CONTROL COORDINATION OF SVCs FOR VOLTAGE REGULATION IN POWER SYSTEMS

by

Abdelhafid Hellal

Department of Electrical Engineering

McGill University

Montreal, Canada

November 1991

A thesis submitted to the Faculty of Graduate Studies and Research
in partial fulfillment of the requirements
of the degree of Doctor Philosophy

ABSTRACT

One of the principal functions of static var compensators (SVCs) in a transmission system is the voltage control at the point of connection. As power and transmission systems have grown considerably in the last decades, many systems have been interconnected for economic reasons. The use of SVCs became more important as the systems were required to operate at higher power levels, which led to a reduction in the stability margin. Increasing the number of SVCs in a network is one of the solutions, but it leads to undesirable interactions among them, which affect the stability limits. Control coordination of these SVCs is considered a good alternative to allow power systems to operate at higher power levels with the required stability margin, as well as to increase the damping of critical modes of oscillation.

This study presents the possibility of improving the effectiveness of SVCs in a system through the concept of SVC control coordination for voltage regulation, in linearized power systems. A concept of coordination of several SVC units, operating on the same system bus of a network, based on averaging the SVC current outputs according to their dynamic reactive capabilities as defined by their slope reactances, has been elaborated. Then, a control coordination concept relevant to many SVC units connected to different buses of the system has been presented and described.

The methodologies used to describe these concepts have been explained, and simulation results were presented.

RÉSUMÉ

Une des principales fonctions des compensateurs statiques (SVCs) dans un réseau de transport d'énergie est la régulation de tension des barres où ils sont connectés. Comme les réseaux de transport et de puissance ont considérablement grandi durant ces dernières décennies, plusieurs systèmes ont été interconnectés pour des raisons économiques. Le besoin d'opérer ces réseaux pour transporter de grandes quantités d'énergie a entraîné une diminution substantielle de la marge de stabilité, ce qui a permis l'emploi grandissant de compensateurs statiques. L'utilisation d'un grand nombre de compensateurs statiques est une des solutions possibles, mais a pour effet l'existence d'interactions mutuelles entre ces dispositifs eux mêmes. Cela affecte aussi les limites de stabilité des réseaux. Aussi, une coordination de contrôle de ces compensateurs statiques peut-être considérée comme une bonne alternative pour permettre de transporter de grandes quantités d'énergie tout en préservant les marges de stabilité requises et améliorer l'amortissement des oscillations des modes critiques.

Cette étude présente au moyen de concepts de coordination de contrôle de compensateurs statiques relatifs à la régulation de tension pour des réseaux linéarisés, une possibilité intéressante d'améliorer l'efficacité de ces dispositifs dans un réseau d'énergie. Un premier concept de coordination de contrôle de plusieurs compensateurs statiques opérant en parallèle sur une même barre du réseau, a été élaboré. Ce concept est basé sur la prise de moyenne des courants de sortie des compensateurs statiques, relatifs à leurs capacités réactives dynamiques défini par leur pente respective. Ensuite, un concept de coordination de contrôle de plusieurs compensateurs statiques localisés sur différentes barres du réseau a été présenté et décrit.

Les méthodologies utilisées pour décrire ces concepts ont été clairement expliqués et des résultats de simulation présentés.

ACKNOWLEDGMENTS

The author wishes to express his most sincere appreciation and gratitude to Dr. M.M. Gavrilovic for his unceasing guidance throughout this study, his useful suggestions and his critical review of this manuscript.

Thanks is also expressed to Mr J.C. DesLauriers, Chef de service and the department Service de Simulation des Réseaux at IREQ (Hydro-Quebec) for allowing me to have access to the computer facilities, photocopier machines, etc,. and financial support by means of a project work. A special note of appreciation for Mr P. Mercier for his encouragements and understanding.

The author would also like to thank all his friends and colleagues from McGill University and IREQ who helped me to conclude this thesis by their support and friendship, especially to my very good friends S.Kamel and R. Kashyap.

A financial support of the government of Algeria is also gratefully aknowledged.

Finally, a very special debt is owed to my parents, brothers and sisters, who were continuously present by their support and unlimited encouragements, especially to Fatah who was very regular in keeping me abreast of the home news during all these years.

CLAIM OF ORIGINALITY

To the best author's knowledge, the following contributions are original :

– a proposition of the concept of coordinating several SVC units, operating in parallel on the same system bus, with regard to voltage regulation of linearized power systems, by means of averaging the SVC current outputs according to their dynamic reactive capabilities, as defined by their slope reactance.

– a proposition of the concept of coordinating many SVC units located at various buses within the power system, with regard to voltage regulation of linearized power systems, by means of a structural change to the SVC controller dynamics, which minimizes the mutual interactions among the SVC controllers and improves their dynamics and stability margin.

TABLE OF CONTENTS

Page

LIST OF FIGURES

CHAPTER I

INTRODUCTION

1.1. STATIC VAR COMPENSATORS AND THEIR APPLICATIONS

Static var compensators (SVCs) are fast acting devices which are being increasingly applied to power systems for a variety of purposes :

- voltage regulation and increasing voltage stability limits (prevention of voltage collapse),
- increase of transient stability limits and power transfer capability,
- increase in power system damping,
- providing of the reactive requirement of HVDC terminals,
- control of voltage flicker,
- phase unbalance of fluctuating loads,
- control of temporary overvoltages, and
- damping of subsynchronous resonance.

At present, the controls of such devices are local and independent. As more and more of these devices are installed within one system, undesirable interactions develop. Such interactions reduce, in general, their stability limits, increasing risks of instability (mutual hunting). For these reasons, slower control settings and dynamics have to be adopted. Some studies indicate that the number of such devices has to be limited in order to ensure their stable operation.

1.2. STATIC VAR COMPENSATORS FOR VOLTAGE REGULATION/ LITERATURE SURVEY

Voltage regulation in power systems has been always a subject of important interest as power systems are sensitive to load variations. Fast voltage regulation in power systems relies primarily on automatic voltage regulation (AVR) of synchronous machines for power generation. Synchronous condensers were the only traditional means for voltage regulation in power transmission systems. Recent development of Static Var Compensators has proved that a relatively inexpensive and reliable fast voltage regulation devices can be build and applied to improve the operation of power systems and extend their transmission capabilities and their transient stability limits [1-8].

Shunt reactive power compensation by means of SVC based on thyristor-controlled reactors (TCR) and thyristors switched capacitors (TSC) as their variable reactive power devices, is now applied in many interconnected power systems as a new and efficient tool for maintaining voltage deviations within specified tolerances.

In conventional SVC systems, thyristor-controlled reactors (TCRs) and thyristor-switched capacitors (TSCs), as variable components, are controlled such as to operate as reactive current sources. SVC systems in development employ gate turn off (GTO) thyristors for forced-commutation of capacitors and reactors, acting as reactive voltage and current sources, respectively [12].

Conventional SVC systems for voltage regulation employ controllers based on local voltage and current measurements. The operation of their TCR, TSC components and GTO thyristors requires phase synchronization, most often based on phase-locked loops (PLLs). Generally, a proportional integral (PI) controller or lead/lag controllers are employed. A PI controller has an internal feedback loop based on the internal (or external) SVC current signal fed through the slope reactance of the SVC. Such control systems are adequate when the number of SVC units is small.

H. W. Schweickardt et al. [9] demonstrated that thyristor-controlled static var compensators meet all transmission system requirements due to their fast control capabilities to regulate the voltage and improve system dynamic performance and its transient stability. They showed also that the SVCs can be controlled so as to enable the damping of system power oscillations. R. L. Hauth et al. [10] and D. McGillis et al. [11] considered the benefits of static var systems in high voltage power systems applications. R. Elsliger et al. [13] presented the strategy of optimization when the shunt compensation is to be applied on a large scale, with a considerable number of SVCs in the system.

L. Gerin-Lajoie et al. [14] considered application of 30 static compensators to Hydro-Quebec power system using the eigenvalue technique. They discovered that when the system becomes weak (i.e, loss of two lines in a section), the SVCs tend to become unstable and in order to preserve the system a recourse must be made to local and remote SVC tripping .

A. J. P. Ramos et al. [15] confirmed, by means of transient network analyzer (TNA) simulations, that the network-SVC and SVC-SVC interactions can develop in a weak power system which is radial and heavily shunt compensated, with three static var compensators of relatively large ratings, installed at short distances from each other.

In order to achieve the best use of static var compensators in a power system, it is necessary to select their strategic locations and ratings. This has been the subject of many technical papers. R.T Byerly et al. [16] considered the application of static var compensators to power transmission systems with an emphasis on stability, regarding to SVC specifications of SVCs, locations, slope reactances, peak reactive power requirements, and control modulation. M. O'Brien et al. [17] proposed a computational by efficient procedure for the determination of SVC locations so as to maximize the damping of electromechanical oscillations. The proposed location criterion is independent of the SVC control scheme to be used. N. Martins et al. [18] developed efficient algorithms for solving two important problems of damping of electromechanical oscillations in large scale systems. The algorithms enable the determination of the most suitable generators for installing power system stabilizers and the most suitable buses in the system for placing static var compensators in order to damp the critical modes of oscillation. S.Granville et al. [19] developed a software named PLANVAR, to be used for improving the voltage profile by means of optimally located shunt var systems.

Optimal control theory has been applied to design optimal controllers, [20–23], SVC controllers in particular [24]. But, it has been shown that optimal control theory assumed a centralized control structure, which requires a great number of feedback loops when the number of SVCs is large. This is a serious drawback from the view point of practical realization. R. L. Kosut et al. [25] proposed a method for designing controllers for linear time-invariant systems whose states are not all available or accessible for measurement and where the structure of the controller is constrained to a linear time-invariant combination of the measurable states of the system. M. M. El Metwally et al. [26] considered the design of decentralized optimal controllers of multi-area power systems. In order to offset the measurement and transmission problems associated with centralized optimal control, localized optimal controls based on the method of minimum error excitation were developed and their performance analyzed as a function of tie line power level. In addition, the effect of feeding back some of the reduced number of remote state variables, on the response of decentralized optimal controls was investigated.

M. Brucoli et al. [27] proposed a decentralized suboptimal control with SVC controllers feeding back only locally available variables. Although some effort has been made to develop SVC adaptive controllers [28–32], the problem of coordination of SVC controllers for voltage regulation is just being recognized.

1.3. CONTROL COORDINATION OF SVCs FOR VOLTAGE REGULATION

Electric utilities are becoming increasingly constrained in regard to construction of new generating plants due to regulatory procedures. There is an increased pressure to build plants far from the major centers, while it becomes more and more difficult to get rights of way for transmission lines.

Power systems become more interconnected for economic reasons. As transmission systems are required to operate at higher power levels, the margin of stability reduces. For these reasons, utilities are increasingly employing static var compensators, series compensation [33], as well as HVDC systems. Therefore, the number of fast voltage control devices on a system is continually increasing, in addition to existing fast, high initial response excitation systems and power system stabilizers.

Control coordination of voltage control devices can reduce undesirable interactions, increase their stability limits, and allow power systems to operate at greater power transfer levels, yet with required stability margins. In addition they will increase damping of critical modes of system oscillations.

Control coordination of static var compensators for voltage regulation can provide a stable and efficient operation especially when their number becomes significant. In the present study, control coordination concepts of static var compensators located on the same bus or various buses of a system, are proposed with regard to voltage regulation of linearized power systems. Such a coordination can be associated to SVC functions, such as coordinated system damping function by static var compensators in support of power system stabilizers and HVDC systems.

1.4. SCOPE AND ORGANIZATION OF NEXT CHAPTERS

Chapter II introduces the power components such as transmission lines, transformers, reactors, capacitors and filters including generators, loads and SVC systems and their linearized representation required in transient and small perturbation studies.

Chapter III gives an introduction to SVC control systems for voltage regulation . Linearized power system with single SVC unit was considered and a modal analysis in s-plane and time domain analysis of that system was presented.

Chapter IV describes the concept applied to coordinate many SVC controllers operating on the same bus of a power system, using linearized single bus equivalent system.

Chapter V presents the concept of coordination of many SVC controllers when the SVC units are connected to different buses within a power system. Analysis of SVC systems with coordinated controllers in s-plane and time domain was made in the case of the linearized IEEE 30-bus power system with up to five SVC units. The results of this analysis are given in Chapter VI.

The conclusions of this study and suggestions of future development were presented in Chapter VII.

CHAPTER II

POWER SYSTEM AND STATIC VAR COMPENSATOR REPRESENTATION

2.1. INTRODUCTION

This chapter deals with the representation of the power system and the SVC systems to be used through this study. Representation of power system components, transmission lines, transformers, reactors, capacitors, filters, generators, loads and SVC systems are described.

2.2 POWER SYSTEM REPRESENTATION

2.2.1. Transmission Lines, Transformers, Reactors and Capacitors

Transmission lines considered in this study are represented by their π -equivalents. One such representation is given in Figure 2.1 ,

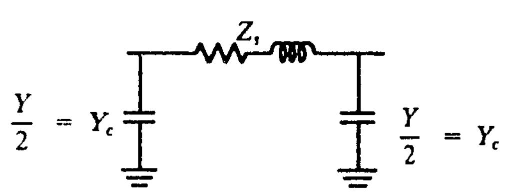

Fig 2.1. π - equivalent line representation

The characteristic parameters of the π-equivalent of the line are :

Z_s – the series impedance between the line terminals, and

$Y_c = Y/2$ – the shunt admittance at each line terminal.

A transformer with a fixed tap setting a can be assumed to consist of its leakage impedance Z_{pq} connected in series with an ideal autotransformer. The π - equivalent of the transformer is shown in Figure 2.2 ,

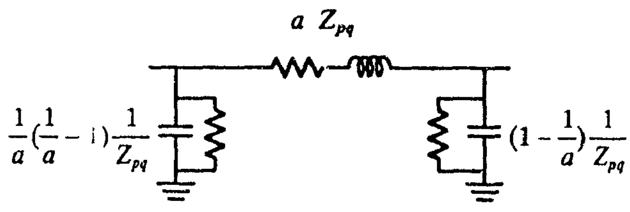

Fig 2.2. π - equivalent transformer representation

On-load tap changing transformers and phase shifters can also be represented by similar π - equivalents.

Linear reactors, capacitors and filters are represented by their relevant impedances.

2.2.2. Generators

Generator dynamics associated with the rotating mass are too slow and do not affect the dynamics of the static var compensators. Even the dynamics of the generator excitation system are relatively slow as compared to the SVC dynamics (ten times slower), so that they can also be neglected, including the dynamics of the associated automatic voltage regulator (AVR). Therefore, the generator can be represented by an equivalent infinite bus behind an internal reactance as shown in Figure 2.3 ,

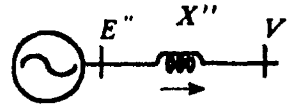

Fig 2.3. Generator representation

where E'' is the voltage behind the subtransient reactance, and

X'' is the subtransient reactance.

The generator which is considered as the slack bus in load flow studies can also be represented by a corresponding infinite bus behind an internal reactance as any other generator within the system.

2.2.3. Loads

Loads consist of thermal and motor loads. Thermal loads are stationary while motor loads are dynamic. However, the dynamics of the motor loads are too slow as compared to SVC dynamics, so that they could be neglected. Therefore, the loads are also considered to be stationary. They are nonlinear with regard to applied voltages. In load-flow studies, the loads are considered in general as ,

$$P = P_o \left(\frac{V}{V_o}\right)^n \qquad n \in [0,2]$$

$$Q = Q_o \left(\frac{V}{V_o}\right)^n$$

For $n = 0$, the load becomes a PQ bus since its active and reactive power are constant.

For $n = 1$, the load becomes a I-bus since its active and reactive currents are constant.

For $n = 2$, the load becomes a Z-bus since its impedance is constant.

In small signal studies of SVC dynamics, the linear representation of the load has to be assumed. Therefore, either a constant current and/or a constant impedance load representation has to be chosen. Load buses are by far the most common, typically comprising more than 80 % of all buses of a network.

2.3 SVC REPRESENTATION

A detailed analysis of SVCs, their functions, characteristics and applications of SVCs has already been elaborated [7]. The sections which follow present a brief review of typical SVC types (TSC and TCR types) as the basis for the SVC control coordination concept.

Then, before establishing the SVC model for transient stability and small disturbances studies, it will be useful to review the SVC representations in load-flow and electromagnetic transient studies.

2.3.1. SVC Functions

In general, static var compensators are used in power systems where continuous and fast reactive power control is required. This requirement has to meet one or more objectives such as (1) improving system voltage condition, (2) providing voltage stability margin, (3) increasing power transfer capability, (4) increasing transient stability margin, and (5) supplying reactive power to AC-DC converters. In addition, they are applied to functionally modulate the voltage in order to (6) damp power system oscillations, (7) damp subsynchronous resonance, (8) balance phase voltages, and (9) control system overvoltages.

2.3.2. TCR / TSC Static Compensators

Among various static var compensators, TCR/TSC types are most often applied, for which reason they will be considered in this study.

A TCR consists of a reactor in series with a bidirectional thyristor valve as shown in Figure 2.4 ,

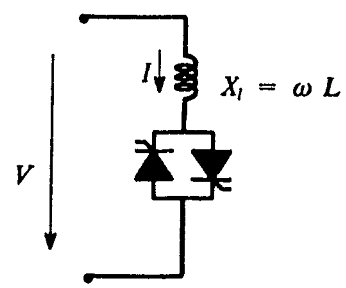

Fig 2.4. TCR configuration

The fundamental frequency current component through the TCR reactor is phase-controlled by closing of the thyristor valve with respect to the zero-crossing of the applied voltage, at angles α between 90° and 180°, at each half-cycle, (Figure 2.5.a) ,

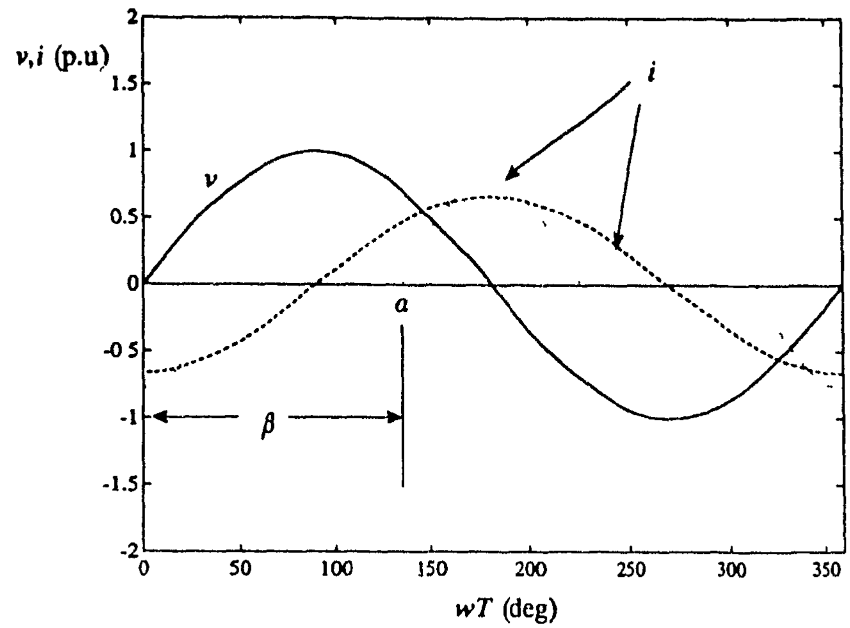

Fig 2.5.a TCR waveforms

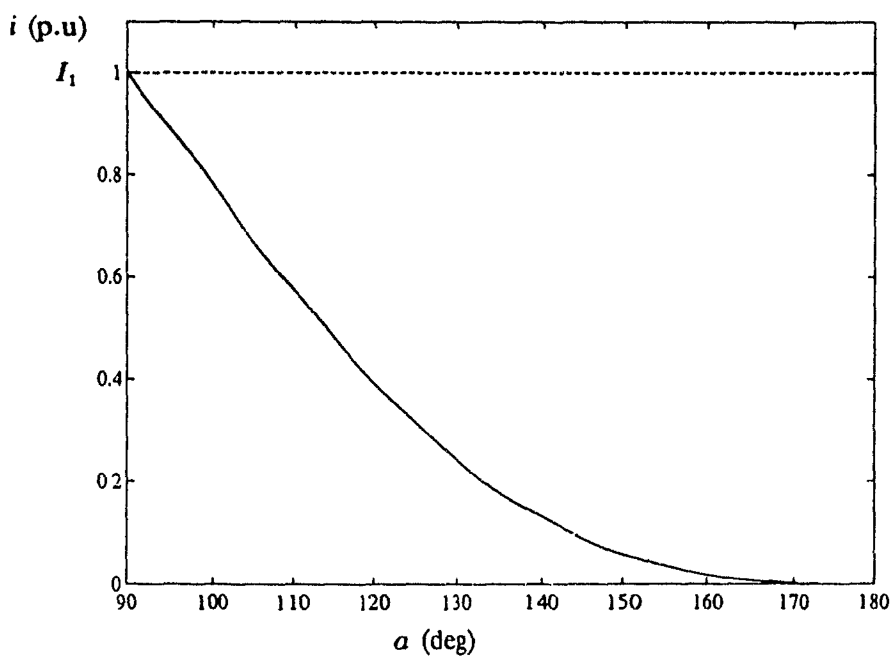

Fig 2.5.b Fundamental current of a TCR as function of the firing angle

The fundamental component I_1, shown in Figure 2.5.b, as a function of the phase a is given by the following expression ,

$$I_1 = \frac{1}{\pi}[2(\pi - a) - \sin 2(\pi - a)]\ p.u.$$

Three TCR units connected in delta comprise a 6-pulse TCR unit which has its triple harmonics ($3n-th$ order harmonics) cancelled. A 12-pulse TCR unit consists of two 6-pulse units, one a wye-connected secondary, the other a delta-connected secondary of the coupling transformer. The 12-pulse TCR unit has its $3rd$, $5th$ and $7th$ harmonics cancelled, the $(6n \pm 1)th$ order harmonics in general.

A TCR/FC compensator consists of 6 or 12 pulse TCR unit with a fixed capacitor bank, a filter (if necessary), a coupling transformer and a controller including the firing (synchronizing) system, the PI or phase lead/lag error processor, internal or external current feedback and the voltage (and current) measurement system, (Figure 2.6),

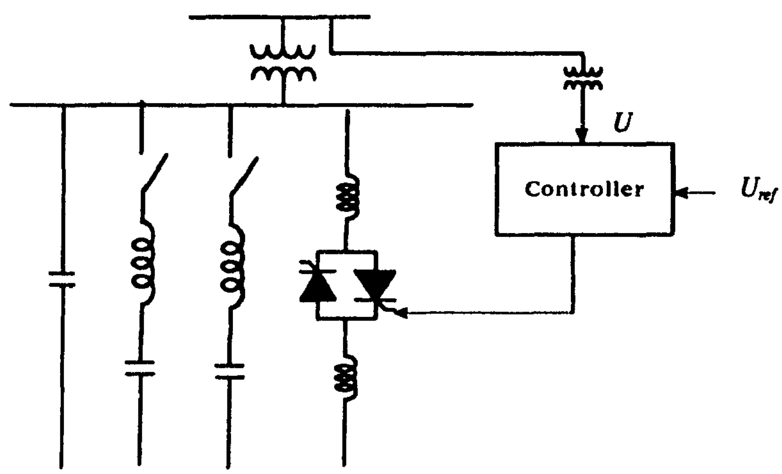

Fig 2.6. Thyristor-Controlled Reactor Compensator

Thyristor-switched shunt capacitor (TSC) consists of a few parallel capacitor banks which are switched on-off individually, using anti-parallel connected thyristors as switching valves as shown in Figure 2.7.

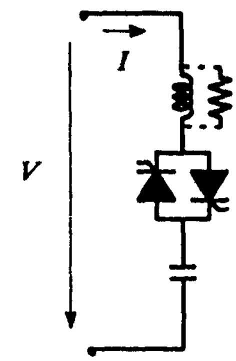

Fig 2.7. TSC configuration

The purpose of the small reactor is to limit the rate of change of the capacitor current. A parallel resistor improves the damping of inrush current transients. In some SVC systems, the limiting reactor is tuned with respect to the capacitor in order to form a filter for a particular harmonic and in order to reduce requirements for additional filtering.

While a TCR reactor unit is characterized by a continuous control, a half-cycle delay (max) response, negligible switching transients and harmonic generation, a TSC is characterized by a stepwise control, a cycle delay (max) response, switching transients but no harmonic generation.

In many applications the SVC systems consist of 6-pulse TCR combined with TSC units as solutions to provide a continuously variable reactive output from fully lagging to fully leading current, while their response is fast and harmonic generation reduced. Such an SVC is illustrated in Figure 2.8 ,

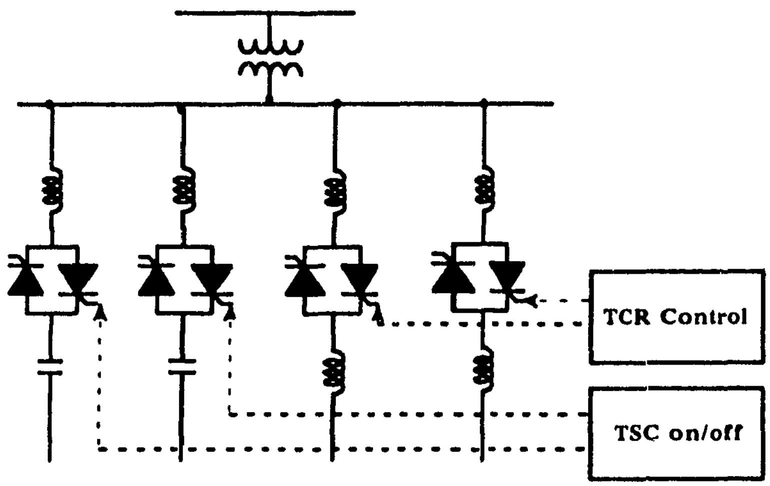

Fig 2.8. TSC/TCR static var compensator

2.3.3. Load Flow Representation of SVCs

The main objectives of a load-flow study are to determine the bus voltages, the active and reactive power flow in transmission lines and transformers, the power losses, the power at the slack bus and the reactive power of generators and shunt elements (e.g SVCs) for a given power system configuration with generators specified as PV buses and loads specified as PQ, I or Z buses.

A load-flow study concerning the SVC applications enables primarily :

- determination of SVC location and preliminary ratings,

- analysis of SVC effects on the system active and reactive power flow and system bus voltage,

- determination of the steady-state for transient stability and/or small perturbation studies.

In a load-flow study, each node of the system is represented either by a PV bus, a PQ bus, an I bus, a Z bus or a slack bus (E bus).

The basic SVC model in load-flow studies is a PV bus where $P = 0$ and $V = V_{ref}$ behind the SVC slope reactance (internal reactance) X_{sl} (Figure 2.9) ,

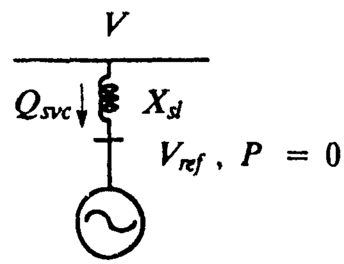

Fig 2.9. SVC model in programs for load-flow studies

The nominal operating range of an SVC is (Q_{max} and Q_{min})

$$1 - X_{sl}\, Q_{svc\,Cm} \leq V \leq 1 + X_{sl}\, Q_{svc\,Lm} \qquad \text{in p.u on the SVC base,}$$

where
$$Q_{svc\,base} = max\,(Q_{svc\,Lm}\ ,\ Q_{svc\,Cm})$$

$$V_{svc\,base} = V_{ref}$$

Outside of this range, the SVC operates as a shunt reactor or capacitor depending on its operating point (Figure 2.10) ,

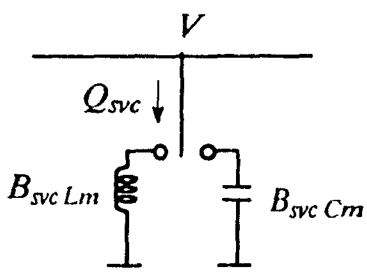

Fig 2.10. SVC model for operation outside nominal range

$$\text{For } V > 1 + X_{sl}\, I_{svc\,Lm} \qquad B_{svc} = -B_{svc\,Lm} = -\,\frac{I_{svc\,Lm}}{1 + X_{sl}\ I_{svc\,Lm}}$$

For $V < 1 - X_{sl}\, I_{svc\,Cm}$ $\qquad B_{svc} = B_{svc\,Cm} = \dfrac{I_{svc\,Cm}}{-X_{sl}\, I_{svc\,Cm}}$

where $\qquad I_{svc\,Lm} = \dfrac{Q_{svc\,Lm}}{1 + X_{sl}\, Q_{svc\,Lm}}$

and $\qquad I_{svc\,Cm} = \dfrac{Q_{svc\,Cm}}{1 - X_{sl}\, Q_{svc\,Cm}}$

The reactive power Q_{svc} at the coupling bus is absorbed/generated according to the SVC characteristic as seen in Figure 2.11 ,

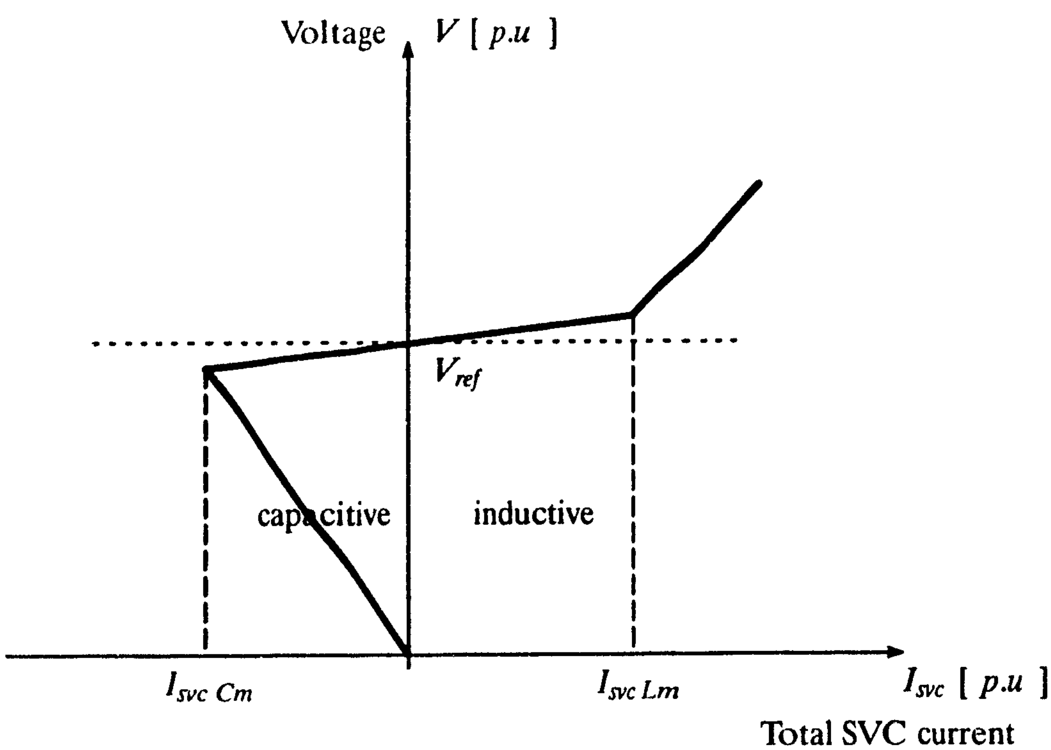

Fig 2.11. Basic SVC characteristic

2.3.4. SVC Representation in Electromagnetic Transient Studies

SVC models in electromagnetic transient studies must accurately represent SVC characteristics in steady-state and transient conditions, for which reason they are three-phase. Depending on the simulation technique being utilized, SVC representation can be analog, digital or a hybrid. Digital models of the SVC power system components consist of implementation of differential and algebraic equations [34], while relevant analog models consist of reactors, capacitors and linear and saturable transformers [35].

Thyristor valves in analog simulation are represented by bidirectional thyristor pairs. Snubber circuits are modelled by passive components. Improved models of thyristor valves employ negative resistance for compensation of excessive voltage drops across their thyristors. Thyristor valve models, based on Field-Effect transistors (FET's) are used in digital simulation, instead of thyristors modelled as ideal valves.

SVC controllers in analog and hybrid simulation are represented either by a physical or an analog or a digital equivalent. Modern digital models and controllers employ microprocessor technology where signal model processing is defined almost entirely in software. The essential component of a digital representation control system is shown in Figure 2.12.

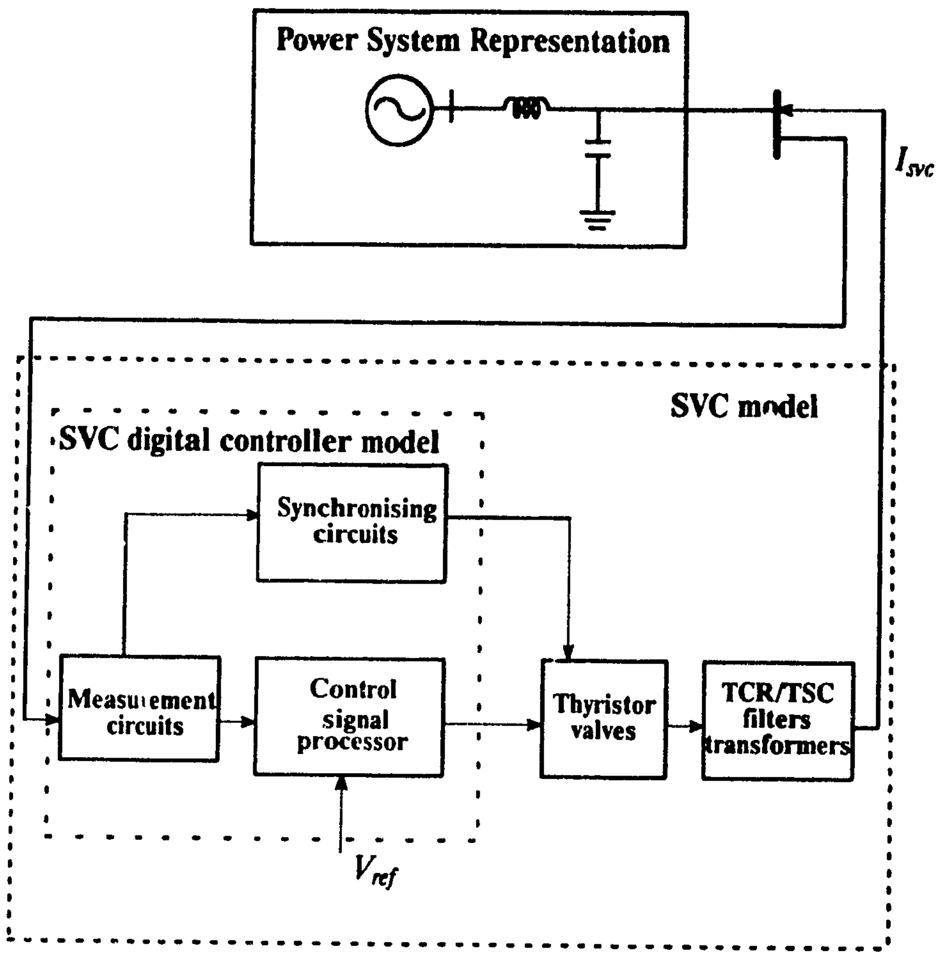

Fig 2.12. Bloc diagram of an SVC model employing a digital controller model

SVC controllers are represented in digital simulation by an equivalent implementation of all controllers, differential, algebraic and logical equations.

2.3.5. SVC Representation for Small Disturbance Studies

Based on SVC modelling in steady-state and electromagnetic transients studies, SVC representation for small disturbance studies has been deduced. This model represent all the relevant dynamic characteristics of the SVC control systems to be analyzed in small disturbance studies. The general block diagram of this model is given in Figure 2.13.

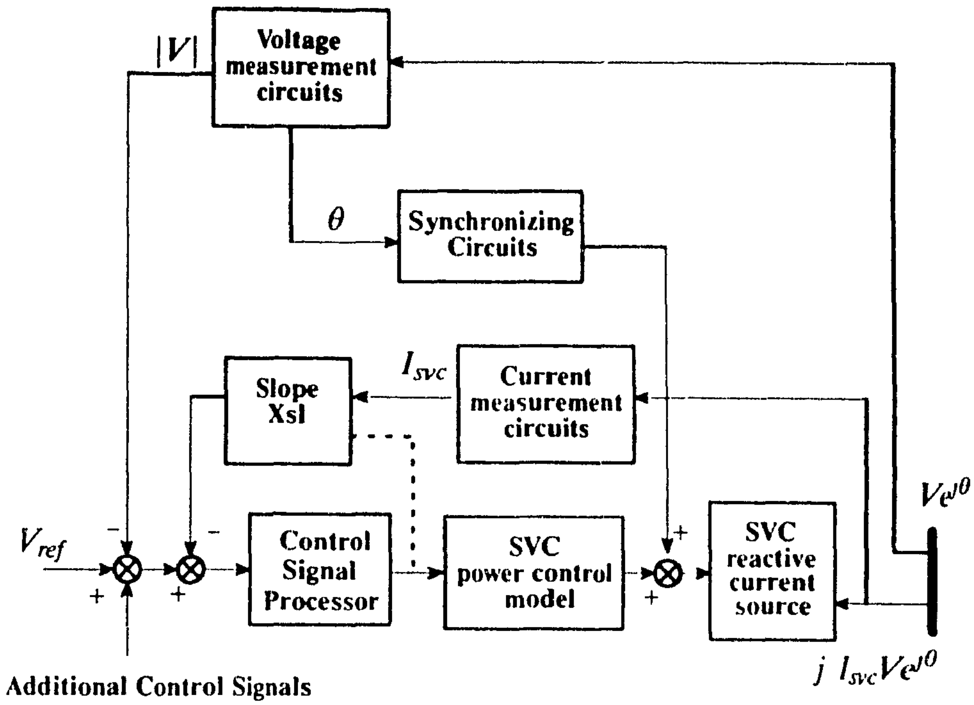

Fig 2.13. Principal SVC Model for Small Signal Studies

Digital computer programs for transient stability and small disturbance studies are based on lumped transmission system components where impedances are considered to remain at their values at nominal frequency during the transients.

In transient stability programs, the power system is described by a set of nonlinear algebraic equations (load-flow problem) and a set of nonlinear differential equations (dynamics of electromechanical system components), which are solved alternately. The load-flow equations are most often solved by Newton-Raphson or Gauss-Seidel methods, while the integration of the differential equations is done in small time steps using trapezoidal techniques.

In programs for small signal stability studies, all system components are linearized around the steady-state operating point, so that the system behavior could be analyzed in Laplace domain, based on system eigenvalues and eigenvectors.

Present SVC controllers are mostly of proportional-integral (PI) type. In some cases proportional controllers are applied with lead/lag filters for an optimal tuning phase processing of voltage error signal. In such cases, the overall controller gain is inversely proportional to the slope reactance,

$$K = \frac{\Delta I_{svc}}{\Delta V_{err}} = \frac{1}{X_{sl}}$$

Integral type voltage controller is frequently applied with the current (reactive power) feedback with a slope reactance as its gain, as an adequate solution instead of proportional-integral controller.

Supplementary control signals related to variation of the system frequency, power flow and phase difference may be also used when SVC systems are applied to improve transient stability and/or system damping.

The nonlinear relationship between the SVC output and the firing angle is compensated by means of a linearizing function in the thyristor phase control circuits.

CHAPTER III

POWER SYSTEM WITH A SINGLE SVC UNIT / MODAL AND TIME DOMAIN ANALYSIS

3.1. INTRODUCTION

The purpose of this chapter is to describe the control model of a single SVC system connected to a power system equivalent, with regard to voltage regulation. The modal analysis of the SVC system in the s-plane is presented as well as step responses in the time domain to various disturbances such as voltage reference variation or load current disturbance.

A review of the significance of eigenvalues, eigenvectors, poles, zeros and residues through modal analysis of linear time-invariant dynamic systems is given in Appendix A.

3.2. POWER SYSTEM WITH A SINGLE SVC UNIT

The linearized power system with a single SVC unit is given in Figure 3.1.

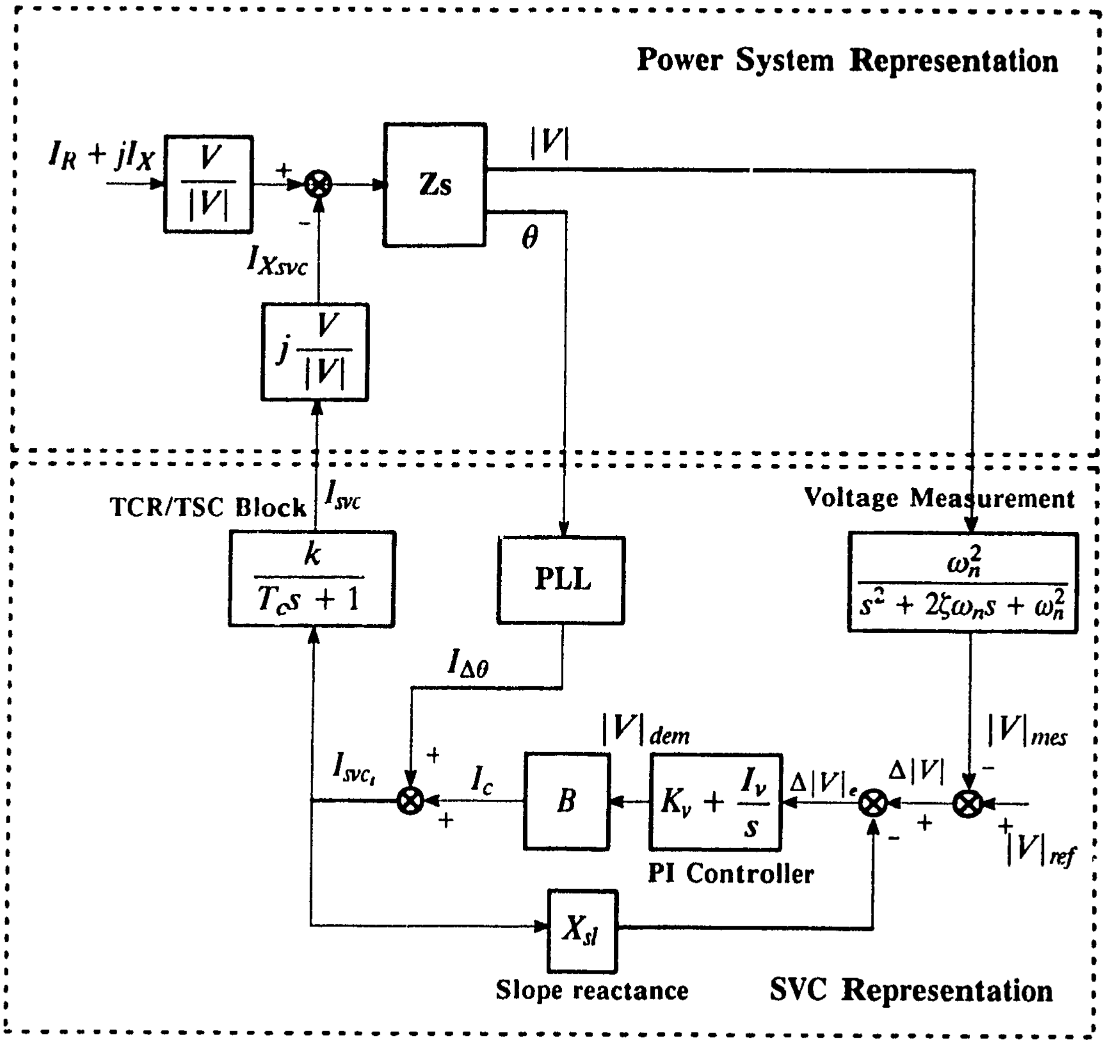

Fig 3.1. Linearized power system with single SVC.

Power System Representation

In this case, the power system is represented by an equivalent impedance block denoted by Zs. In more details the block Zs is shown as follows, in Figure 3.2,

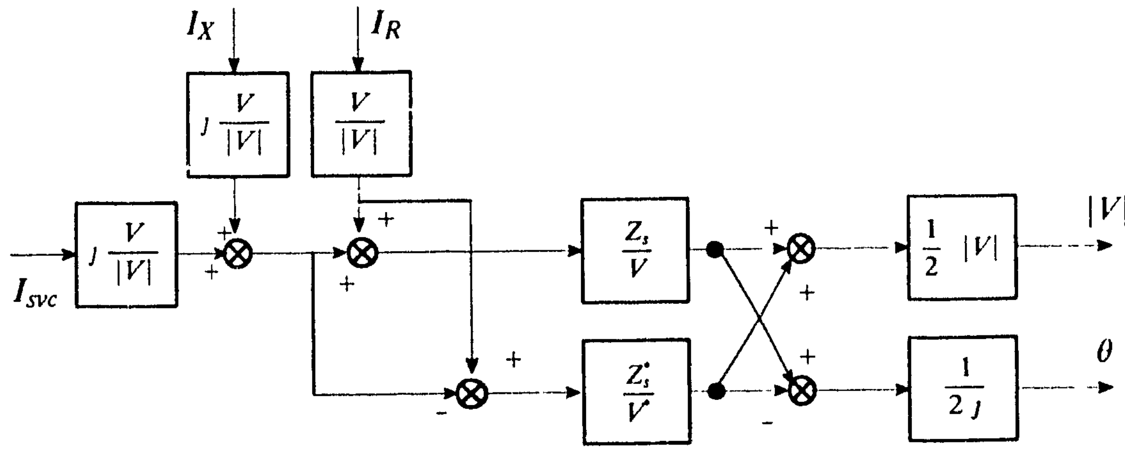

Fig 3.2. Linearized power system block diagram

The voltage magnitude $|V|$ and the phase θ represent the outputs of the power system, while the inputs are the SVC current I_{svc} and the reactive and active load currents I_X and I_R. These outputs are expressed by the following linearized equations,

$$|V| = \frac{\partial|V|}{\partial I_{svc}}|_0\, I_{svc} + \frac{\partial|V|}{\partial I_X}|_0\, I_X + \frac{\partial|V|}{\partial I_R}|_0\, I_R \tag{3.1}$$

$$\theta = \frac{\partial\theta}{\partial I_{svc}}|_0\, I_{svc} + \frac{\partial\theta}{\partial I_X}|_0\, I_X + \frac{\partial\theta}{\partial I_R}|_0\, I_R \tag{3.2}$$

where $\frac{\partial|V|}{\partial I_{svc}} = \frac{\partial|V|}{\partial I_X} = j\,\frac{1}{2}\,[Z_s - Z_s^*]$,

$$\frac{\partial|V|}{\partial I_R} = \frac{1}{2}\,[Z_s + Z_s^*],$$

$$\frac{\partial\theta}{\partial I_{svc}} = \frac{\partial\theta}{\partial I_X} = \frac{1}{2}\,\frac{1}{|V_0|}\,[Z_s + Z_s^*],$$

$$\frac{\partial\theta}{\partial I_R} = \frac{1}{2j}\,\frac{1}{|V_0|}\,[Z_s - Z_s^*].$$

At a selected operating point, V_0 is constant, as well as $|V_0|$. The power system block diagram, is therefore clearly defined as linear since the system outputs $|V|$ and θ are linear functions of system intputs I_{svc}, I_R and I_X.

SVC Representation

SVC systems considered in this thesis are represented by a generalized block diagram shown in Figure 3.1. It comprises a TCR/TSC block, a valve firing unit, a phase-locked loop unit, a PI controller, a slope reactance feedback and a voltage measurement unit.

The voltage magnitude is filtered, then compared to a reference signal, the difference being the input to the PI controller. The PI controller has an internal feedback loop based on the internal (or external) SVC current fed through the slope reactance of the SVC.

The phase-locked loop is assumed to consist of a voltage controlled oscillator, a PI controller, a filter and a phase discriminator. The VCO is represented by an integrator, a PI controller and a filter, while the phase discriminating multiplier is linearized as shown in Figure 3.3,

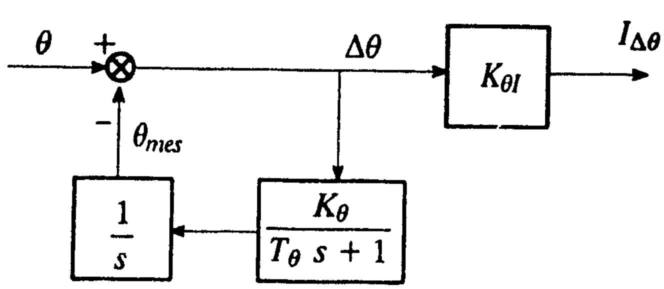

Fig 3.3 Linearized block diagram of the PLL

The TCR/TSC valve triggering is performed taking the voltage zero-crossing for its reference which is provided by the phase-locked loop (PLL). However, the PLL circuit introduces a phase tracking delay $\Delta\theta$ during transients. This causes a disturbance $I_{\Delta\theta}$ to the current order. The linearized PLL circuit is represented by a second order system. Details of the PLL models have been elaborated in reference [36].

The SVC current is finally realized by TCR/TSC components with a response time constant T_c.

The admittance of the TCR/TSC block is a nonlinear function of the controlled firing angle and the PLL synchronization error of their valves. In order to present the linearization of a such function, a TCR/FC block is considered for simplicity.

The controllable susceptance of the TCR is given as follows :

$$\frac{B}{B_l} = \frac{1}{\pi} \left[(\beta - \Delta\theta) - \sin(\beta - \Delta\theta) \right] \tag{3.3}$$

where B_l is the susceptance of the reactor,

β is the valve conduction angle, and

$\Delta\theta$ is the PLL phase synchronization error.

The susceptance of the FC is expressed by :

$$\frac{B}{B_c} = 1 \tag{3.4}$$

where B_c is the capacitor bank susceptance.

For the combined TCR/FC systems of equal inductive and capacitive ratings, the controllable susceptance is given by the sum of (3.4) and (3.5) , which is :

$$B = 1 - \frac{2}{\pi} \left[(\beta - \Delta\theta) - \sin(\beta - \Delta\theta) \right] \tag{3.5}$$

when B is the TCR/FC susceptance in p.u. values, its base being

$$B_{base} = B_c = \frac{B_l}{2}$$

From Figure 3.3, the following relation can be deduced :

$$I_{\Delta\theta} = K_{\theta I}\, \Delta\theta = |V_0| \frac{\partial B}{\partial \Delta\theta}\, \Delta\theta \tag{3.6}$$

where $\frac{\partial B}{\partial \theta}$ is the SVC susceptance sensitivity constant coefficient, as

$|V_0|$ is the steady-state voltage magnitude

For small PLL synchronization errors $\Delta\theta$ around the steady-state values β_0 and $\Delta\theta_0 = 0$, the following linearized expression can be deduced from expression (3.5) :

$$\frac{\partial B}{\partial \Delta\theta} |_{\beta_0,\, \Delta\theta_0 = 0} = \frac{2}{\pi}\,(1 - \cos\beta_0) \tag{3.7}$$

Therefore we have :

$$K_{\theta I} = |V_0|\, \frac{2}{\pi}\,(1 - \cos\beta_0) \tag{3.8}$$

On the other side, when $\Delta\theta$ is small, the expression (3.5) reduces to :

$$B = 1 - \frac{2}{\pi}\,[\beta - \sin\beta\,] = f\,(\,\beta\,) \tag{3.9}$$

The nonlinearity $f\,(\,\beta\,)$ is eliminated by means of the linearizing function $f^{-1}\,(B)$ which is regularly implemented on the SVC controllers.

The TCR/FC response dynamics is represented by a simple delay as shown in Figure 3.1.

3.3. STATE-SPACE SYSTEM REPRESENTATION

In general, this block-diagram representation (given in Figure 3.1) can be transformed into a state-space form where load currents I_R and I_X as disturbances and $|V|_{ref}$ as voltage reference are the system inputs, and the variables such as the

SVC currents, the voltage magnitude at the bus, etc.. are the system outputs as shown in Figure 3.4 :

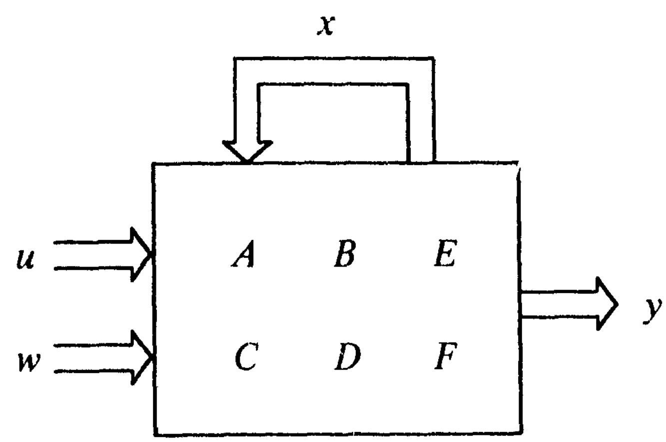

Fig 3.4. State-space block diagram

The general form of this state-space form is given by the following equations,

$$x = A\,x + B\,u + E\,w \tag{3.10}$$

$$y = C\,x + D\,u + F\,w \tag{3.11}$$

where $u = [\,|V|_{ref}]$ and $w = \begin{bmatrix} I_R \\ I_X \end{bmatrix}$ are the disturbance inputs,

$y = \begin{bmatrix} |V| \\ I_{svc} \\ \cdot \\ \cdot \\ \cdot \end{bmatrix}$ is the output vector,

x is the state variable vector, and

A , B , C and D are the system matrices.

The system matrices were formed by simulation using MATLAB software. For reasons of illustration, the state-space representations of the principal dynamic blocks of the system given in Figure 3.1 were derived analytically and presented below.

Voltage Magnitude Measurement Block

The state-space representation of the voltage magnitude measurement block is given by the following expressions :

$$x_m = A_m x_m + B_m u_m \tag{3.12}$$

$$y_m = C_m x_m + D_m u_m \tag{3.13}$$

where $x_m = \begin{bmatrix} |V|_{mes} \\ |V|_{mes} \end{bmatrix}$ is the state vector,

$u_m = |V|$ is the input vector,

$y_m = |V|_{mes}$ is the output vector, while the system matrices A_m, B_m, C_m and D_m are :

$$A_m = \begin{bmatrix} 0 & 1 \\ -\omega_n^2 & -2\zeta\omega_n \end{bmatrix}, \qquad B_m = \begin{bmatrix} 0 \\ \omega_n^2 \end{bmatrix},$$

$$C_m = \begin{bmatrix} 1 & 0 \end{bmatrix} \qquad \text{and} \qquad D_m = [0].$$

PI Error Processor Block

The PI error processor can be represented as follows :

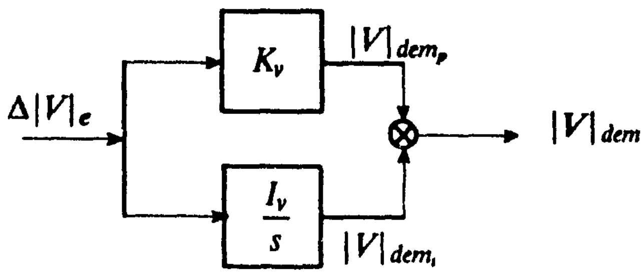

Fig 3.5. Developed PI controller representation

The state-space representation of the PI error processor block is given by the following expressions :

$$x_{PI} = A_{PI}\, x_{PI} + B_{PI}\, u_{PI} \tag{3.14}$$

$$y_{PI} = C_{PI}\, x_{PI} + D_{PI}\, u_{PI} \tag{3.15}$$

where $x_{PI} = |V|_{dem_i}$ is the state vector,

$u_{PI} = \Delta|V|_e$ is the input vector,

$y_{PI} = |V|_{dem}$ is the output vector, while the system matrices A_{PI}, B_{PI}, C_{PI} and D_{PI} are :

$A_{PI} = [0]$, $B_{PI} = [1]$,

$C_{PI} = [1]$ and $D_{PI} = [K_v]$.

<u>TCR/FC Block</u>

The TCR/FC state-space representation is given by the following expressions :

$$x_d = A_d\, x_d + B_d\, u_d \tag{3.16}$$

$$y_d = C_d\, x_d + D_d\, u_d \tag{3.17}$$

where $x_d = I_{svc_{des}}$ is the state vector,

$u_d = \begin{bmatrix} I_{X_{svc}} \\ I_{\Delta\theta} \end{bmatrix}$ is the input vector,

$y_d = I_{svc_{des}}$ is the output vector, while the system matrices A_d, B_d, C_d and D_d are :

$$A_d = [-\frac{1}{T_c}], \qquad B_d = [\frac{1}{T_c} \quad 1],$$

$$C_d = [1] \qquad \text{and} \qquad D_d = [0 \quad 0].$$

where T_c represents the TCR/FC response time constant.

Phase Locked-Loop Block

The phase locked-loop state-space representation (Figure 3.3) is given by the following expressions :

$$x_\theta = A_\theta \, x_\theta + B_\theta \, u_\theta \tag{3.18}$$

$$y_\theta = C_\theta \, x_\theta + D_\theta \, u_\theta \tag{3.19}$$

where $x_\theta = \begin{bmatrix} \theta_{mes} \\ \theta_{mes} \end{bmatrix}$ is the state vector,

$u_\theta = \theta$ is the input vector,

$y_\theta = \Delta\theta$ is the output vector, while the system matrices A_θ, B_θ, C_θ and D_θ are :

$$A_\theta = \begin{bmatrix} 0 & 1 \\ -\frac{K_\theta}{T_\theta} & -\frac{1}{T_\theta} \end{bmatrix}, \qquad B_\theta = \begin{bmatrix} 0 \\ \frac{K_\theta}{T_\theta} \end{bmatrix},$$

$$C_\theta = [-1 \quad 0] \qquad \text{and} \qquad D_\theta = [0].$$

By combining the state-space equations of the described blocks (equations 3.12 to 3.19) with the algebraic equations for $\Delta|V|$ and $\Delta|V|_e$ deduced from Figure 3.1 one can form the state-space equations of the SVC system. Then interconnecting this SVC system state-space representation with the power system (equations 3.1 and 3.2), the complete state representation of Figure 3.4 is defined.

Using the MATLAB software and its Control System Toolbox [37], the system matrices were formed in two steps. First, the state-space representations of the controller and the PLL were formed from their block diagrams using the *'transfer function-to-state space'* conversion function. Secondly, the state-space representation of the whole system was formed by interconnecting the controller and the PLL state-space representation with the power system into a complete system using the *'connect'* function.

3.4. MODAL ANALYSIS OF THE POWER SYSTEM WITH A SINGLE SVC

The principal phase of the modal analysis consists of determining the system eigenvalues. The oscillation frequencies (modes) are associated with corresponding complex eigenvalues pairs, while aperiodic transient components are associated with real eigenvalues.

The eigenvalues of the system are the roots of the characteristic equation associated with the system matrix A.

For example, a power system with a short circuit power of 14000 MVA, a system voltage of 735 kV and an SVC of 660 Mvar are represented in p.u. values based on the SVC rating by the following parameters:

Impedance of power system equivalent : $Z_s = (0.942 + j47.115).10^{-3}$ p.u.

Slope reactance of SVC : $X_c = 0.03$ p.u.

Filter parameters : $\omega_n = 200$; $\zeta = 0.3$;

PI controller parameters : $K_v = 1$; $I_v = 800$;

Time constant : $T_d = 0\ 005$;

Phase-locked loop parameters : $K_t = 533$; $P_t = 1$; $T_t = 0.0038$;

Using MATLAB, the following system eigenvalues have been determined (Figure 3.6) :

$$[-29.95,\ -244.89,\ -30.64 \pm j209.81,\ -266.52 \pm j263.02]$$

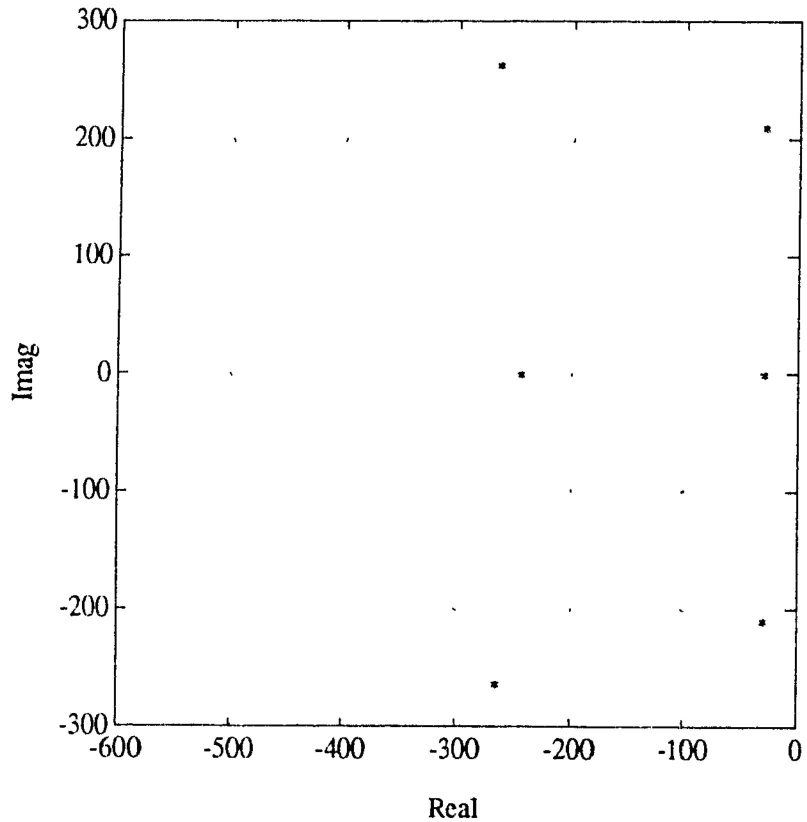

Fig 3.6. Eigenvalues of a power system with single SVC

From Figure 3.6 two oscillatory modes can be revealed, represented by the two pairs of complex eigenvalues and the two aperiodic modes represented by two real eigenvalues.

The position of eigenvalues in the s-plane determine the system stability and its dynamics. These eigenvalues move when parameters vary, whether those of the system (i.e the equivalent impedance Zs of the network due to its topological changes), or those of the controller (i.e gain, integration constant, PLL parameters, etc..).

Root loci foı different parameter variations reveal impact of various parameters upon the system dynamics. Such root loci are given on Figure 3.7 when the impedance of the equivalent network is varied.

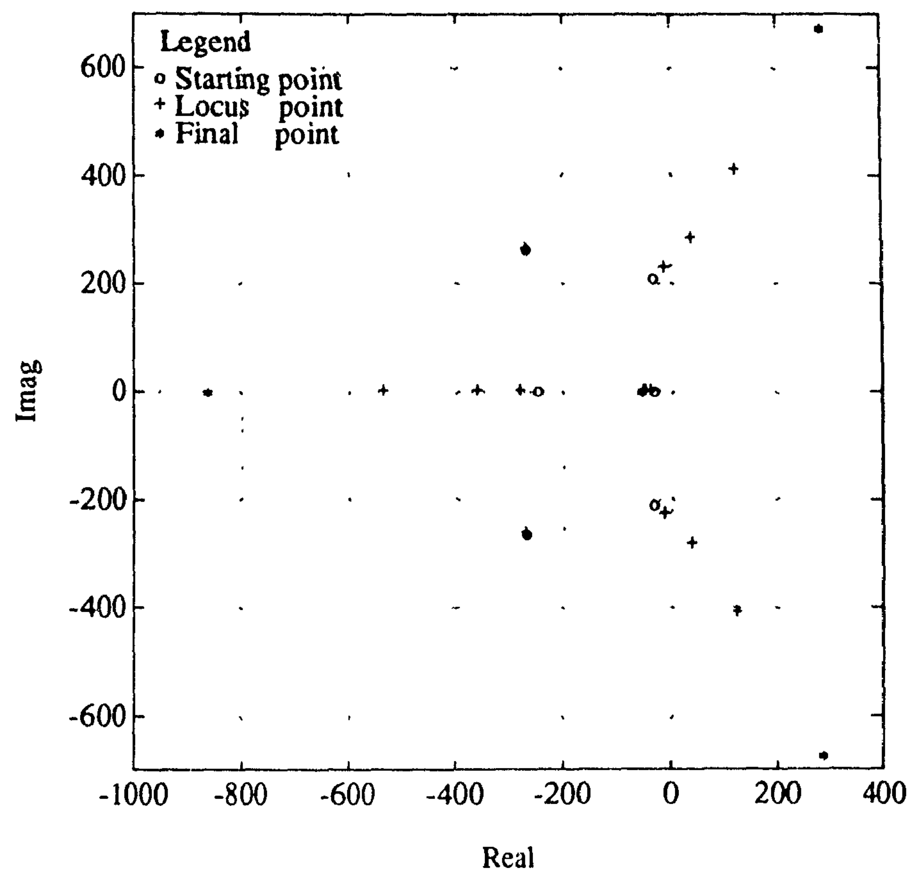

Fig 3.7. Root loci when equivalent of the network impedance with a single SVC system is varied

Figure 3.7 illustrates the displacement of the eigenvalues of the studied system when the impedance of the equivalent netwoık increases two to five times the original value of Z_s. We can see that as the system impedance increases, (i.e. the power system becomes weaker), a pair of complex conjugate eigenvalues (due to the measurement filters) move to the right, the system becomes less damped while its margin of stability diminishes. The other pair of complex eigenvalues (due to the PLL) remains unchanged, but the real eigenvalues move. One of these real eigenvalues is shifted far to the left half plane which gives to its corresponding aperiodic response a shorter time constant. The other real eigenvalue is shifted slightly to the left,, yielding slightly shorter time constant to the relevant aperiodic mode.

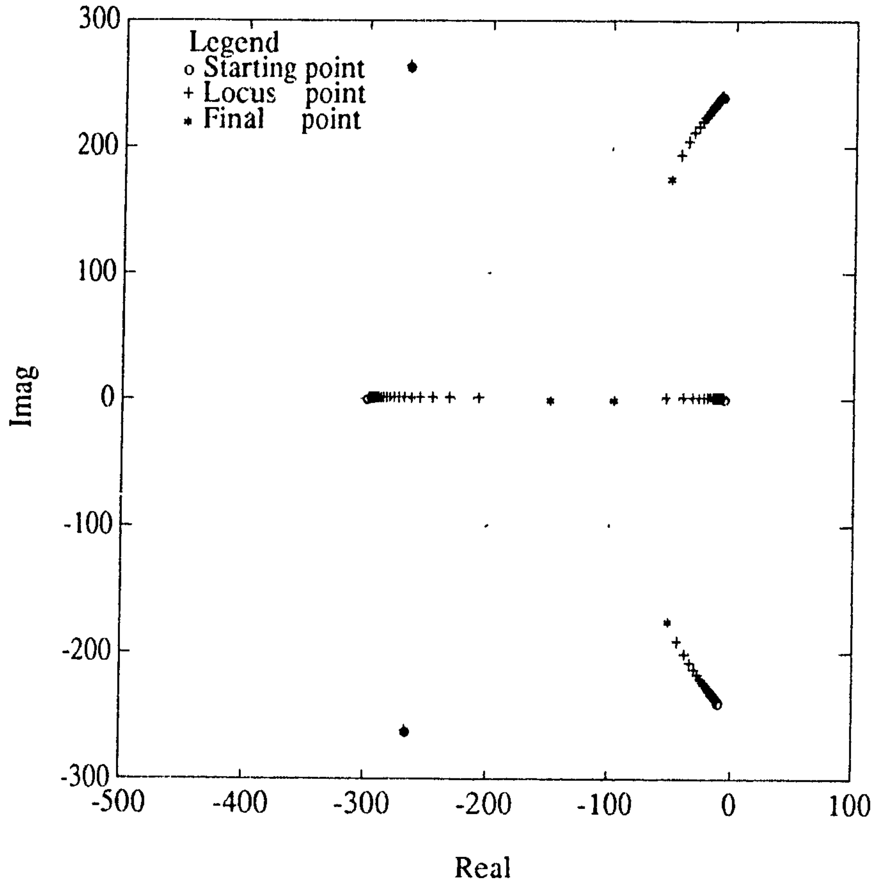

Fig 3.8. Root loci of the system eigenvalues for a variable controller gain

Figure 3.8 illustrates the root loci of the system eigenvalues for varying controller gain K_v from 100 to 0 by steps of 5. The plot shows that for higher gains the system has smaller stability margin. If the gain is increased somewhat above 100, the system becomes unstable since the pair of complex eigenvalues move to the right half plane.

The pair of complex eigenvalues due to the PLL remains unaffected. A decrease of the gain moves one of the real eigenvalue to the right, while the other is moved to the left.

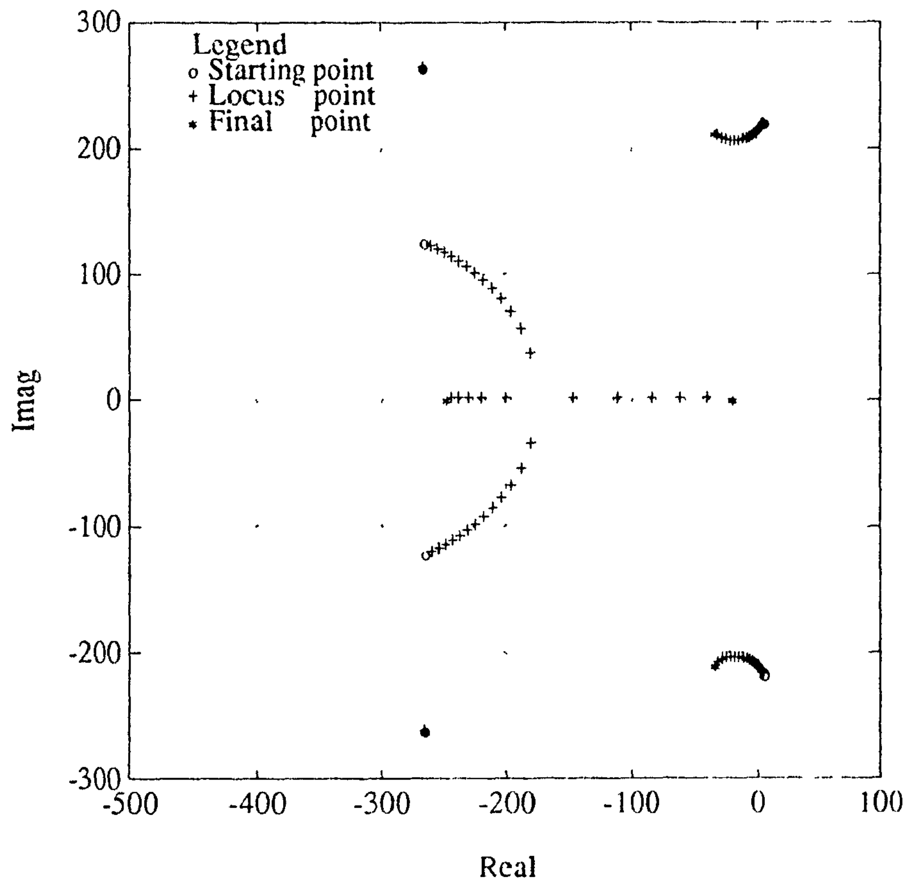

Fig 3.9. Root loci of the system eigenvalues for variable integration constant of the SVC controller

Figure 3.9 shows the root loci for variation of the controller integration constant I_v as it decreases from the value 10000 to 20 by steps of 500. The system is taken from unstable to stable region, since the critical complex pair of eigenvalues move from the right half plane to the left half plane. Another complex pair of eigenvalues transforms into two real eigenvalues, one moving to the left, the other to the right from double value position on the real axis. The complex pair of eigenvalues due to PLL remains at its original location.

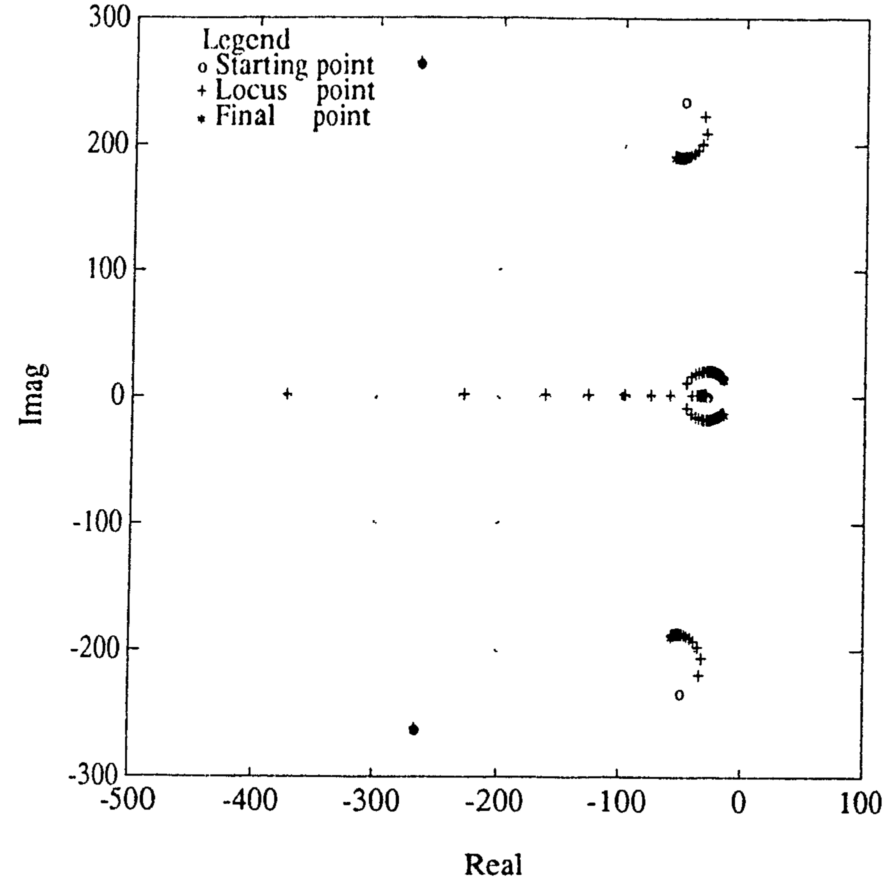

Fig 3.10. Root loci of the system eigenvalues for variable time constant

Time constant T_d due to delayed reaction of the thyristor valves does not have a great effect on the stability of the system as shown in Figure 3.10 when it was varied from 0.0005 to 0.1 seconds by steps of 0.0025, as shown in Figure 3.10. The controller parameters were chosen to provide a stable operation to the system.

3.5. STEP RESPONSE OF THE SYSTEM WITH A SINGLE SVC UNIT

Dynamic performance of an SVC system is often specified in time domain. For that reason, step responses of the systems to reference and disturbance inputs are of prime interest to system engineers. Time responses are determined by system eigenvalues, their locations and types, as well as by location and magnitudes of system disturbances.

Real eigenvalues correspond to aperiodic modes, while pairs of complex eigenvalues correspond to oscillatory modes.

Applying step disturbances, one can determine, using numerical simulation, how an SVC responds in time-domain to such disturbances.

Different step disturbances and relevant system responses have been determined and given in the following figures. The system and controller parameters are chosen to be the same as those selected in section 3.4.

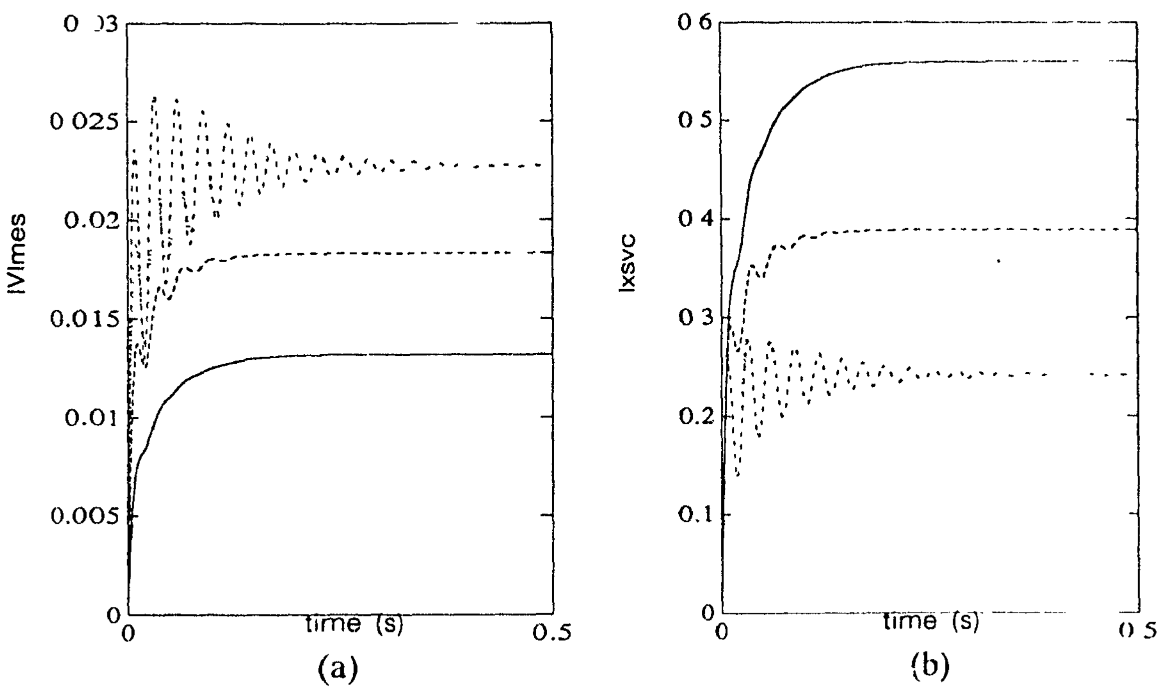

Fig 3.11. Time responses to the reference voltage step variation for various network impedance values (Z/Zs = 0.5 p.u. to 2 p.u.)
(a) voltage magnitude (b) SVC current

Figure 3.11 shows the time responses of the voltage magnitude and the SVC current to a reference step variation of $V_{ref} = 0.03$ p.u. when the impedance of the equivalent network varies from $\frac{Z}{Z_s} = 0.5\ p.u.\ \ to\ \ 2\ p.u.$, where

$Z_s = (0.942 + j47.115).10^{-3}$ p.u. . As the impedance Z_s increases (the network becomes weaker), the voltage magnitude and the SVC current change from almost aperiodic to oscillatory, revealing a significant degradation of the damping of the system.

The slope can also be verified using the following expression,

$$X_{slope} = \frac{\Delta|V|}{I_{svc_f}} \tag{3.20}$$

where I_{svc_f} and $\Delta|V|$ (see Figure 3.1), are to be taken after being settled to their steady-state values.

For example, for the case given in Figure 3.10, when the equivalent impedance of the network is $Z_s = (0.942 + j47.115)10^{-3}\ p.u.$, one obtains the following values :

$\Delta|V| = 0.0117\ p.u.$

$I_{svc_f} = 0.3890\ p.u.$

which gives $X_{slope} = 0.0301\ p.u.$ or 3.01%, equal to the value that was originally set.

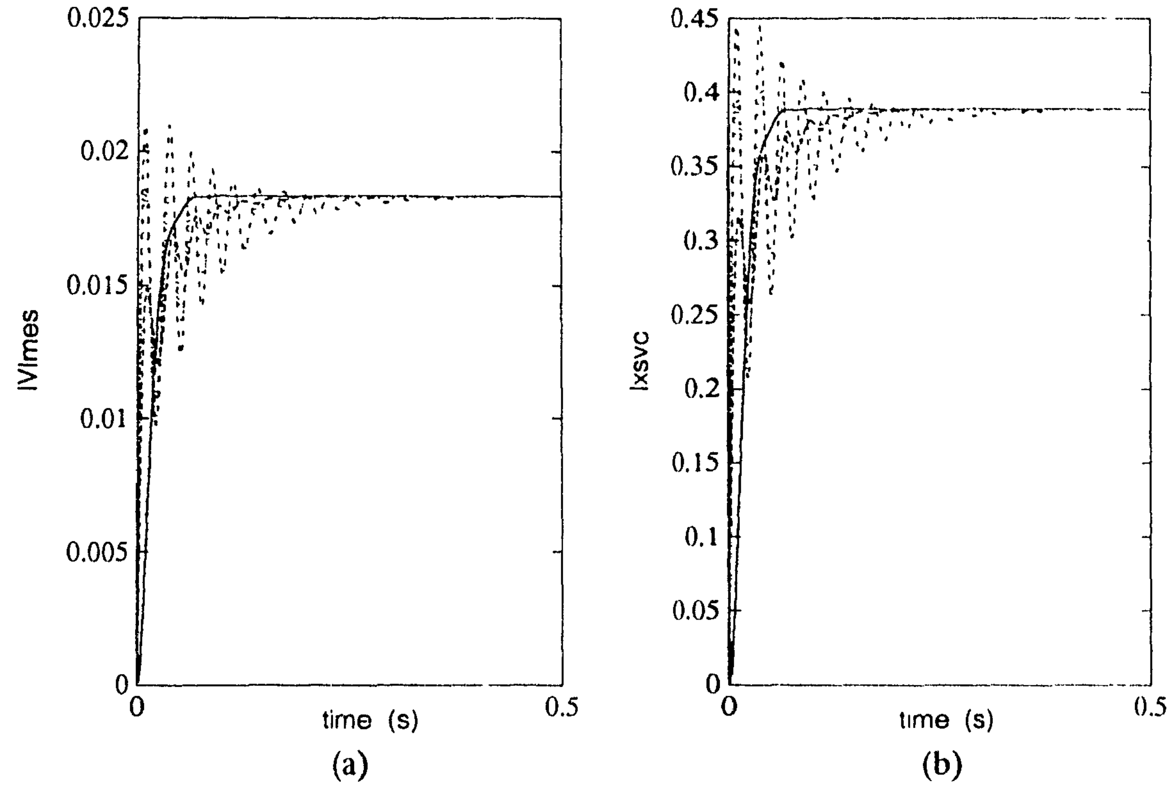

Fig 3.12. Time responses to a step variation of the reference voltage when the controller gain varies
(a) voltage magnitude (b) SVC current

Similarly, an identical step voltage variation is applied to the power system when the controller gain K_v varies, and the resulting time responses are illustrated in Figure 3.12. One can see the effect of the increase of the gain. When $K_v = 0$, both of the measured voltage magnitude and SVC current are aperiodic, but when it increases, the output responses become more oscillatory.

Once again, a similar step voltage reference is applied, but this time the integration constant I_v varies as shown in Figure 3.13.

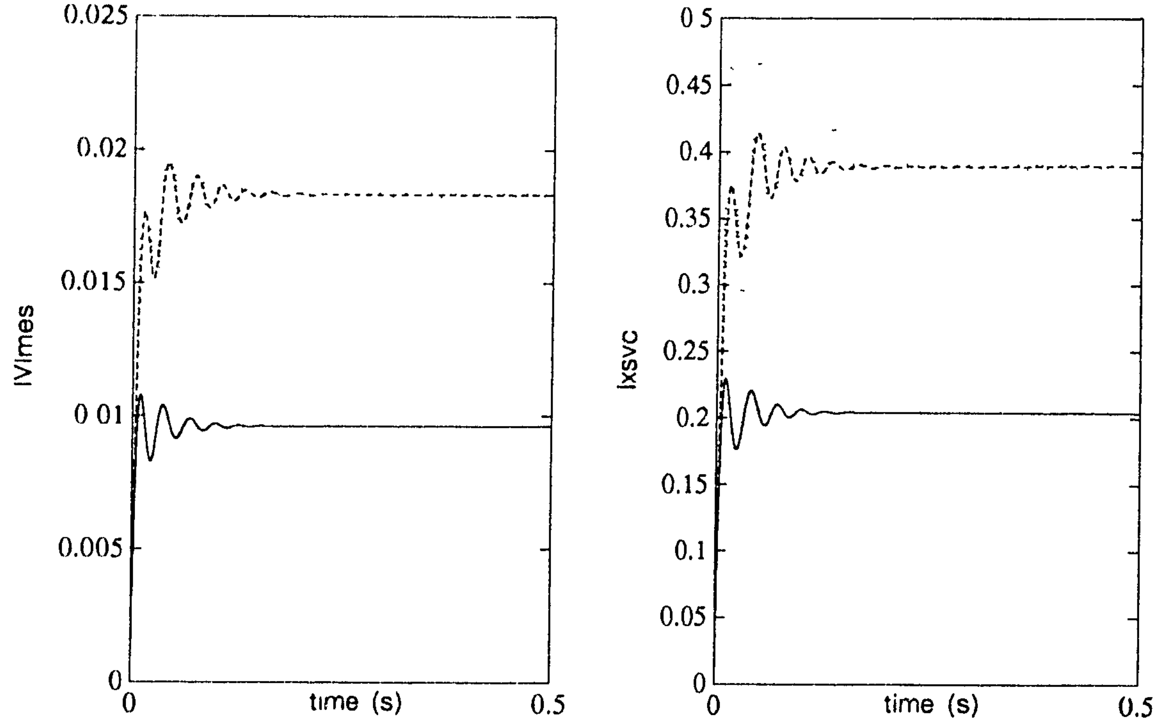

(a) (b)

Fig 3.13. Time responses to a step variation of the reference voltage when the integration constant varies
(a) voltage magnitude (b) SVC current

In a similar way, we have applied other disturbances to the system, without varying any of the parameters of the controllers or the system. The system and controller parameters are chosen to be the same as those selected in section 3.4.

Figure 3.14 and 3.15 show the step responses of the measured voltage magnitude and the SVC current to a variation of the reactive load current $I_X = 0.9\ p.u.$, and a variation of the active load current $I_R = 0.9\ p.u.$. One can see that the time responses are not well damped. For the chosen set of controller parameters, it is important to notice that the effect of the reactive load current variation is significantly greater than that of the active load current variation. The slope was also verified by input-vs-output measurements and 3% was regularly obtained.

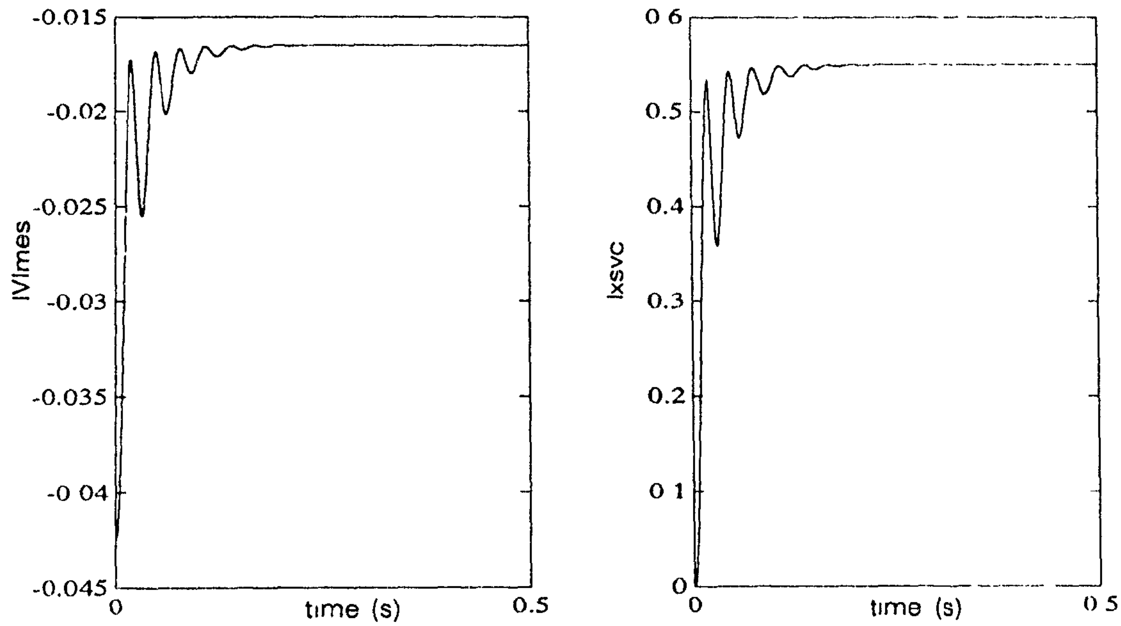

(a) (b)

Fig 3.14. Time responses to a step disturbance of reactive load current
(a) voltage magnitude (b) SVC current

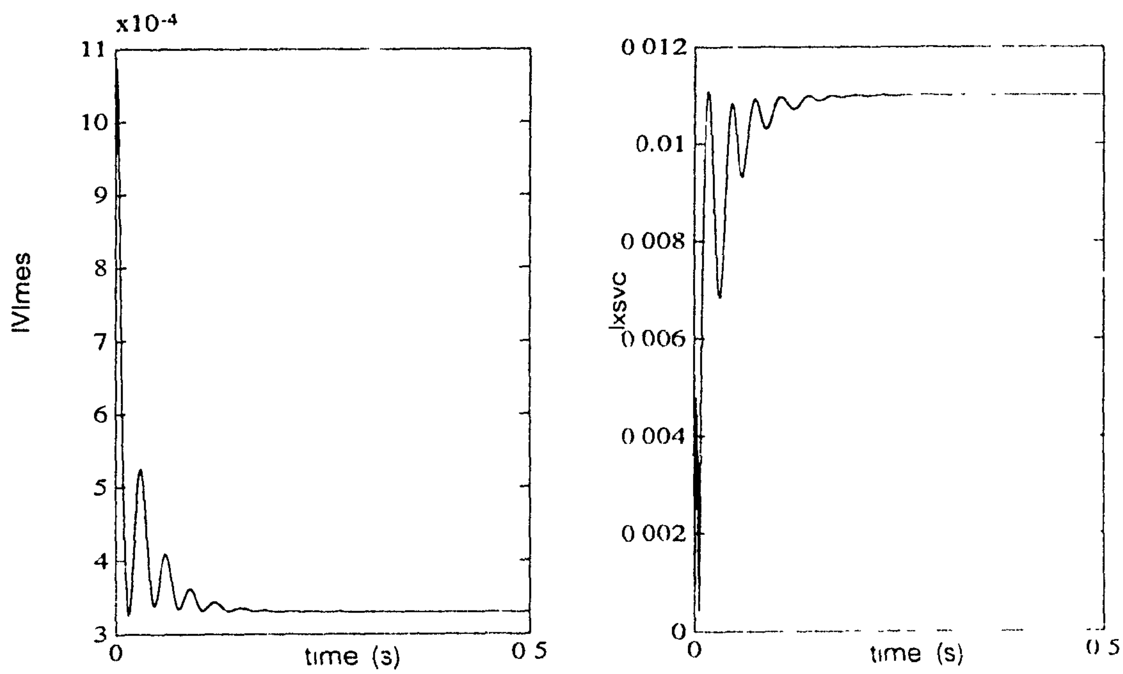

(a) (b)

Fig 3.15. Time responses to a step disturbance of active load current
(a) voltage magnitude (b) SVC current

For curiosity reasons, we have applied (Figure 3.16) a combined step disturbance of active and reactive load current $I = 0.9 + j0.9$ $p.u.$. As seen in Figures 3.14 and 3.15, the reactive load current variation has a dominant impact upon the system responses, while the impact of the active current variation was small.

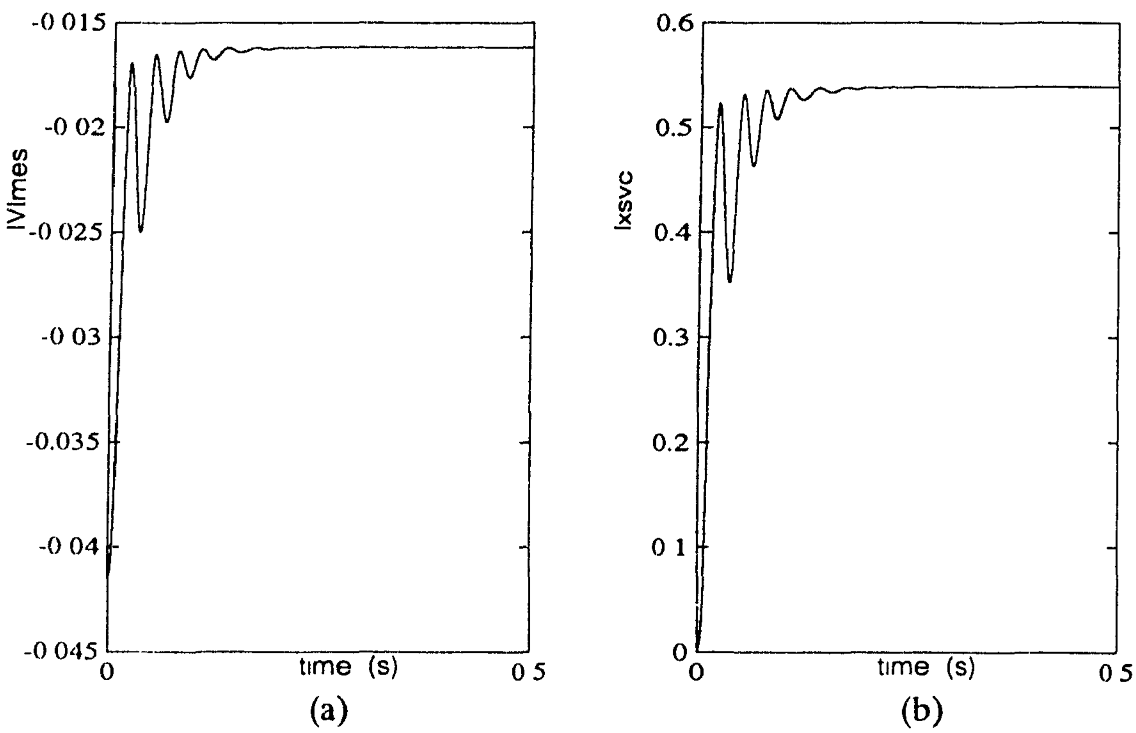

Fig 3.16. Time responses to a step disturbance of the active current combined with the reactive load current
(a) voltage magnitude (b) SVC current

Finally, a disturbance has been applied, consisting of a step variation of the reference voltage $|V|_{ref} = 0.03$ $p.u.$ and a complex load current $I = 0.9 + j0.9$ $p.u.$, illustrated by Figure 3.17. As the impact of the active current variation is small (Figure 3.15) the response obtained in Figure 3.17 is mainly due to the effect of the reference voltage and reactive current load disturbance.

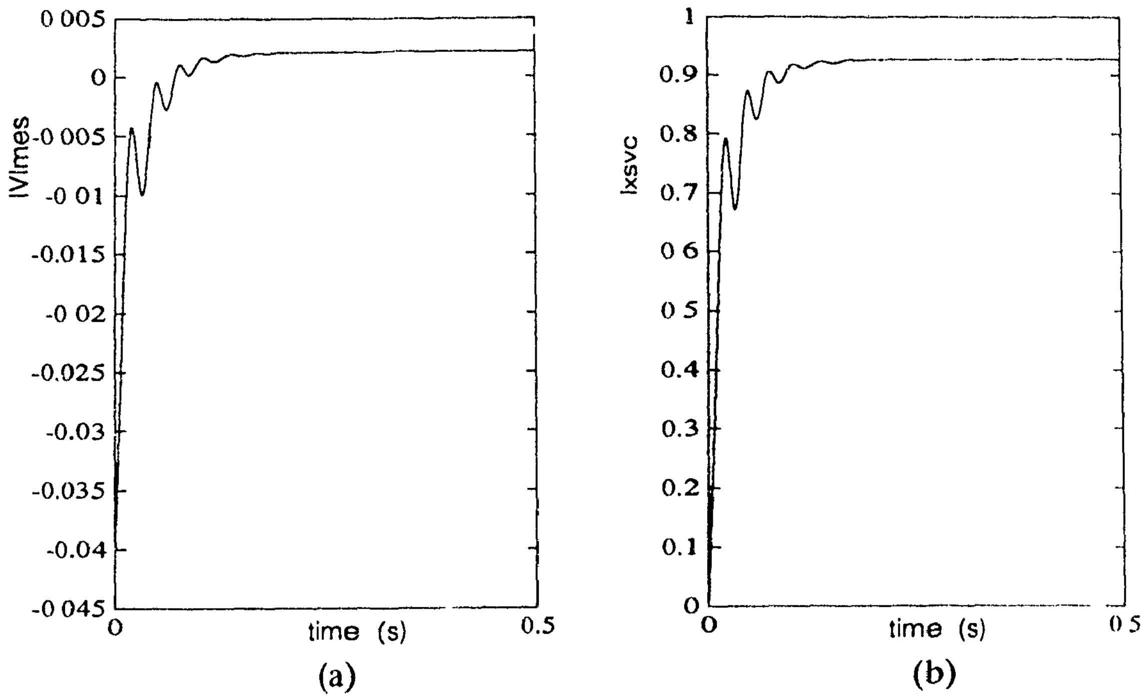

Fig 3.17. Time responses to simultaneous step changes in the voltage reference and active and reactive load current
(a) voltage magnitude (b) SVC current

CHAPTER IV

CONTROL COORDINATION OF SVCs IN PARALLEL OPERATION

4.1. INTRODUCTION

This chapter deals with coordination of several SVCs operating in parallel on the same system bus. The coordination concept of such systems, proposed in this thesis is based on equalization of the SVC outputs, accoruing to their dynamic reactive capabilities as defined by their slope reactances. In this case, the SVCs can be considered as operating in parallel on a single bus equivalent system without any loss of generality.

4.2. POWER SYSTEM WITH TWO OR MORE SVC UNITS OPERATING ON THE SAME BUS

In many SVC applications, more than one SVC unit are installed on the same bus. Many reasons can justify that, the most important being an increased reliability of multi-unit systems, especially on high voltage systems for large bulk power transmission.

In such cases, SVC units are designed to operate in parallel, independently, without any control coordination.

4.2.1. Uncoordinated SVC Units Operating on the same Bus

Let us consider two SVC units similar to the one in Figure 3.1, to be connected to the same bus as illustrated in Figure 4.1 :

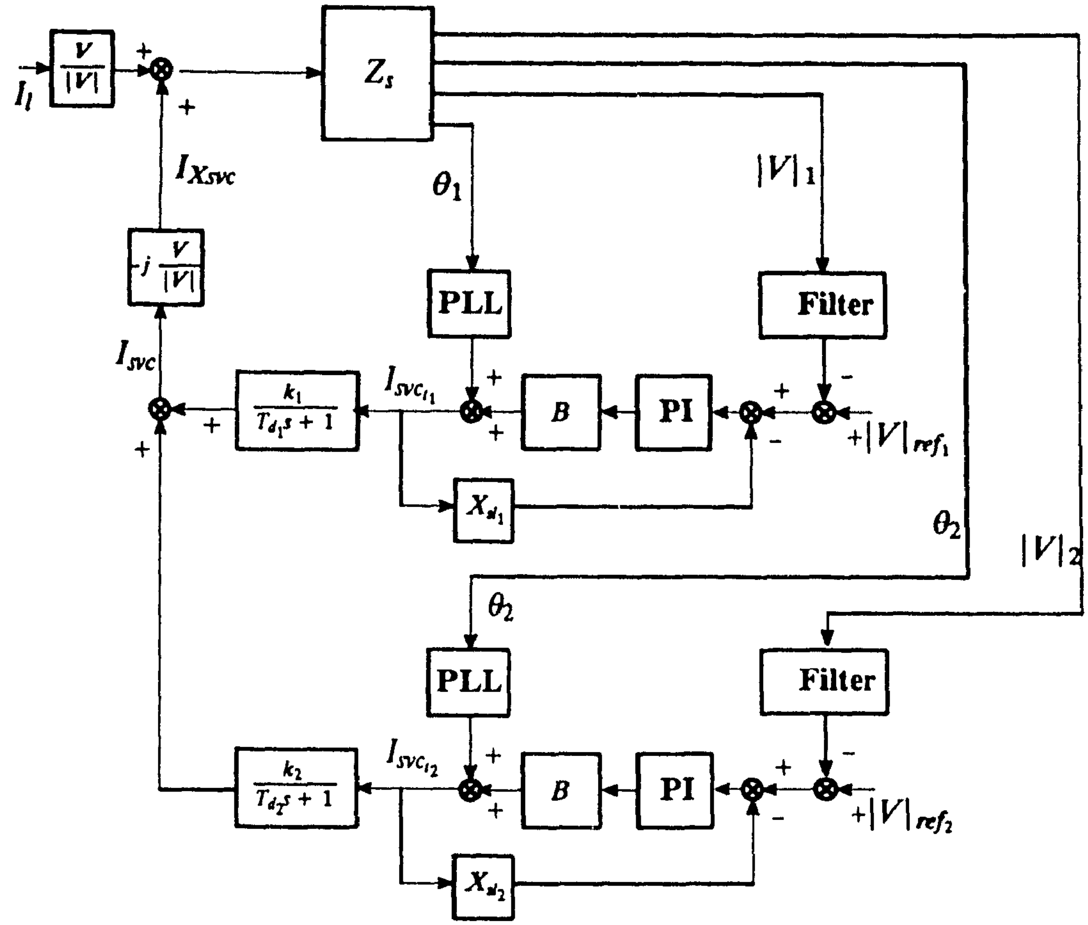

Fig 4.1. Block diagram of a power system with two uncoordinated SVC units

The two SVC units with identical controller parameters were chosen as those presented in Section 3.4, each of them rated 330 Mvars, half the rating of the single SVC unit chosen in Section 3.4. Therefore, the equivalent SVC has a rating of 660 Mvars. It is interesting, for a chosen SVC power rating, to compare the behavior of a single SVC unit with the two equivalent SVC units operating in parallel on the same bus.

For a power system with a single SVC, the eigenvalues describe the dynamic interactions between the SVC and power system, while for two or more SVCs, some eigenvalues describe SVC-power system interactions while others describe the interactions among SVCs, as illustrated in Figures 4.2 and 4.3. Figure 4.2a shows the eigenvalues of a single SVC unit, describing interactions of the SVC with the power system. Figure 4.2b illustrates the case of two identical uncoordinated SVC units, where some of the eigenvalues are located identically as those shown in Figure 4.2a, which means that the equivalent SVC which consists of the two identical units operating on the same bus exhibits identical interactions with the system as the single SVC unit of equivalent rating. Other eigenvalues shown in Figure 4.2b are associated with mutual interactions between the SVC units themselves. It should be noticed that pair of complex eigenvalues due to the phase-locked loop (PLL) is double. Figure 4.3 is similar to 4.2 and it shows the poles of Figure 4.2a and 4.2b on the same plot.

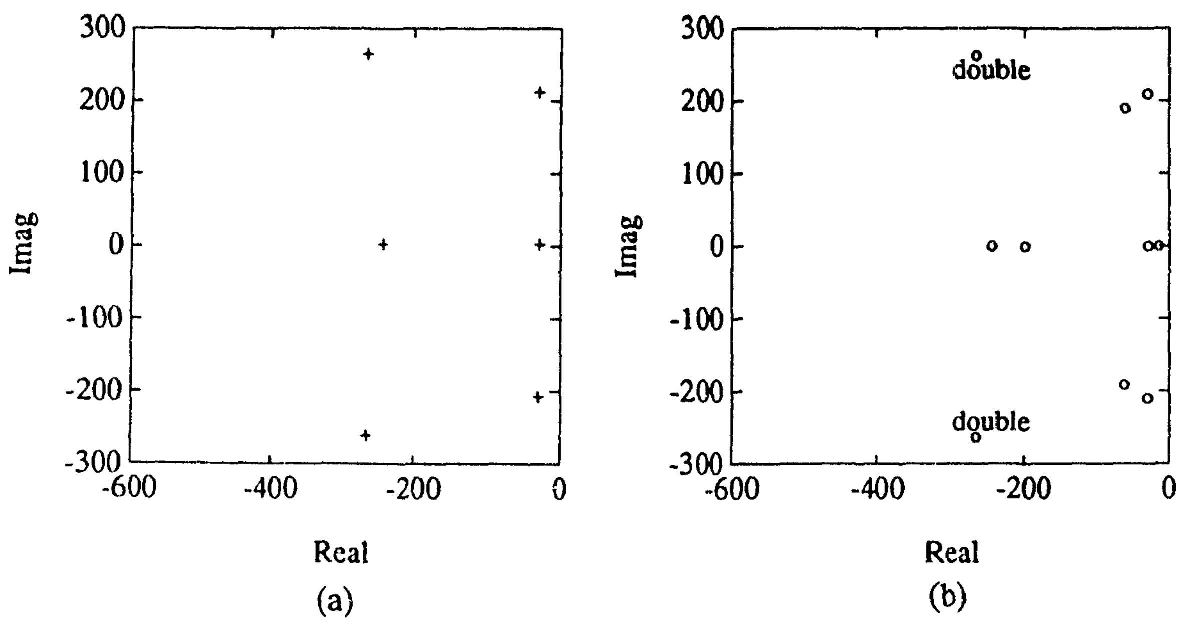

Fig 4.2. (a) Eigenvalues of a power system with a single SVC
(b) Eigenvalues of the power system with two identical uncoordinated SVC units

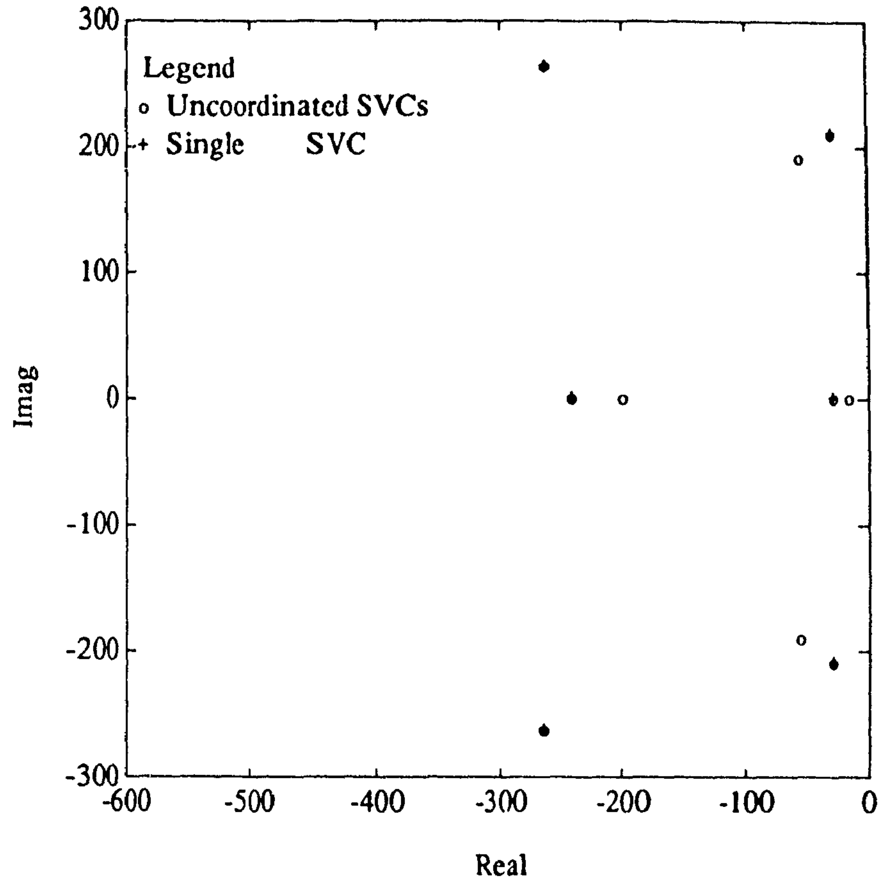

Fig 4.3. Eigenvalues of a power system with a single SVC or two identical uncoordinated SVCs

Table 4.1

Single SVC unit	Two identical uncoordinated SVC units
-29.95	-16.03
-244.89	-29.95
-30.64 ± j 209.81	-200.00
-266.52 ± j 263.14	-244.89
	-30.64 ± j 209.81
	-60.00 ± j 190.72
	-266.50 ± j 263.02
	-266.52 ± j 263.14

The calculated eigenvalues of the single SVC unit and the equivalent system consisting of two identical uncoordinated SVC units are given in Table 4.1.

The eigenvalues shown in Figure 4.2b which are not associated with interactions of the SVCs with the power system, describe the mutual interactions between the SVC units themselves. Therefore, if the parameters of the two identical uncoordinated SVC units are kept unchanged, the eigenvalues describing their mutual interactions remain unchanged when the network equivalent impedance is varied. However the eigenvalues describing the interactions of the SVCs with the network change (move). This is well illustrated by Figure 4.4, which shows that the eigenvalues due to mutual SVC interactions do not move while the network equivalent impedance varies when the network becomes too weak and when the eigenvalues cross into the right half plane (unstable region).

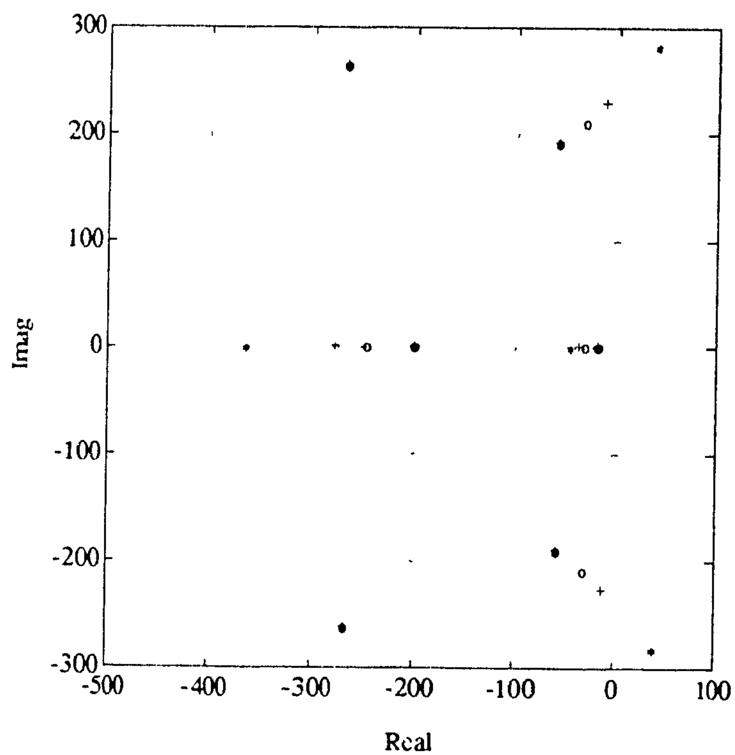

Fig 4.4. Eigenvalues system with a two identical uncoordinated SVC units for various values of the network equivalent impedance

4.2.2. Coordinated SVCs on the same Bus / Coordination Concept.

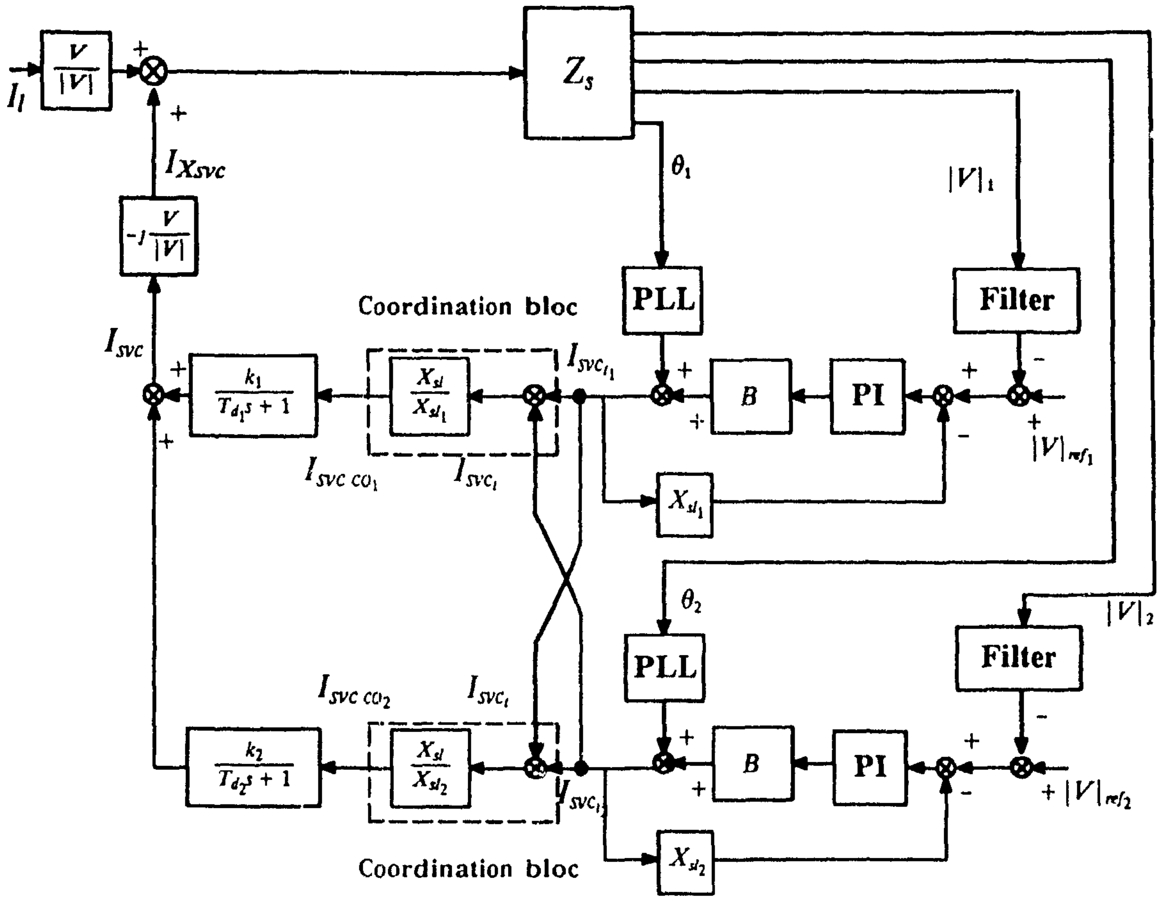

Fig 4.5. block diagram of a power system with two coordinated SVCs

The coordination of SVC units operating in parallel on the same bus is realized by coordination blocks as controller extension units. Each coordination block forms an equivalent SVC controller output I_{svc_t} which is multiplied by the factor X_{sl}/X_{sl_i} in order to form the coordinated controller output $I_{svc\,co_i}$,

$$I_{svc\,co_i} = \frac{X_{sl}}{X_{sl_i}} I_{svc_t} \tag{4.1}$$

where $I_{svc_t} = \sum_{i=1}^{n} I_{svc_{l_i}}$

and $$\frac{1}{X_{sl}} = \frac{1}{X_{sl_1}} + \frac{1}{X_{sl_2}} + \dots = \sum_{i=0}^{i=n} \left(\frac{1}{X_{sl_i}} \right)$$

The block diagram representation of the network with two SVC units with their coordinated controllers outputs is given in Figure 4.5.

The coordination or action coordination was made possible by averaging the SVC currents at the output of their controllers. The current output of each SVC controller was first summed with other SVC outputs, then multiplied by the ratio of its slope admittance and the equivalent slope admittance relevant to the SVC units all together.

The proposed coordination modifies the general structure dynamics of the SVC units operating on the same bus of the system. It has for effect to reduce the interactions among the SVC controllers and tends to transform the SVC units into one equivalent. In fact it will be shown in Figures 4.8 and 4.9 that this coordination achieves a relatively good regrouping of the eigenvalues in the s-plane, approaching the situation of a single SVC unit operating on a bus bar. It will also be shown that with this coordination the SVC current outputs behave in phase although the parameters of the SVC controllers can be totally different.

4.3. MODAL ANALYSIS OF POWER SYSTEM WITH TWO OR MORE COORDINATED SVC UNITS OPERATING ON THE SAME BUS

The series of plots below show the effects of the proposed SVC coordination with regard to the system eigenvalues location in the s-plane.

To implement the effect of this coordination, an example of two SVC units connected to a single bus is considered. In the case of identical SVCs with identical control parameters and ratings, the coordination cannot improve the system dynamics, as shown by Figures 4.6 and 4.7. Controller parameters, ratings and power system parameters are taken equal to those of the SVC unit considered in Section 3.4. From Figures 4.6 and 4.7, one can see the identical locations of the eigenvalues for the system with coordinated and uncoordinated SVC units.

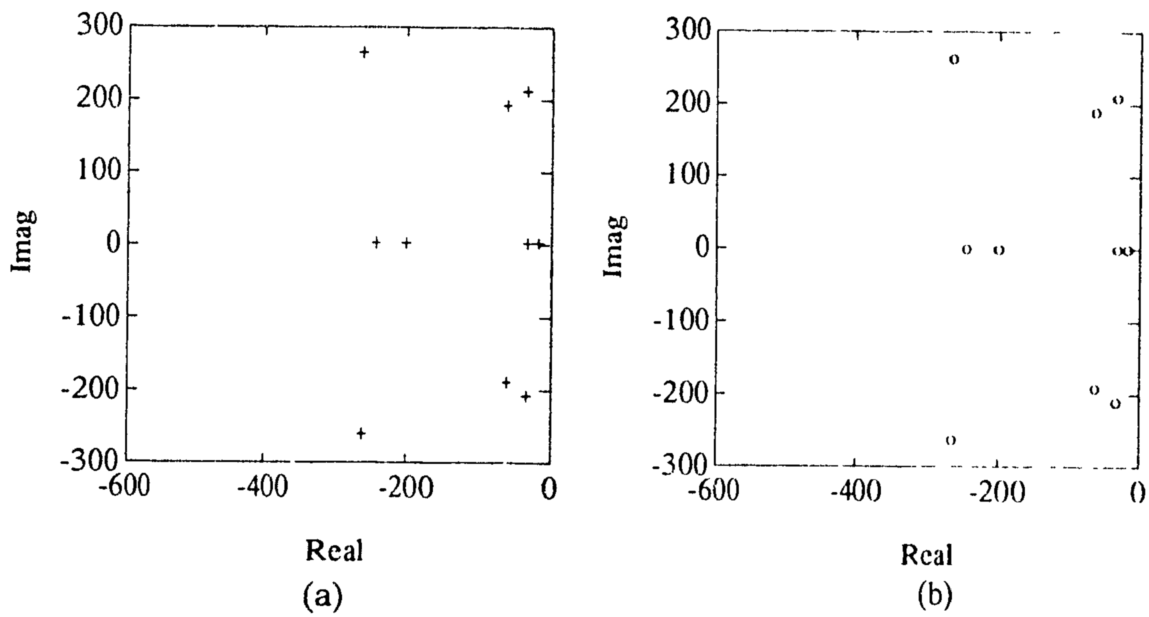

Fig 4.6. Eigenvalues of a power system with two identical SVC units
(a) SVCs with coordinated controllers
(b) SVCs with uncoordinated controllers

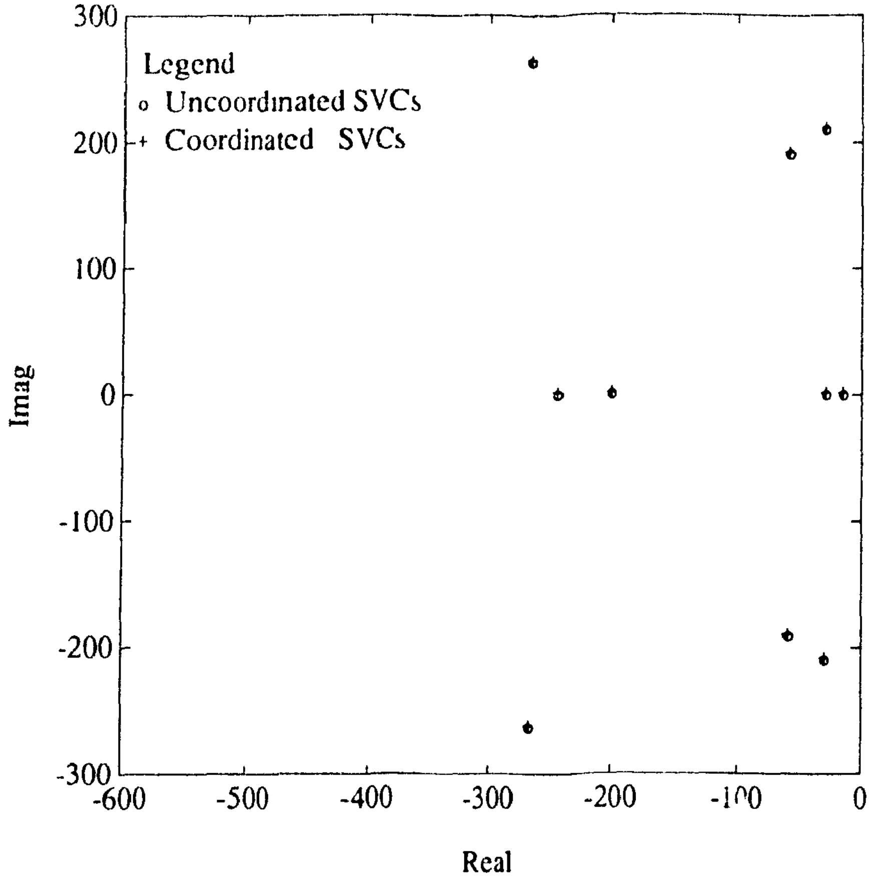

Fig 4.7. Eigenvalues of a power system with two identical SVC units with coordinated and uncoordinated controllers

Table 4.2

Coordinated SVCs	Uncoordinated SVCs
−16.03	−16.03
−29.95	−29.95
−200.00	−200.00
−244.89	−244.89
-30.64 ±j 209.81	-30.64 ± j 209.81
-60.00 ± 190.79	-60.00 ± j 190.79
-266.50 ±j 263.14	-266.50 ± j 263.14
-266.52 ±j 263.02	-266.52 ± j 263.02

Table 4.2 displays identical eigenvalues for the three coordinated and uncoordinated SVC unit systems.

The coordination effect appears when the dynamics SVC controllers are different.

Figures 4.8 and 4.9 show the case when controller parameters are set to be different from one SVC unit to the other (Parameters of the system and the SVC controllers are given in Appendix C).

Table 4.3

Coordinated SVCs	Uncoordinated SVCs
-224.16	-272.53
-999.54	-999.69
-46.45 ±j 112.02	-28.26 ± j 119.19
-78.59 ±j 109.02	-101.25 ± j 72.23
-202.43 ± 372.77	-182.15 ± j 96 18
-210.92 ±j 24.42	-202.36 ± j 372.76
-266.40 ±j 263.10	-266.50 ± j 263.08

The eigenvalues of the two different SVC units for coordinated and uncoordinated SVC unit systems are shown in Table 4.3.

Figures 4.8 and 4.9 illustrate the locations of the system eigenvalues of the coordinated and uncoordinated SVC units. One can see a relative regrouping of eigenvalues for the coordinated system. One can see also an improvement in the margin of stability considering the eigenvalues which are closer to the imaginary axis of the s-plane.

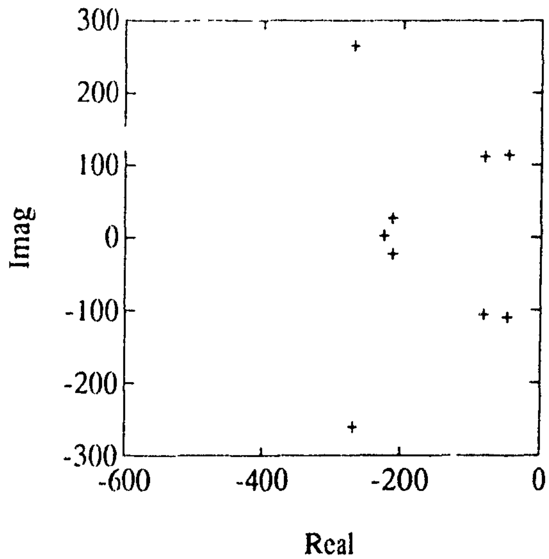

(a)

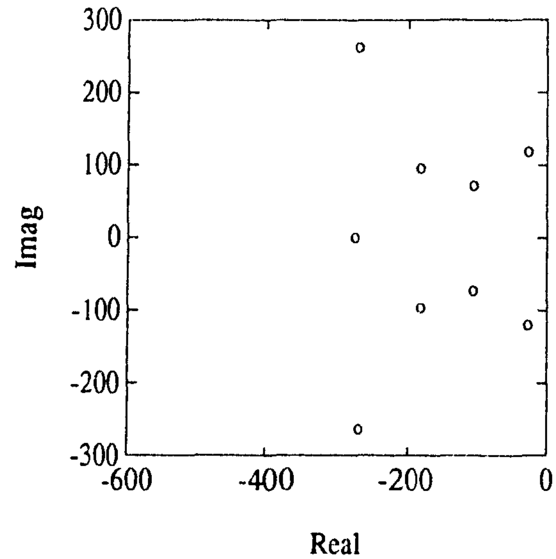

(b)

Fig 4.8. Eigenvalues of a power system with two SVC units
(a) with coordinated controllers
(b) with uncoordinated controllers

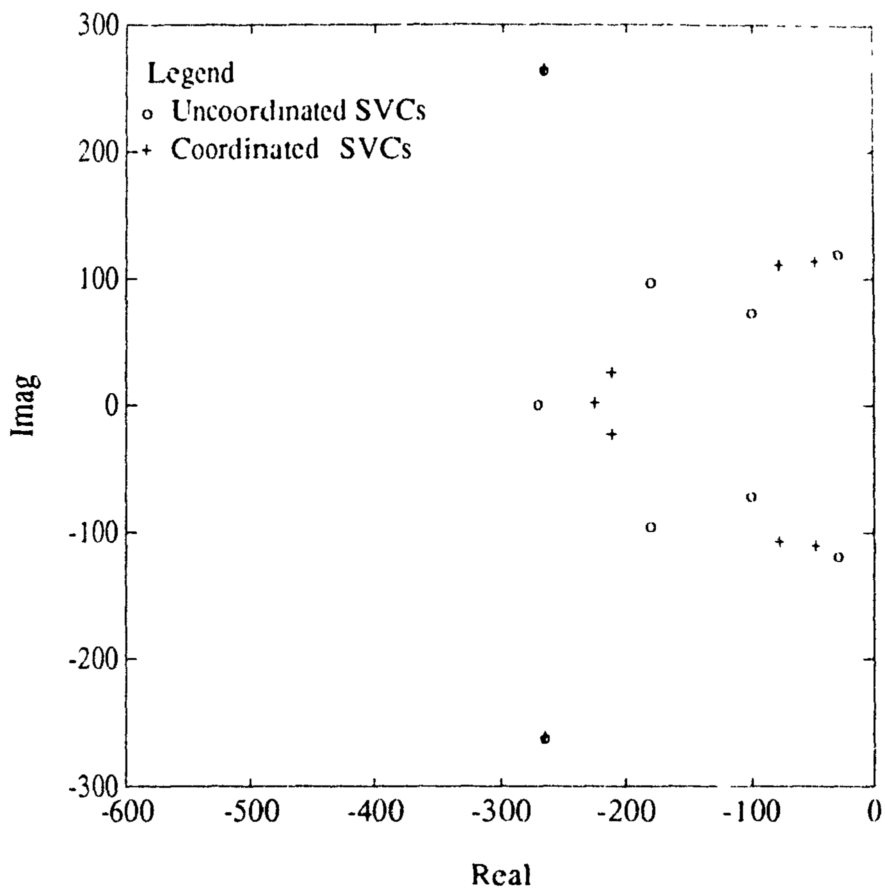

Fig 4.9. Eigenvalues of a power system with two different SVC units with coordinated and uncoordinated controllers

To prove the impact of the coordination effects, let us consider a variation of the equivalent admittance of the network. Figures 4.10 and 4.11 illustrate the movement of the eigenvalues in the s-plane when the network is weakened (one to five times the value of Z_s). One can see that for the third step of variation, the coordinated system remains in the stable region while the uncoordinated system cross to the unstable region. On another hand, the coordinated system eigenvalues of Figure 4.11 are kept relatively regrouped and therefore maintain reduced interactions among SVC units, while Figure 4.10 show through the distribution of the uncoordinated system eigenvalues a greater effect of the mutual interactions which subsist among the SVC units.

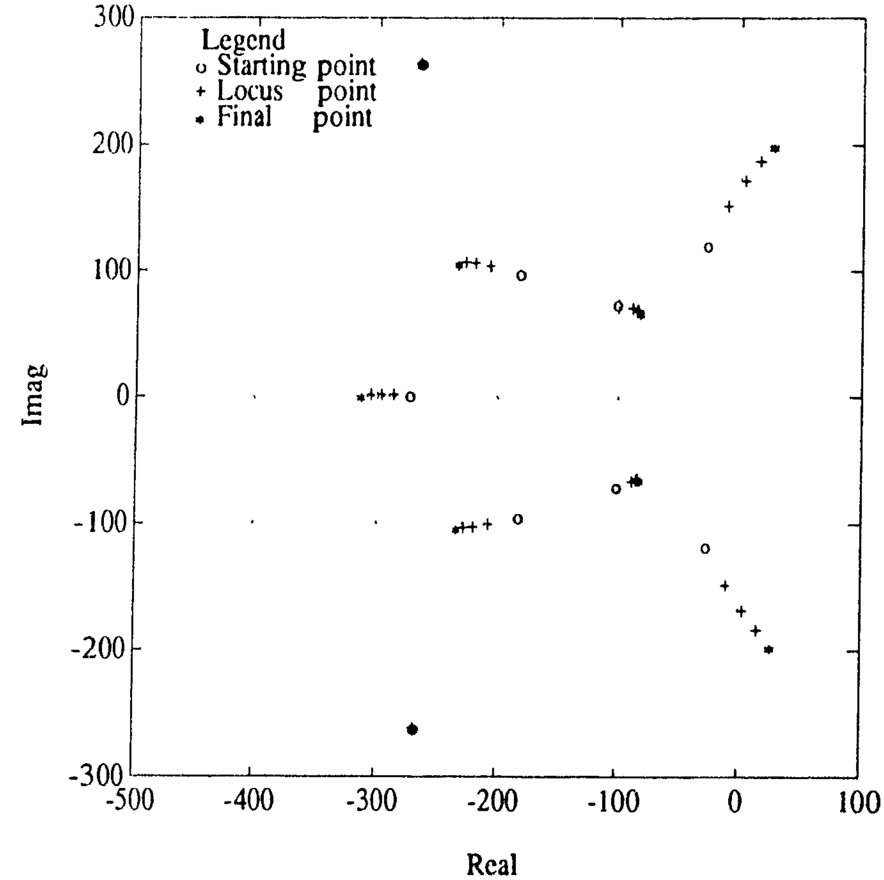

Fig 4.10. Eigenvalues system with a two different uncoordinated SVC units for various values of the network equivalent impedance

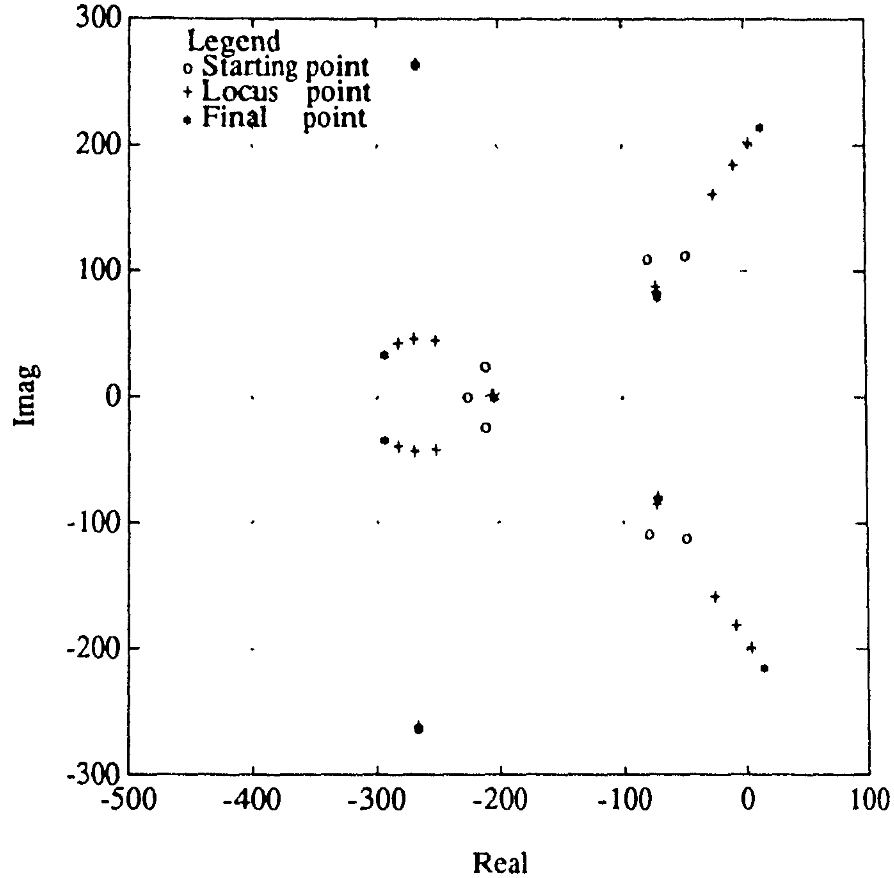

Fig 4.11. Eigenvalues system with two different coordinated SVC units for various values of the network equivalent impedance

Let us analyze some other root loci through different variations of the controller parameters. One can see from Figures 4.12 and 4.13, the illustration of the variation of the integrator constants I_{v_1} and I_{v_2}. I_{v_1} is increased from 3000 to 13000 while I_{v_2} is decreased from 10000 to 0. One can see that a pair of complex eigenvalues (relevant to the phase-locked loop) remain unchanged while others move. In the coordinated system (Figure 4.13), a pair of complex eigenvalues transform to two real eigenvalues which eliminate the oscillations of their relevant time responses, while the uncoordinated system (Figure 4.12) show the same pair of eigenvalues kept complex. For the other eigenvalues, the movements are relatively similar for both coordinated and uncoordinated systems.

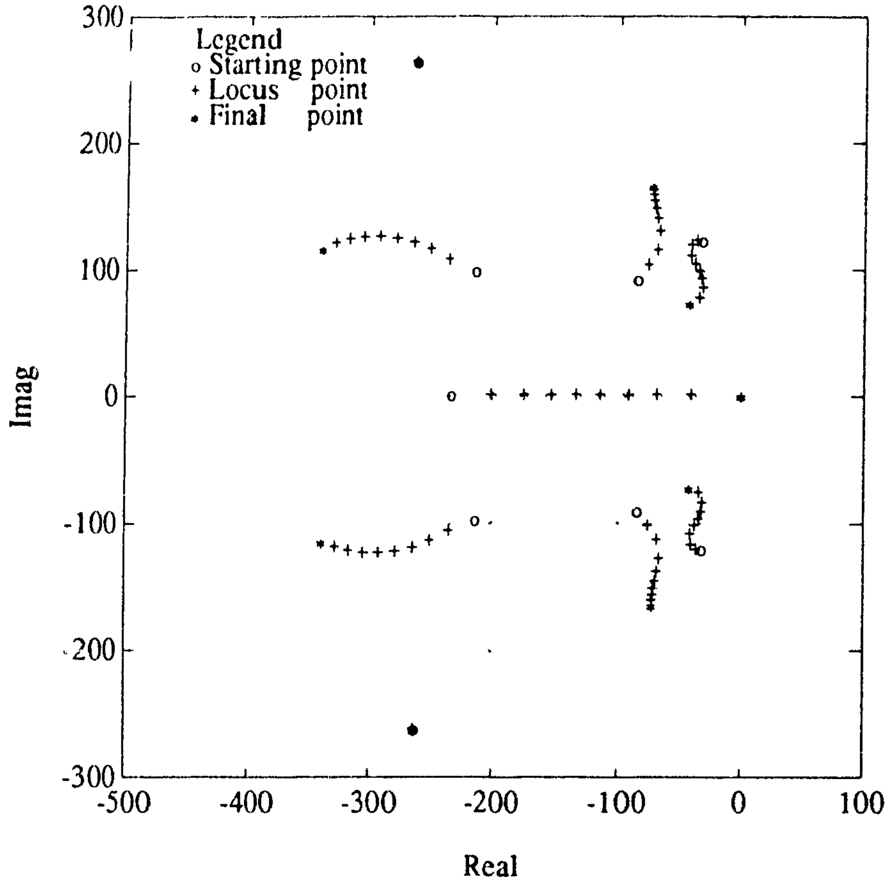

Fig 4.12. Root loci of the system eigenvalues for variable integration constants of the two uncoordinated SVC controllers

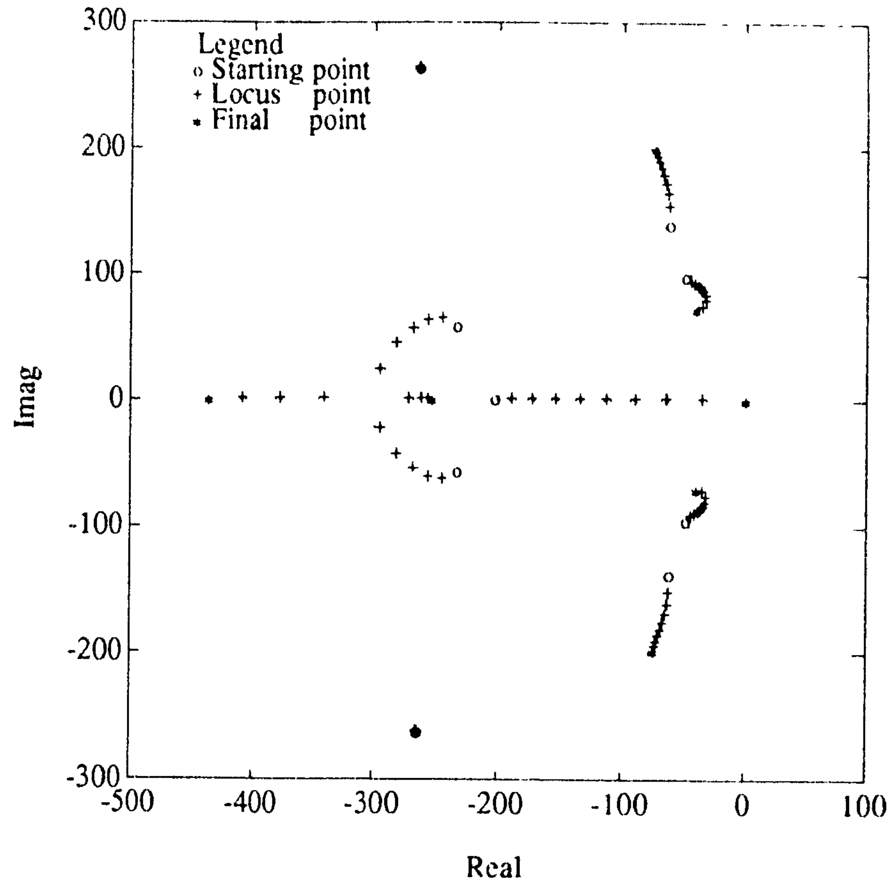

Fig 4.13. Root loci of the system eigenvalues for variable integration constants of the two coordinated SVC controllers

Let us now vary the gains of the SVC controllers. Figures 4.14 and 4.15 illustrate an increase of K_{v_1} from 2 to 7 while K_{v_2} is decreased from 5 to 0. Once again the coordinated system of Figure 4.15 shows the transformation of a pair of complex eigenvalues to two real eigenvalues, while the same eigenvalues are still complex in the uncoordinated system of Figure 4.14. Some other pairs of complex eigenvalues do not move or move very little, while the remaining eigenvalues have relatively similar shifts in both the coordinated and uncoordinated SVC unit systems.

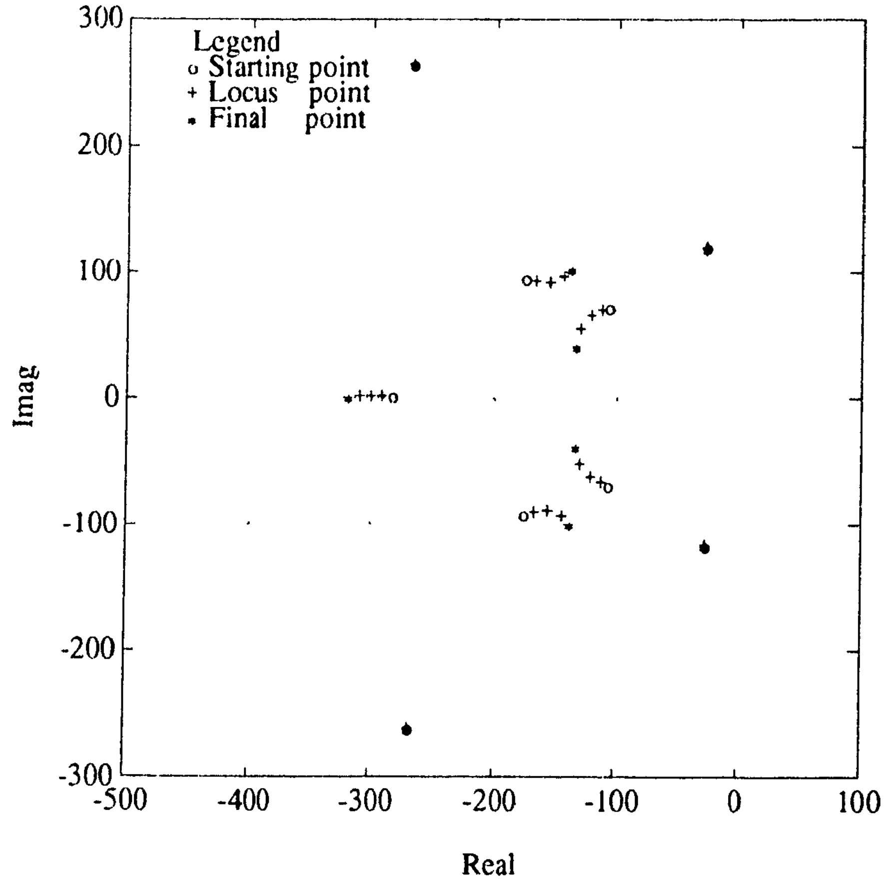

Fig 4.14. Root loci of the system eigenvalues for variable gains of the two uncoordinated SVC controllers

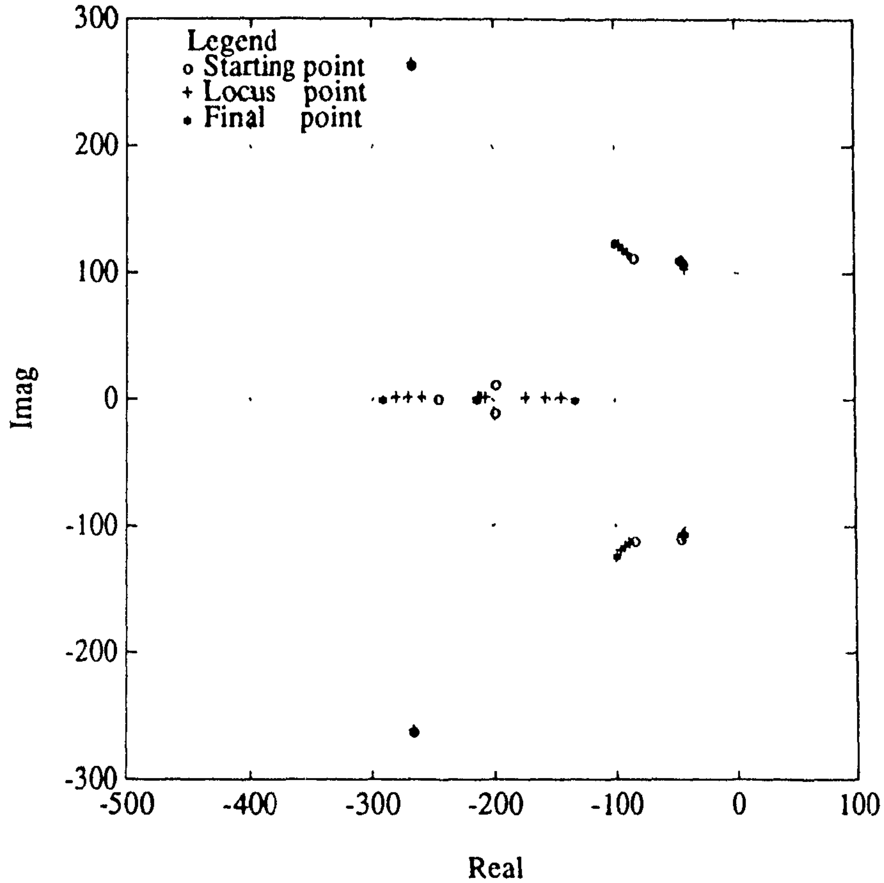

Fig 4.15. Root loci of the system eigenvalues for variable gains of the two coordinated SVC controllers

Instead of varying differently the gains K_{v_1} and K_{v_2}, let us vary their sum $K_{v_1} + K_{v_2}$ keeping their ration constant. It is assumed that the sum $K_{v_1} + K_{v_2}$ corresponds to the gain of the two SVC unit equivalent system. Figures 4.16 and 4.17 show the root loci corresponding to an increase of $K_{v_1} + K_{v_2}$ from one to ten times its original value. One can see that in both coordinated and uncoordinated systems a pair of complex eigenvalues transform into two real eigenvalues. An other pair of complex eigenvalues remain unchanged, while an other one move slightly in both of the Figures 4.16 and 4.17. The last pair of complex eigenvalues show an improvement of the margin of stability in Figure 4.17 (coordinated system) without affecting the damping, while from Figure 4.16, (uncoordinated system) the move of the same pair of complex eigenvalues improve the stability but deteriorates its damping. The real eigenvalue, in both coordinated and uncoordinated systems show similar displacement.

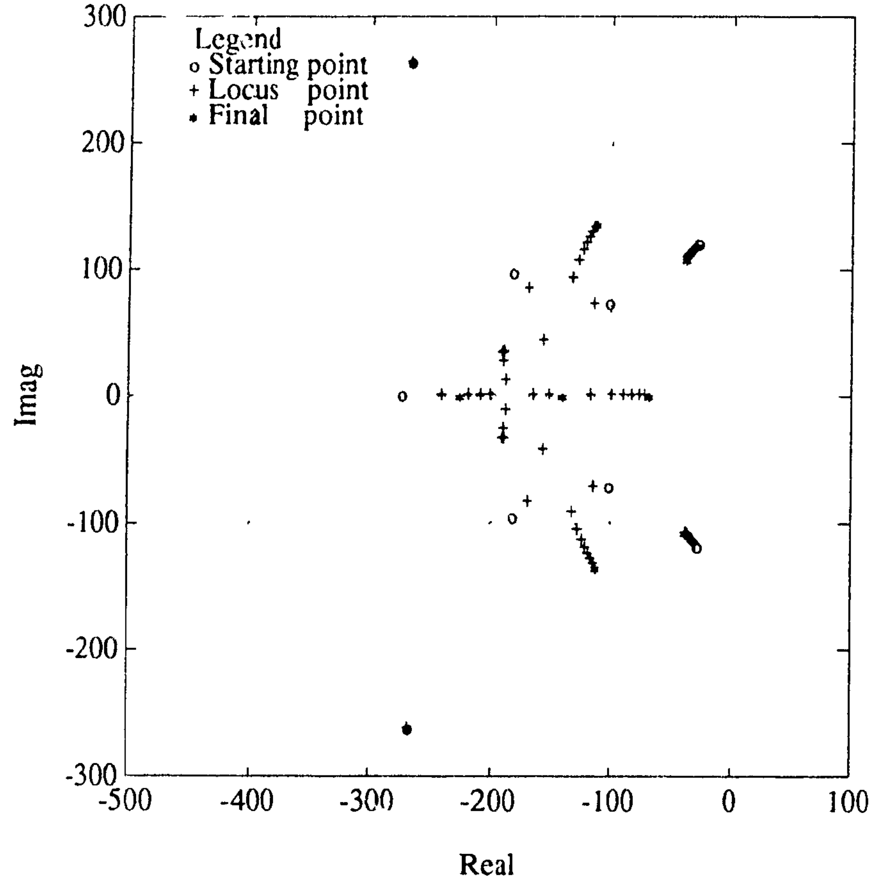

Fig 4.16. Root loci of the system eigenvalues for variable equivalent gain of the two uncoordinated SVC controllers

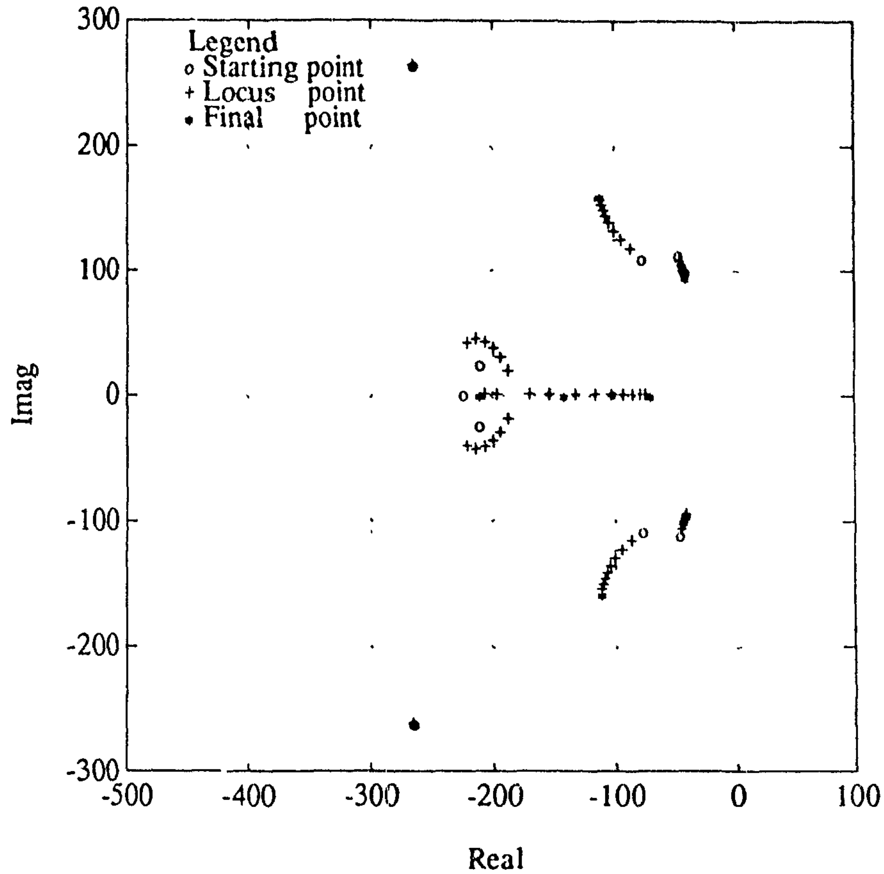

Fig 4.17. Root loci of the system eigenvalues for variable equivalent gain of the two coordinated SVC controllers

The presented illustrations demonstrate that the coordinated SVCs have an advantage over the locally controlled SVCs with regard to their stability margins. This is particularly important for system contingencies when the network becomes weak and when stability of SVCs is of prime concern.

4.4. STEP RESPONSES OF POWER SYSTEM WITH TWO OR MORE SVC UNITS ON THE SAME BUS

Applying step disturbances to the voltage reference input, the responses of various system variables in time domain are generated by MATLAB. This is illustrated by

Figures 4.18 to 4.20 for two identical SVC unit systems and by Figures 4.21 to 4.23 for two different SVC unit systems. One can observe the comparisons between the time responses for systems with coordinated SVC units and systems with uncoordinated SVC units. The SVC coordination, when they are different (frequent case in practice) improves significantly the power system stability.

Figures 4.18 to 4.19 display step responses of a power system with two identical SVC units. All parameters are identical and correspond to the parameters considered in the single SVC unit example of Section 3.4. An identical voltage reference voltage variation $|V|_{ref} = 0.03$ p.u. is applied to each of the two SVC units of the system.

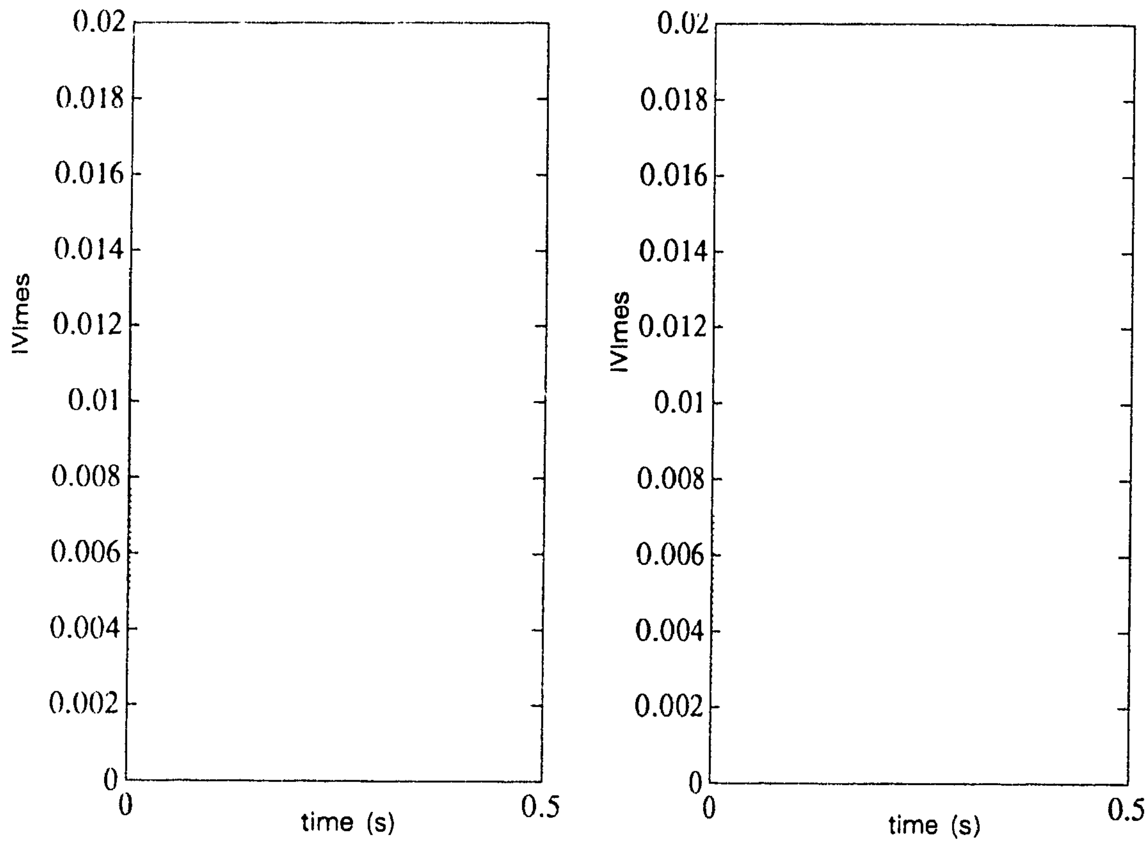

(a) (b)

Fig 4.18. Magnitude voltage response to voltage reference step variation
(a) system with two identical coordinated SVC units
(b) system with two identical uncoordinated SVC units

Figure 4.18 illustrates a step response of the magnitude voltage of the system. One can see an identical response for both coordinated (Figure 4.18a) and uncoordinated (Figure 4.18b) SVC unit systems with identical parameters.

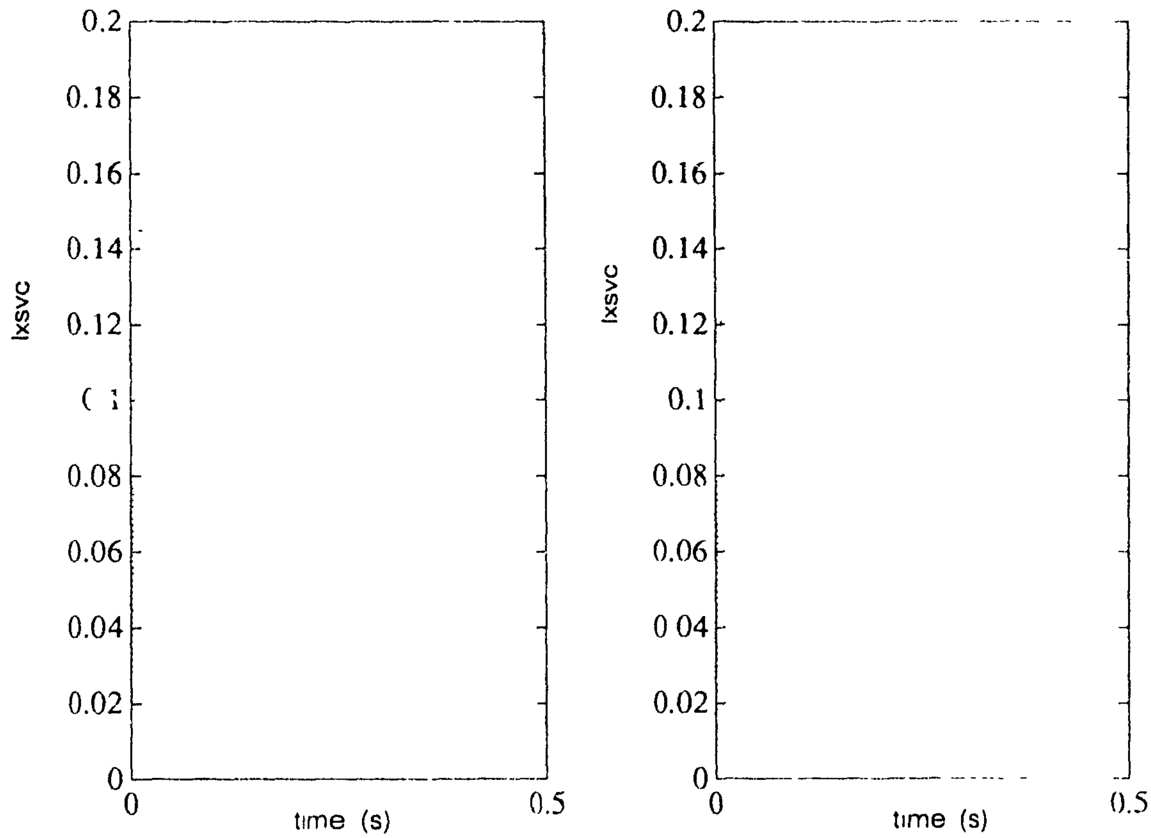

(a) (b)

Fig 4.19. SVC current responses to voltage reference step variation
(a) system with two identical coordinated SVC units
(b) system with two identical uncoordinated SVC units

Figure 4.19 shows the SVC current step responses to the same voltage reference variation $|V|_{ref} =$ 0.03 p.u. applied to all SVC units. Similarly, the response is identical for both coordinated (Figure 4.18a) and uncoordinated (Figure 4.18b) SVC unit systems. Moreover, the curves seen on Figure 4.19a and 4.19b represent only the current output of one SVC unit. Within one system, the two current SVC outputs are identical.

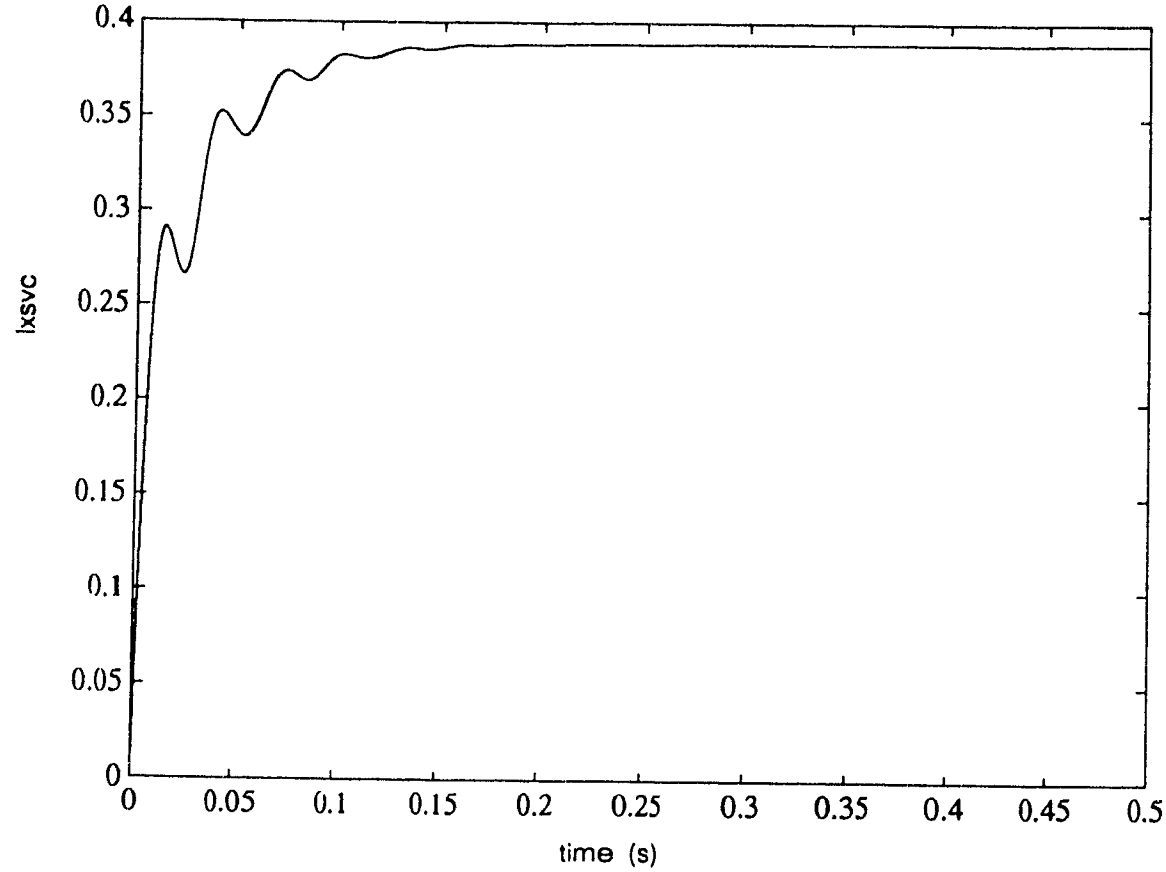

Fig 4.20. Total SVC current responses to voltage reference step variation of the system with two identical coordinated or uncoordinated SVC units
________ Coordinated system
.... Uncoordinated system

Figure 4.20 illustrates the total SVC current response of the system. One cannot distinguish on this figure the coordinated from the uncoordinated response. For identical SVCs with identical parameters, the responses show no difference, as for responses of Figures 4.18 and 4.20. Figure 4.20 show the total SVC current, which is the sum of all SVC currents.In addition, it has been verified for each SVC unit, that the relation (3.21) gives the same value (3%) for X_{slope} than what was originally set.

The next figures consider the same example of power system with different parameters of the SVC units (Parameters of all two SVC units are given in

Appendix C). The disturbance considered is also a step voltage reference variation $|V|_{ref} = 0.03$ p.u. applied to each of the two SVC units of the system.

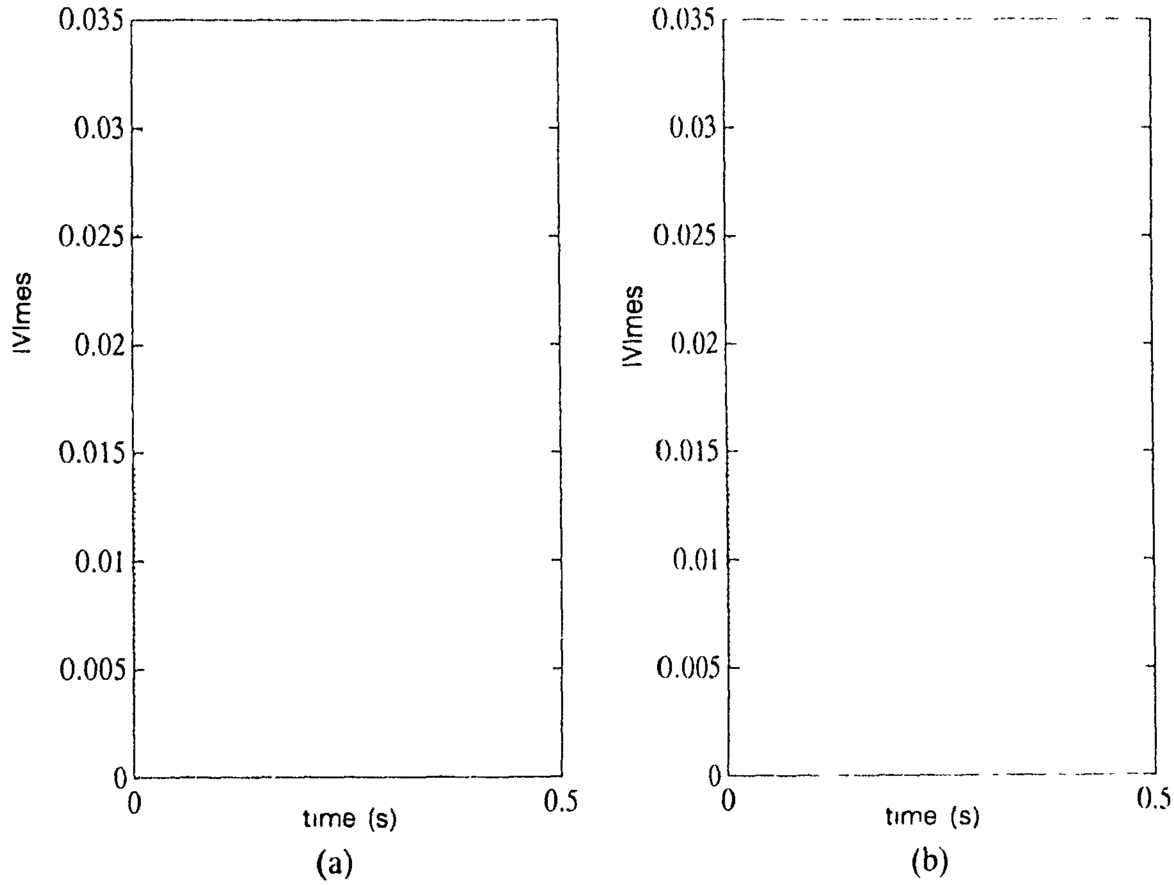

Fig 4.21. Magnitude voltage response to voltage reference variation
(a) system with two different coordinated SVC units
(b) system with two different uncoordinated SVC units

Figure 4.21 shows the magnitude voltage step responses. One can see the effect of the coordination by comparing with the response waveforms of Figure 4.21a and Figure 4.21b. The coordinated response present a better damping waveform with a reduced maximum percentage overshoot over the steady-state response.

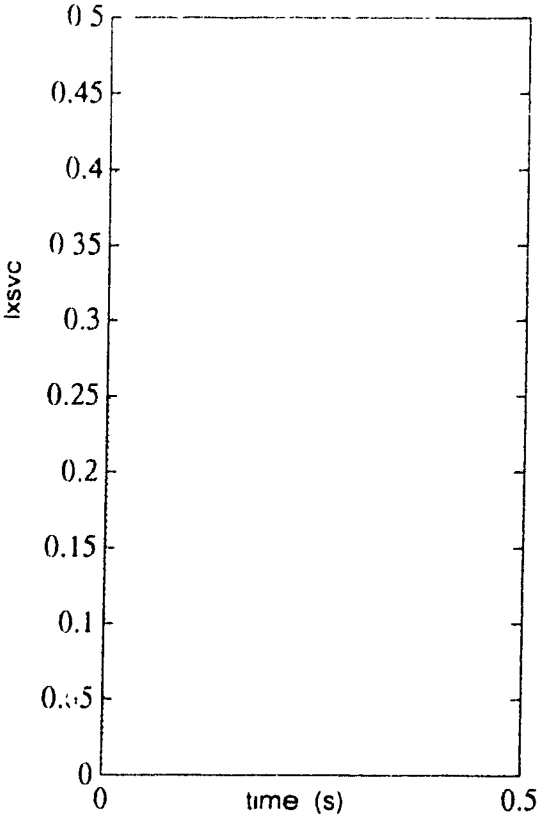

(a)

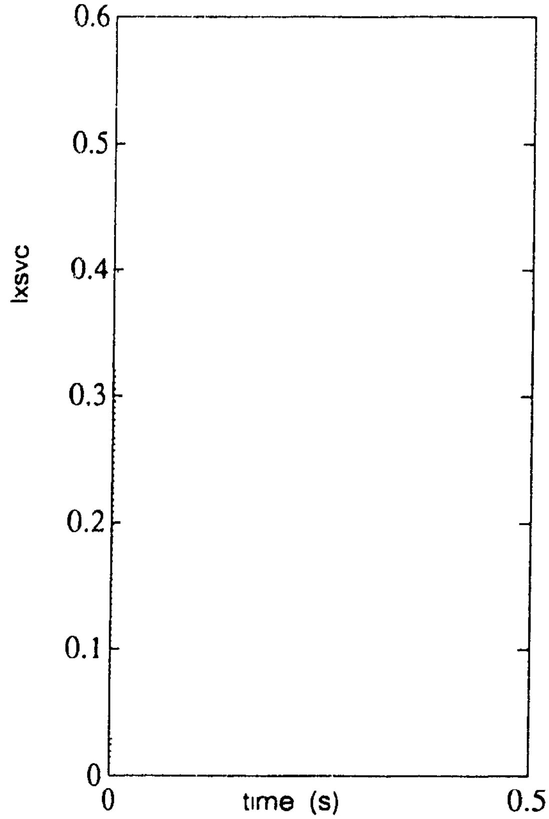

(b)

Fig 4.22. SVC current responses to voltage reference step variation
(a) system with two different coordinated SVC units
(b) system with two different uncoordinated SVC units

Figures 4.22a and 4.22b illustrate the SVC current output of each unit for relevant coordinated and uncoordinated systems. As noticed, the coordinated responses give a better damped waveforms, and the coordination action of the controllers dynamics is a real improvement for coordinated SVCs as their reactions are synchronized. One can also see that the corresponding SVC currents have the same steady-state value for both coordinated and uncoordinated systems.

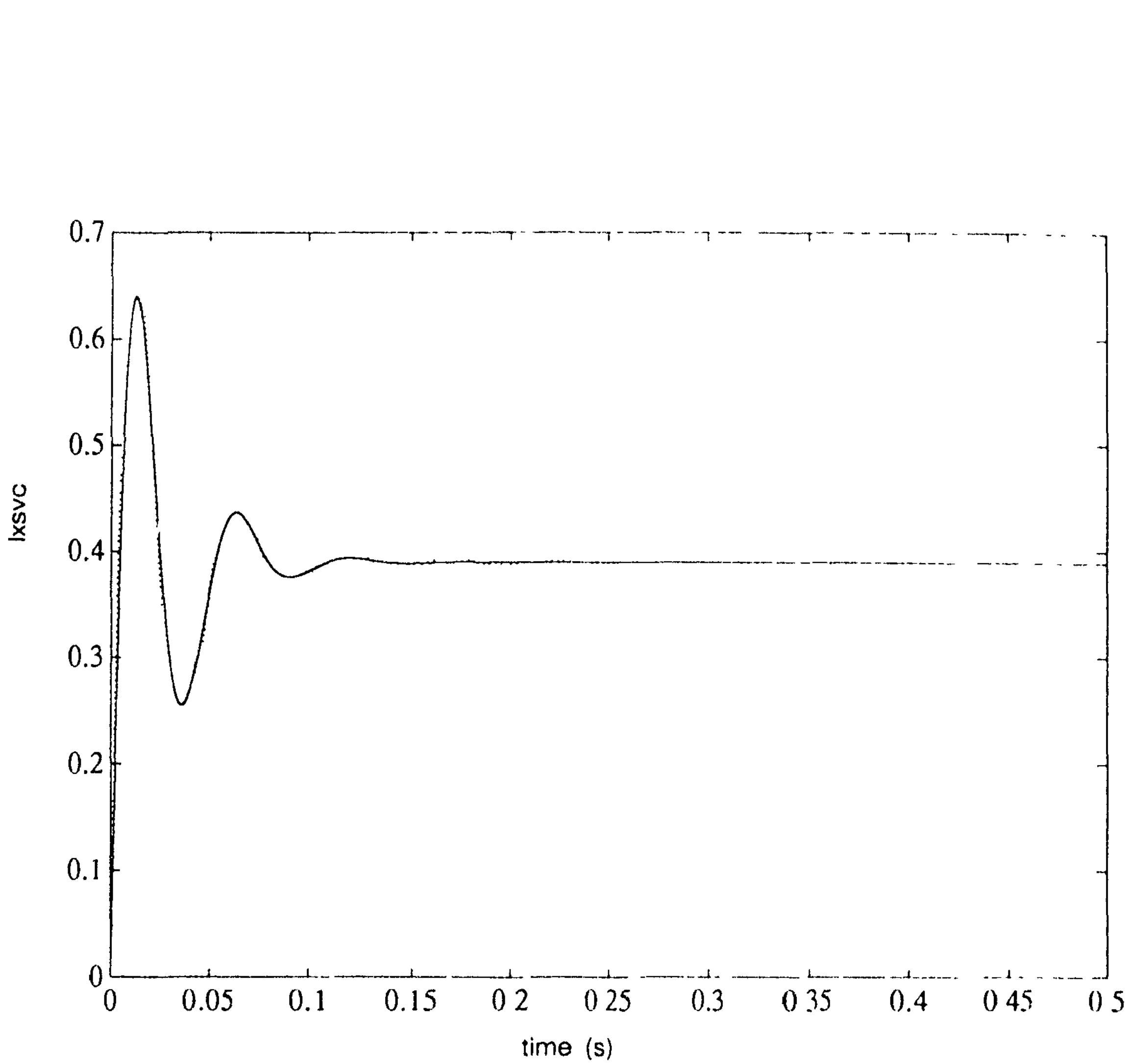

Fig 4.23. Total SVC current responses to voltage reference step variation of the system with two different coordinated or uncoordinated SVC units
________ Coordinated system
. . .. Uncoordinated system

Finally, Figure 4.23 shows the total SVC current responses for coordinated and uncoordinated systems. the percentage overshoot is seen to be reduced with coordination and the damping has been improve . Once again, one can also see that the steady-state value is identical for both cases. In addition, it has also been verified that the relation (3.21) gives the same value (3%) for X_{slope} than what was originally set.

The coordination has not changed the steady-state value of the time responses. It shows clearly the structural modification of the SVC controllers dynamics by synchronizing their reaction and improving the damping of the oscillations.

CHAPTER V

CONTROL COORDINATION OF SVCs CONNECTED TO VARIOUS BUSES WITHIN THE POWER SYSTEM

5.1. INTRODUCTION

SVCs are required to support the system voltage at various locations within the transmission system in order to stabilize the voltage and its power transfer capability and to increase its transient stability margin. The fast acting SVCs provide fast responses to system voltage disturbances. However, their speed is limited by stability constraints relevant to interactions among SVCs as well as SVCs interactions with the system.

Some studies were addressed to these issues in order to enable parameter optimization of the SVC controllers as well as to enable an identification of other problems related to addition of series compensation, or interactions between SVCs and the HVDC systems.

5.2. VOLTAGE REGULATION AS A MULTI-INPUT/MULTI-OUTPUT CONTROL PROBLEM

5.2.1. Problem Statement and Linearization

Assuming that all the linear components of the network are represented by constant impedances and by voltage or current sources, if the voltage sources are represented by their current equivalents, the voltages on the system buses are described by the Norton equation,

$$YV = I_G - I_{SVC} - I_L \tag{5.1}$$

where	Y	is the system admittance, (matrix),
	V	is the bus voltage, (vector),
	I_G, I_{SVC}, I_L	are the respective generator, SVC and load current, (vectors).

If the voltage is expressed in terms of its orientation and magnitude vectors, the following equation is obtained,

$$Yv|V| = v[(I_{Rg} - I_{Rl}) + j(I_{Xg} - I_{Xsvc} - I_{Xl})] \tag{5.2}$$

where	$v = e^{j\Theta}$	is the voltage orientation, (diagonal matrix), being the voltage phase (diagonal matrix),
	$\|V\|$	is the voltage magnitude, (vector),
	I_{Rg}, I_{Xg}	is the active and reactive generator current, (vectors)
	I_{Rl}, I_{Xl}	is the active and reactive load current, (vectors)
	I_{Xsvc}	is the SVC current, (vector) with all currents referred to the bus voltage.

When equation (2) is resolved, the following two equations are obtained for the voltage magnitude and orientation as functions of the load and SVC current,

$$|V| = \mathrm{Re}(v^*Y^{-1}v)(I_{Rg} - I_{Rl}) - \mathrm{Im}(v^*Y^{-1}v)(I_{Xg} - I_{Xsvc} - I_{Xl}) \tag{5.3}$$

$$0 = \mathrm{Im}(v^*Y^{-1}v)(I_{Rg} - I_{Rl}) + \mathrm{Re}(v^*Y^{-1}v)(I_{Xg} - I_{Xsvc} - I_{Xl}) \tag{5.4}$$

If equation (5.2) is linearized in terms of the voltage magnitude and phase variations as well as the variations of the SVC and load current around the steady-state operating point, the following equation is obtained,

$$\mathbf{Y}\mathbf{v}_0\ (|V| + j|\mathbf{V}_0|\theta) = -\ \mathbf{v}_0[I_{Rl} + j(I_{Xsvc} + I_{Xl})] \tag{5.5}$$

where $|V|$ is the voltage magnitude variation, (vector),

$|\mathbf{V}_0|$ is the voltage magnitude at the steady-state operating point, (diagonal matrix), and

θ is the voltage phase variation, (vector)

I_{Rl}, I_{Xl} is the active and reactive load current variation, (vectors), and

I_{Xsvc} is the SVC current variation, (vector).

Linearized form of expressions (5.3) and (5.4) are obtained by solving equation (5.5) for $|V|$ and θ,

$$|V| = -\ \mathrm{Re}(\mathbf{v}_0^*\mathbf{Y}^{-1}\mathbf{v}_0)I_{Rl} + \mathrm{Im}(\mathbf{v}_0^*\mathbf{Y}^{-1}\mathbf{v}_0)(I_{Xl} + I_{Xsvc}) \tag{5.6}$$

$$\theta = -\ |\mathbf{V}_0|^{-1}[\mathrm{Im}(\mathbf{v}_0^*\mathbf{Y}^{-1}\mathbf{v}_0)I_{Rl} + \mathrm{Re}(\mathbf{v}_0^*\mathbf{Y}^{-1}\mathbf{v}_0)(I_{Xl} + I_{Xsvc})] \tag{5.7}$$

The voltage regulation problem of the linearized system described by equations (5.6) and (5.7) is stated as follows:

Control the SVC current variation so as to maintain the voltage magnitude variation as close to the reference voltage variation as the SVC slope reactance permits, as defined by equation (5.8), in order to reduce the effects of load variation,

$$\Delta|V| = |V|_{ref} - |V| = \mathbf{X}_{sl}\ I_{Xsvc} \tag{5.8}$$

where $\Delta|V|$ is the voltage magnitude error variation, (vector),

$|V|_{ref}$ is the reference voltage magnitude variation, (vector), and

$\mathbf{X_{sl}}$ is the SVC slope reactance, (diagonal matrix).

5.2.2. Controller Optimal Adjustment

Optimization of the controller adjustment is based on a performance index defined in terms of the output vector which gives the measure of the system behavior in the time domain for a specified disturbance.

The most commonly used performance index is given by the following expression :

$$\mathbf{J} = \frac{1}{2}\int_{t_0}^{T} (\mathbf{y}'\ \mathbf{Q}\ \mathbf{y})\ dt \tag{5.9}$$

where $\mathbf{Q}$ is a positive semidefinite symmetric matrix,

(the factor $1/2$ in the integrand is sometimes omitted. Its presence merely indicates an averaging of the integrand).

An optimal controller performance is achieved when the controller parameters are chosen so as to minimize the specified performance index, as defined by the following expression,

$$min \int_{0}^{\infty} \Delta|V|_{tr}'\, q_v\, \Delta|V|_{tr}\, dt \tag{5.10}$$

where $\Delta|V|_{tr} = \Delta|V| - \Delta|V|_{t\to\infty}$ is the transient voltage magnitude error variation, (vector),

q_v are the weighting factors (diagonal matrix).

Another performance index which includes input vector in addition, is also applied frequently. This performance index is defined by the following expression,

$$min \int_0^{\infty} (\Delta|V|_{tr}' \, q_v \, \Delta|V|_{tr} + \Delta I_{Xsvc}' \, r_i \, \Delta I_{Xsvc}) \, dt \tag{5.11}$$

where $\Delta|V|_{tr} = \Delta|V| - \Delta|V|_{t\to\infty}$ is the transient voltage magnitude error variation, (vector),

$\Delta I_{Xsvc} = I_{Xsvc} - I_{Xsvc\, t\to\infty}$ is the transient SVC current variation, (vector),

q_v and r_i are the weighting factors (diagonal matrices).

The voltage regulation in power systems is obviously a multi-input/multi-output control problem.

5.3. SVC COORDINATED CONTROL

Analysis of expressions (5.6) and (5.7) reveals that the voltage magnitude is mostly affected by the reactive load and SVC currents, while the voltage phase is mostly affected by the active load current, due to negligible transmission losses. It is important to notice that a control action of an SVC current by its reactive current affects the voltages on all other buses. This is why the locally controlled SVC systems mutually interact.

5.3.1. Control Coordination Concept

In order to eliminate mutual interference, the control concept presented in this thesis assumes a coordination of SVC currents in order to decouple voltage control actions, as the first design step. The derivation of the control coordination expression is based on expressions (5.6) and (5.8). The voltage magnitude variation caused by the SVC current according to expression (5.6), is given by,

$$|V| = \mathrm{Im}(\mathbf{v}_o^* \, \mathbf{Z} \, \mathbf{v}_o) \, I_{Xsvc} \tag{5.12}$$

where $\mathbf{Z} = \mathbf{Y}^{-1}$

In order to produce this voltage magnitude variation, taking into account the voltage drop across the slope reactance, the following voltage demand has to be made,

$$|V|_{dem} = |V| + X_{sl}\, I_c \tag{5.13}$$

As variations of I_c lead to negligible variations of $I_{\Delta\theta}$, one can assume that $I_{Xsvc} \approx I_c$. Hence, introducing equation (5.12) into (5.13), the following expressions for $|V|_{dem}$ and I_c are obtained,

$$\begin{aligned} |V|_{dem} &= [\mathrm{Im}(\mathbf{v}_o^{*}\, \mathbf{Z}\, \mathbf{v}_o + j\, X_{sl})]\; I_c \\ I_c &= \mathbf{B}_{co}\, |V|_{dem} \end{aligned} \tag{5.14}$$

where $\mathbf{B}_{co}$ is the coordination susceptance, (matrix), with

$$\mathbf{B}_{co} = [\mathrm{Im}(\mathbf{v}_o^{*}\, (\mathbf{Z} + jX_{sl})\, \mathbf{v}_o)]^{-1} \tag{5.15}$$

In general, $\mathbf{B}_{co} = \left(\dfrac{\partial I_{c\,i}}{\partial |V|_{dem_j}} \right)$, (Jacobian matrix).

This control coordination requires a communication network interconnecting all SVC controllers, similar to those applied in DC transmission.

5.3.2. Power System Representation

The linearized power system block diagram is represented by Figure 5.1

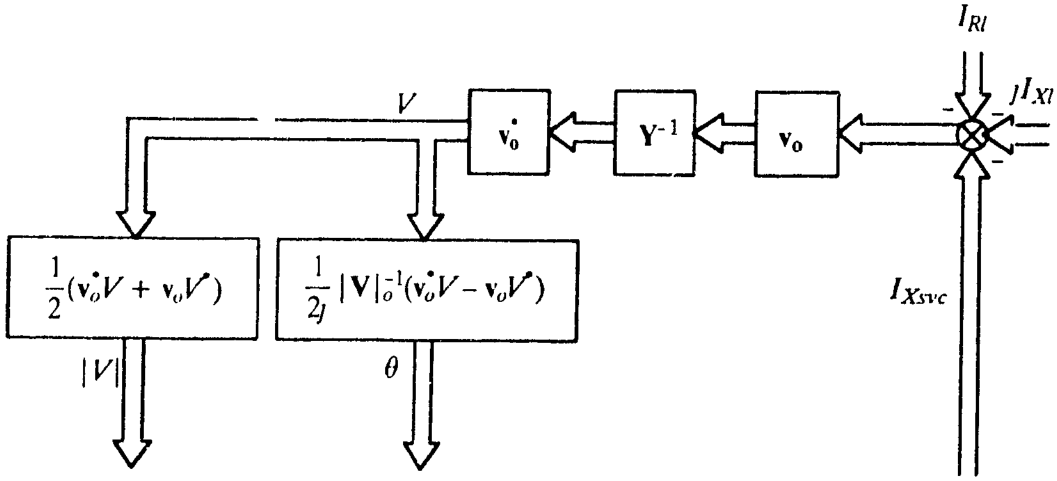

Fig 5.1. Block diagram of the power system

The voltage magnitude $|V|$ and the phase θ represent the outputs of the power system, while the SVC current I_{Xsvc}, the reactive and the active load currents I_{Xl} and I_{Rl} represent its inputs. The expressions of the linearized outputs as given by expressions (5.6) and (5.7) are as follows :

$$|V| = -\operatorname{Re}(\mathbf{v}_0^* \mathbf{Y}^{-1} \mathbf{v}_0) I_{Rl} + \operatorname{Im}(\mathbf{v}_0^* \mathbf{Y}^{-1} \mathbf{v}_0)(I_{Xl} + I_{Xsvc}) \tag{5.16}$$

$$\theta = -|\mathbf{V}_0|^{-1}[\operatorname{Im}(\mathbf{v}_0^* \mathbf{Y}^{-1} \mathbf{v}_0) I_{Rl} + \operatorname{Re}(\mathbf{v}_0^* \mathbf{Y}^{-1} \mathbf{v}_0)(I_{Xl} + I_{Xsvc})] \tag{5.17}$$

5.3.3. SVC System with Coordinated Controllers

The block diagram of the SVC system with the coordinated controllers is given in Figure 5.2.

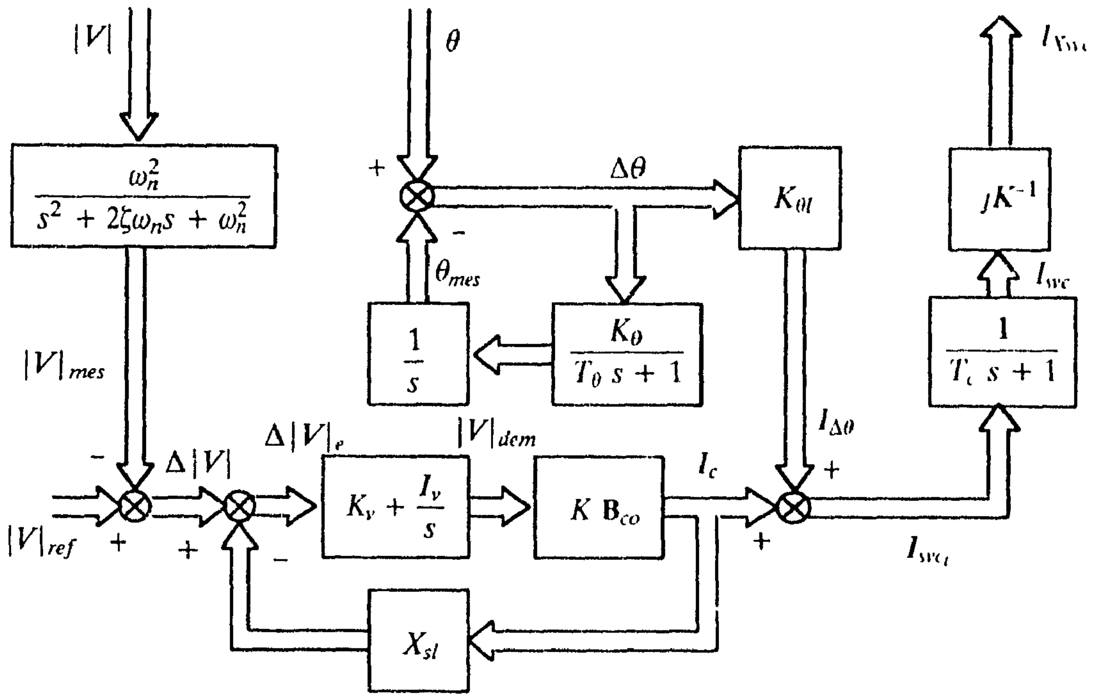

Fig 5.2. Block diagram of the SVC system with coordinated controllers

In each SVC unit (as assumed in chapter III), the bus voltage magnitude (scaled to its p.u. value) is measured and filtered by a second order low pass filter. The voltage drop across the slope reactance assumes SVC current which is either measured or computed internally. The measured voltage magnitude and voltage drop across the slope reactance are subtracted from the reference voltage magnitude to form an error signal. Based on this error, proportional and integral terms form the voltage magnitude demand. The controller subsystem consists of PI error processors where K_v are the controller gains and I_v are the integration coefficients. The internal current feedback loops have the slope reactances as their gains. The notch filter blocks are included to eliminate undesired effects of the lowest system resonance frequencies in the measurement of the voltage magnitudes.

In order to achieve a coordinated voltage control action, each controller communicates its demand to other SVC controllers, and also it receives theirs. Each controller can now compute its reactive current demand $I_{svc\,dem}$ according to equation (5.14) in order to satisfy voltage demands of all other controllers.

The control coordination concept is therefore based on equations (5.14) and (5.15) with the coordination susceptance matrix $\mathbf{B}_{co}$ being of the principal importance (Figure 5.3).

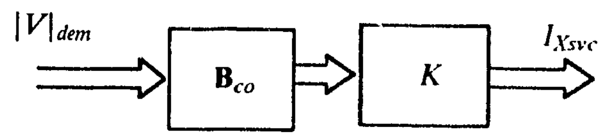

Fig 5.3. Control coordination block diagram

The current order of each SVC unit is computed according to expression (5.14),

$$I_{Xsvc\,i} = k_i \, B'_{co\,i} \; |V|_{dem} \tag{5.18}$$

where $B_{co\,i}$ is the relevant coordination vector, (i-th column of matrix B_{co}), $B'_{co\,i}$ being its transpose

$k_i = \dfrac{P_{svc_i}}{P_{sys}}$ is the factor for p.u. base conversion from system to SVC values.

The SVC coordinated control system as a multi-input/multi-output system consists of an assembly of classical local controllers and coordination blocks, which interchange their local voltage magnitude demands so that each controller determines its current so to respond correctly and immediately to all voltage magnitude demands, as specified by equation (5.18). In the absence of this communication, each controller determines its current order in response to its local voltage magnitude demand only, according to the following expression,

$$I_{X_{svc\,i}} = k_i \; B_{co\,ii} \; |V|_{dem\,i} \tag{5.19}$$

where $\quad B_{co\,ii} \quad$ is the relevant coefficient, (diagonal element of the coordination susceptance matrix $\mathbf{B}_{co}$).

In this case, the SVC coordinated control system reduces to the SVC uncoordinated control system, which consists of an assembly of classical local SVC controllers.

The SVC system is a dynamic subsystem which can be defined in state-space in the same way it was shown in Chapter III.

5.3.4. State-Space Representation of the System with SVCs

The global state-space of the system including the active load disturbances input will be represented by Figure 5.4,

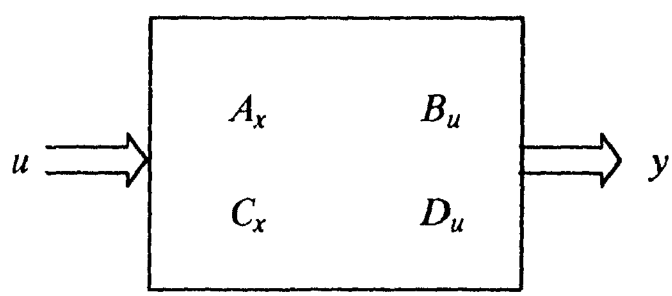

Fig 5.4. State-space block diagram of the complete system

The state-space representation of the complete system is given by the following equations :

$$x = A_x \; x + B_u \; u \tag{5.20}$$

$$y = C_x \; x + D_u \; u \tag{5.21}$$

where $x = \begin{bmatrix} |V|_{mes} \\ |V|_{mes} \\ \theta_{mes} \\ \theta_{mes} \\ |V|_{dem} \\ I_{Xsvc} \end{bmatrix}$, $u = \begin{bmatrix} |V|_{ref} \\ I_{X1} \\ I_{R1} \end{bmatrix}$, and $y = \begin{bmatrix} |V| \\ \Delta\theta \\ \Delta|V| \\ I_{svc_i} \\ \cdot \\ \cdot \end{bmatrix}$.

x, u, y being the state-space, input and output vectors, and

A_x, B_u, C_x and D_u are the system matrices.

For a power system having n SVCs, the order of the system of equations (5.18) and (5.21) becomes $6n$.

Details of the complete mathematical derivations of the state-space matrices of the complete system are given in Appendix B.

The system matrices were formed by means of MATLAB software. First, the state-space representations of the controllers without their coordination units were formed using the block diagram to the *'transfer function-to-state space'* conversion function from the MATLAB software and its Control System Toolbox [37]. Secondly, the state-space representation of a complete system was formed by interconnecting all the controllers with the control coordination and power system blocks using the *'connect'* function.

CHAPTER VI

ANALYSIS OF THE SYSTEM WITH COORDINATED SVCs AT VARIOUS LOCATIONS

6.1. STUDIED SYSTEM

In order to analyze and evaluate the proposed control coordination concept, the IEEE 14-bus and the IEEE 30-bus power systems were chosen [38]. Various number of SVCs were considered on each system. For a chosen number of SVCs, tests were made with different types of disturbances such as active, reactive step variations, voltage reference step variations and combinations of them. However, only the results concerning the IEEE 30-bus system with five SVC units are presented, since the tests with different number of SVCs gave similar results in principle. The IEEE 30-bus power system is specified in Appendix D.

As shown in Figure 6.1, five SVCs units rated at 5, 5, 5, 10 and 1 Mvars, were connected to buses 2, 13, 15, 19, and 23, respectively. The slope reactance of each SVC system was assumed to be 3% on its rating. The determination of the SVC locations and ratings were based on the load flow study made with the objective to minimize the total reactive power required for voltage regulation. The load flow program was also applied to determine the system voltage magnitude $|V|_o$ and phase θ_o at the steady-state operating point. Next, the system admittance were formed, while all the voltage sources and were linearized and transformed into relevant current sources.

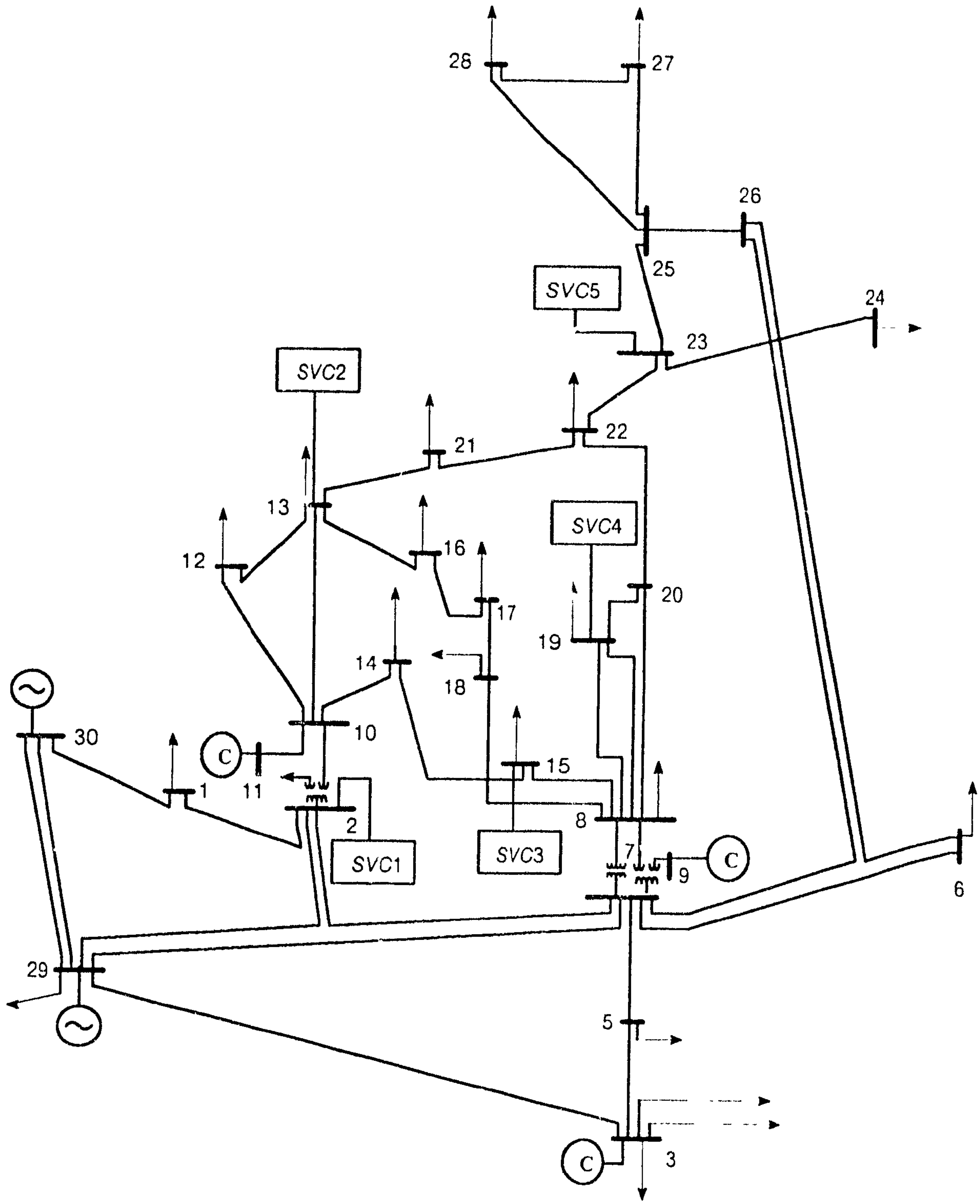

Fig 6.1. IEEE 30-bus power system with five SVC units

—Ⓒ Synchronous Condensers

$\boxed{SVC}$ Static Var Compensators

Then the system was reduced to an equivalent system containing only those buses where SVCs were connected. This reduction is not necessarily required, but it is advantageous in computation while it does not have any effect upon neither simulation nor analysis. However, this reduction limits the disturbances to the retained buses of the considered system. If a load disturbance is assumed at the bus where an SVC is not connected, the complete network has to be considered.

The SVC coordinated controllers were assumed with the following filter and PLL parameters :

$\omega_n = 120$; $\zeta = 0.707$;

$K_\theta = 533$; $T_\theta = 0.038$;

$K_{\theta I} = 0.955 \ rad^{-1}$;

The assumed TCR/TSC response time constant is :

$T_c = 8.3 \ 10^{-3} \ s$.

The proportional and integral gains of the controllers were considered adjustable.

The control coordination susceptance matrix $\mathbf{B}_{co}$ was calculated, from which the coordination susceptance vectors $B_{co\,i_{(i\,=\,1,2,\ldots,5)}}$ equation (5.18) were deduced.

For comparative evaluation the uncoordinated SVC controllers were considered as an alternative, with the same fixed parameters, while the diagonal elements of the coordination susceptance matrix were taken as susceptance factors coefficients, equation (5.19). The proportional K_v and integral gains I_v of the uncoordinated controllers were also considered adjustable.

Block Diagram of the SVC System with Improved Coordinated Controllers

The coordinated SVC controller system has also been improved (Figure 6.2) by adding a filter in the slope block of each controller. These filters are identical to those used for voltage magnitude measurement. This allows for an effective dynamic decoupling of the coordination operation, so that each SVC controller reacts as an equivalent isolated single SVC unit system. An attractive alternative is to relocate the measurement filter to filter the voltage error $\Delta|V|_e$. Of course, the added filters increase the number of eigenvalues, without deteriorating the performance of the coordinated SVC controllers with regard to voltage regulation.

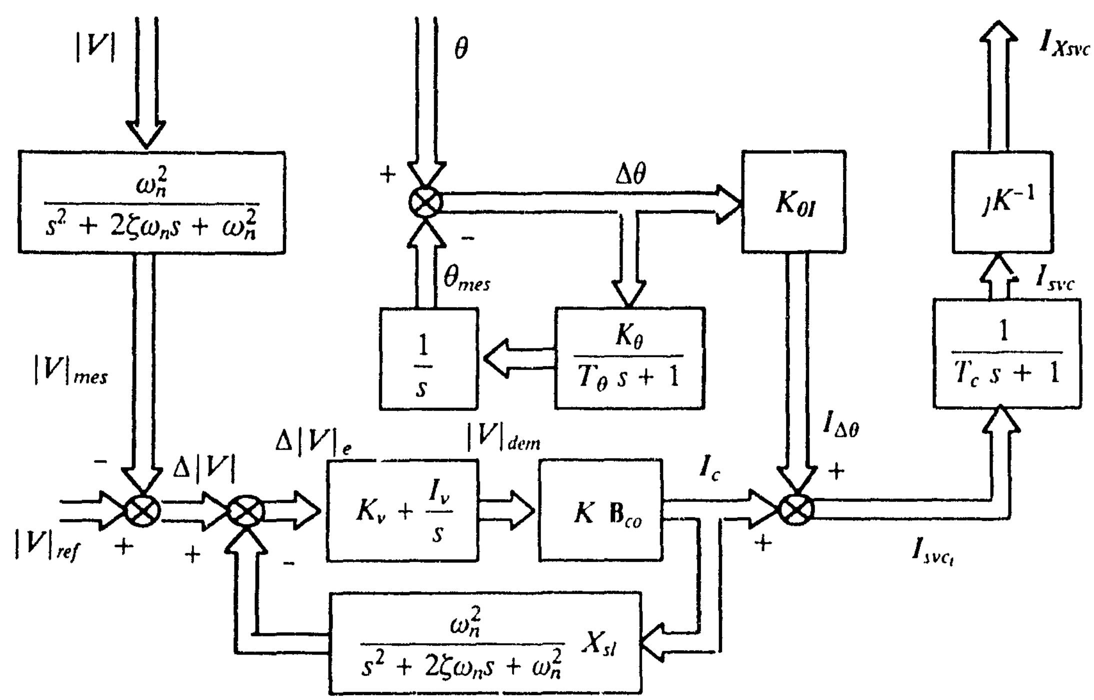

Fig 6.2. Block diagram of the SVC system with improved coordinated controllers

6.2. COMPARATIVE SYSTEM ANALYSIS AND EVALUATION

Analysis and evaluation of the SVC systems with and without control coordination was performed in s-plane and time domain, by means of the MATLAB software and its Control System Toolbox.

It is well known that when the system short circuit impedance increases (weaker system), the SVC dynamic performance as well as its stability margin would degrade. In extreme cases, this results in the loss of stability.

When two or more SVC units operate on the system, they mutually interact. This interaction degrades their performance, reducing their margin of stability. To illustrate this, a comparative analysis was done of the SVC systems comprising one to five locally controlled SVC units. In each case, the SVC controllers were optimally adjusted, according to the expression

$$min \int_0^{\infty} \Delta|V|' \, q_v \, \Delta|V| \, dt$$

with regard to their integral gains (proportional gains were kept at zero), as it is usually done in SVC controllers with internal current measurements. The optimal adjustment of the SVC controllers was done in the time domain applying the Monte-Carlo technique.

The minimization process of the performance index defined above, not only allowed to determine the optimal values of the integral gains of the SVC controllers, but also to compare the optimal performance indices obtained for the coordinated and uncoordinated systems.

The cumulative performance index which provides an evaluation of the system of SVC's with regard to the step-inputs applied to every SVC reference voltage in sequence, consists of a sum of the performance indices. The optimal parameters of the

SVC controllers (integral gains, for example) are determined so to minimize this performance index as defined by the following expression :

$$\min \mathbf{J} = \min \sum_{i=0}^{n} \mathbf{J}_i \tag{6.1}$$

where $\mathbf{J}_i = \int_0^{\infty} \Delta|V|_i' \, q_V \, \Delta|V|_i \, dt$ is the performance index with step input set only to the voltage reference of the i-th SVC unit (among the n SVC units connected).

Let us analyze now the system of uncoordinated SVCs in the s-plane and time domain.

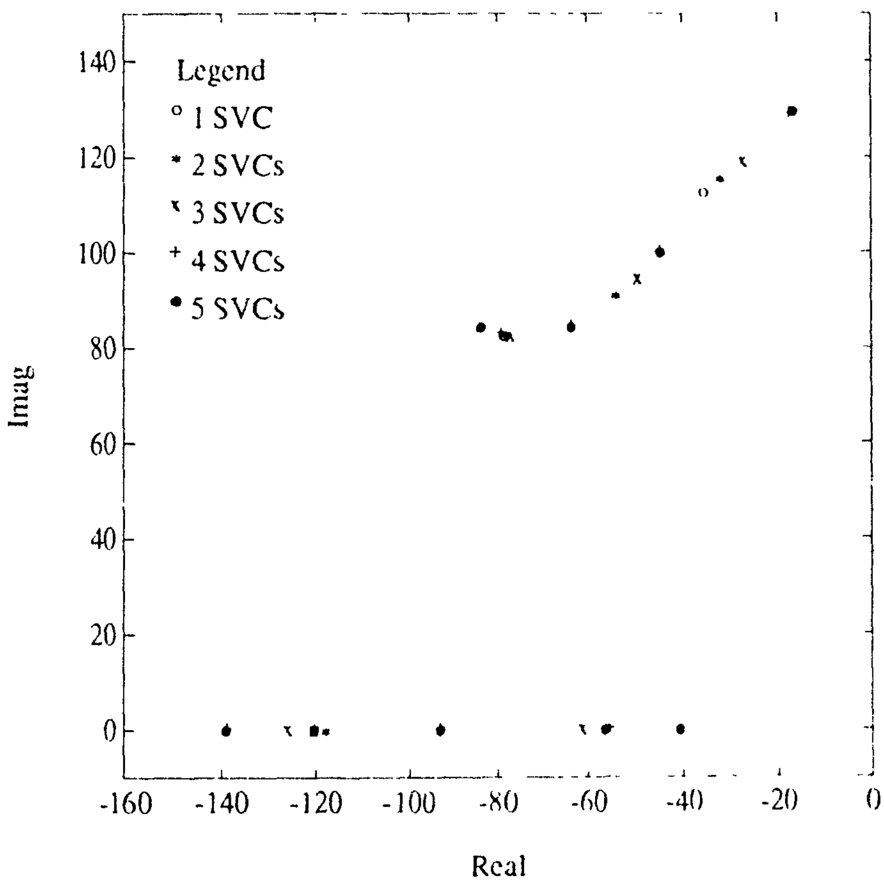

Fig 6.3. Eigenvalues of the system with 1, 2, 3, 4 and 5 uncoordinated SVC units.

Figure 6.3 gives the displacement of eigenvalues of the system with 1, 2, 3, 4, and 5 uncoordinated SVC units, in the upper left quadrant of the s-plane. In all these cases, the controller parameters were chosen such that they optimize their relevant performance indexes as defined by expression (6.1). It can be seen that the system with five uncoordinated SVC units has much smaller stability margin than the system with a single SVC unit. This indicates that, due to mutual interactions, the stability margin reduces when the number of SVC units increases.

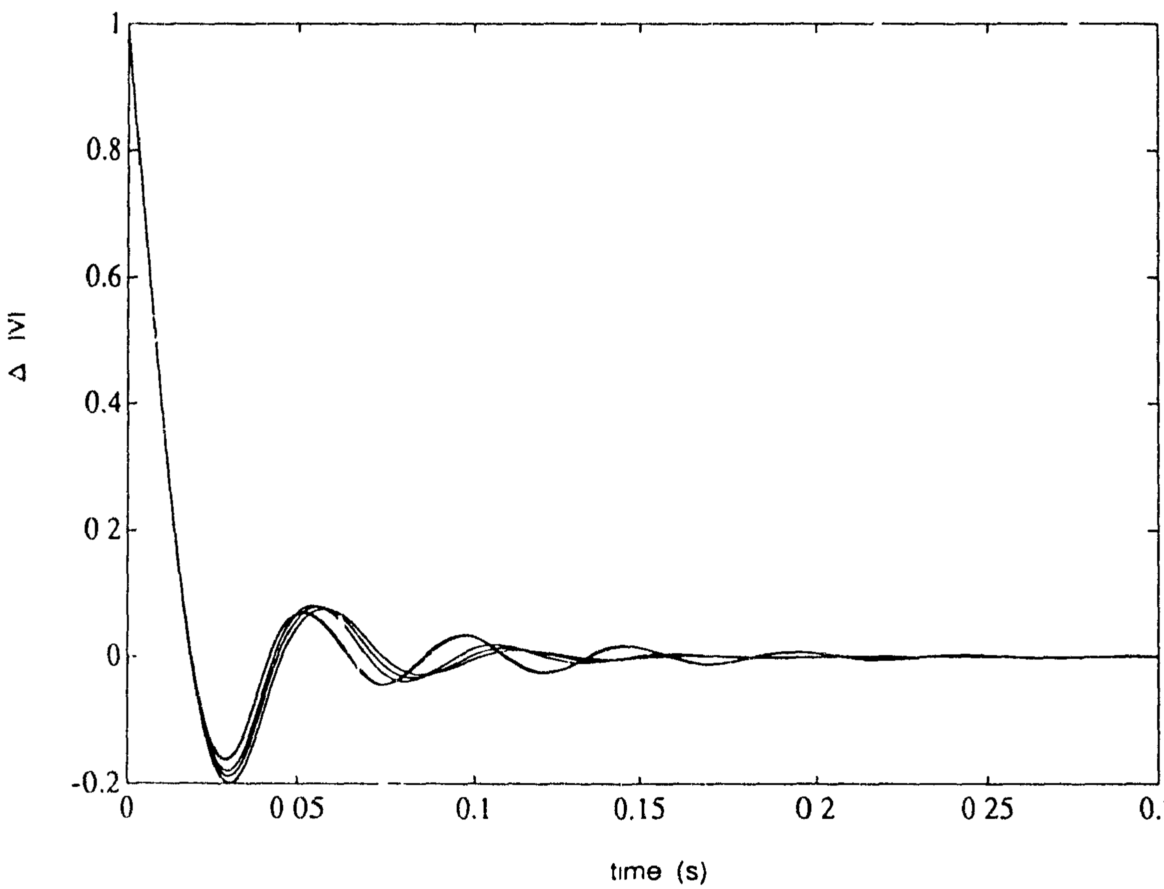

Fig 6.4. Voltage error step response $\Delta|V|_{svc1\ trans}$ of the system with 1, 2, 3, 4, or 5 uncoordinated SVC units

Again, for all cases of Figure 6.4, the controller parameters were chosen such that they optimize their corresponding performance indices. The figure shows the transient components of the voltage error step-responses of the first SVC unit when it operates alone and together with 1, 2, 3, and 4 other uncoordinated SVC units. As the number of SVC units increases the step response becomes more oscillatory. For many SVC units the system could become unstable.

Based on expression (6.1), the minimization of the performance indexes was carried out for the case of five uncoordinated SVC controllers, with the following integral gains obtained :

$$\begin{aligned} I_{v_1} &= 150.22 \\ I_{v_2} &= 102.18 \\ I_{v_3} &= 73.64 \\ I_{v_4} &= 124.24 \\ I_{v_5} &= 44.23 \end{aligned}$$

the performance index $\mathbf{J}_{unco\,\min}$ being:

$$\mathbf{J}_{unco\,\min} = 0.2546$$

Before considering the parameter optimization of the coordinated SVC units, let us use the integral gains determined previously for uncoordinated SCV units and calculate the performance index $\mathbf{J}_{co}$ for the coordinated SVC units. The value obtained is :

$$\mathbf{J}_{co} = 0.1663$$

For both, coordinated and uncoordinated SVC system, the voltage reference step-input to each SVC unit was equal to 1 p.u.

One can already notice that J_{co} has a lower value than $J_{unco\ min}$. This indicates that the integral measure of the voltage error variation is smaller in the coordinated system than in the uncoordinated system.

A comparative analysis and evaluation in the s-plane and the time domain was carried out for the system with five coordinated SVC units and with five uncoordinated SVC units.. The eigenvalues of both systems are given in Table 6.1, and shown in Figures 6.5 and 6.6.

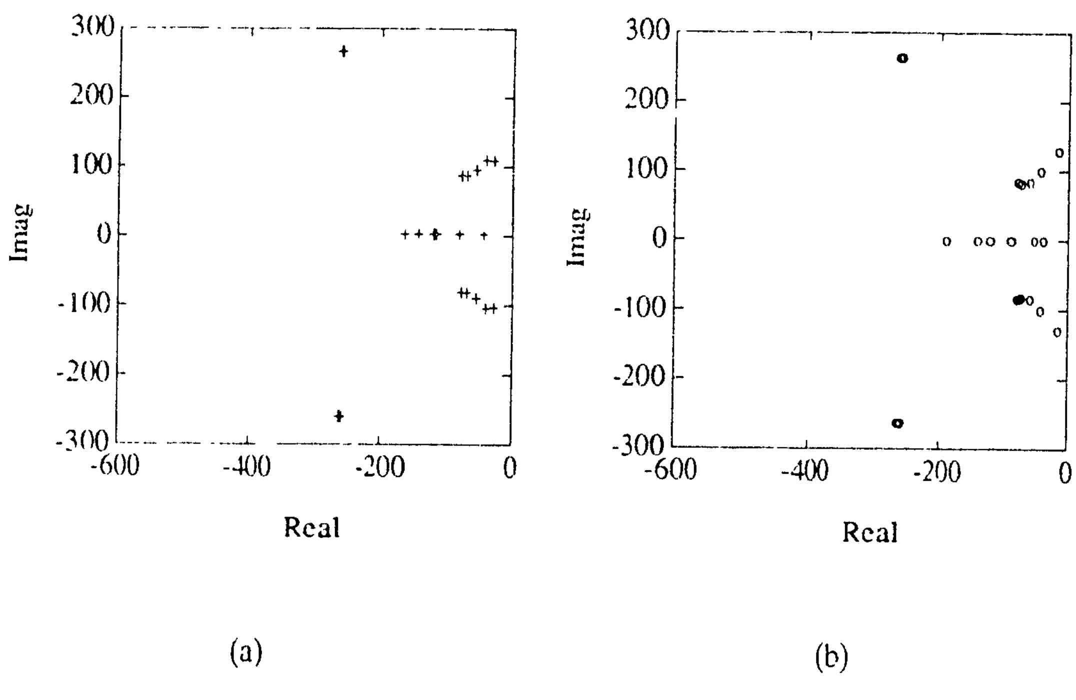

Fig 6.5. Eigenvalues of the system with five SVC units
(a) SVC units with coordinated controllers
(b) SVC units with uncoordinated controllers

Table 6.1

Coordinated SVCs	Uncoordinated SVCs
-46.13	-40.74
-87.13	-56.24
-120.48	-92.90
-120.48	-120.48
-120.48	-120.48
-120.48	-120.48
-120.48	-120.48
-124.36	-120.48
-145.46	-139.02
-164.39	-189.59
-28.90 ±j 105.54	-16.43 ± j 129.47
-42.80 ±j 106.61	-44.99 ± j 99.88
-58.80 ± 93.07	-63.55 ± j 84.19
-74.39 ±j 84.62	-78.55 ± j 82.49
-83.24 ±j 84.15	-83.56 ± j 84.19
-263.37 ±j 263.21	-263.44 ± j 263.23
-263.87 ±j 263.10	-263.85 ± j 263.18
-265.62 ±j 263.15	-265.63 ± j 263.15
-266.25 ±j 263.14	-266.25 ± j 263.14
-266.34 ±j 263.14	-266.34 ± j 263.14

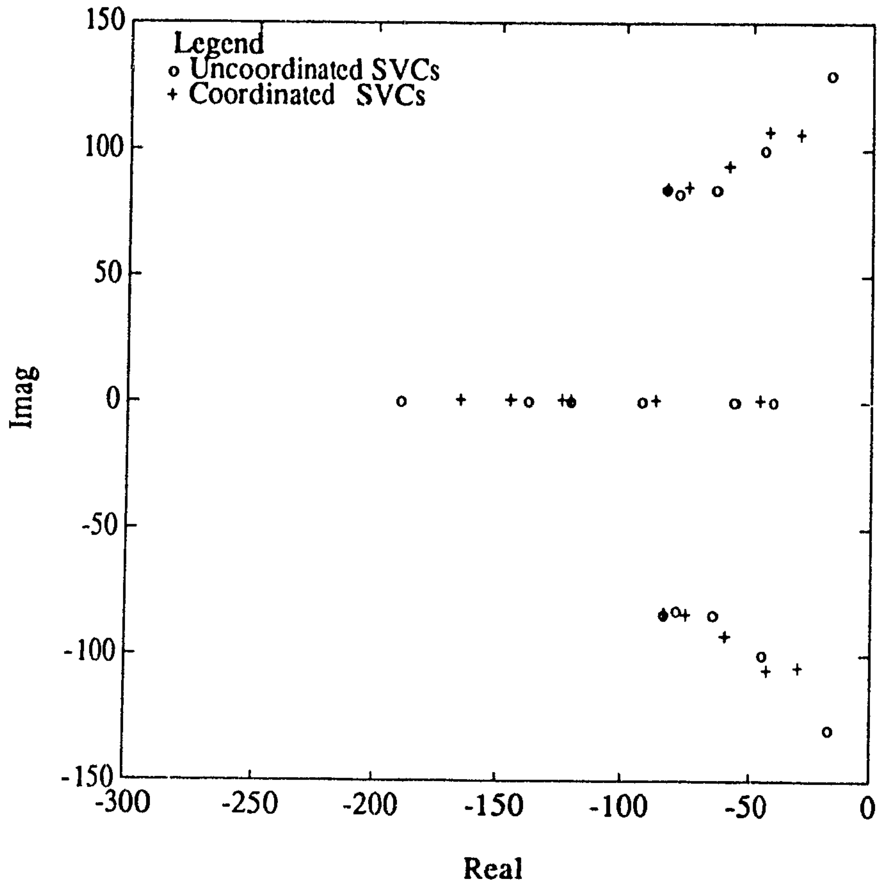

Fig 6.6. Eigenvalues of the system with five coordinated or uncoordinated SVC units

Analysis of the eigenvalue displacement reveals that the system with coordinated SVC controllers has much greater margin of stability than the system with local SVC controllers. Figure 6.6 also shows that eigenvalues of the coordinated SVC system have a tendency to regroup which can attributed to the coordination which eliminates the mutual interactions among SVCs.

Figures 6.7 and 6.8 show respectively the step responses of the measured voltage magnitude $|V|_{mes}$ and the transient voltage error of each SVC controller with and without coordination, the step-input being applied to the reference voltage of the fourth SVC unit. As it can be observed, the step responses of the coordinated SVC controllers are much more damped, with smaller overshoots than were the responses of the local SVC controllers.

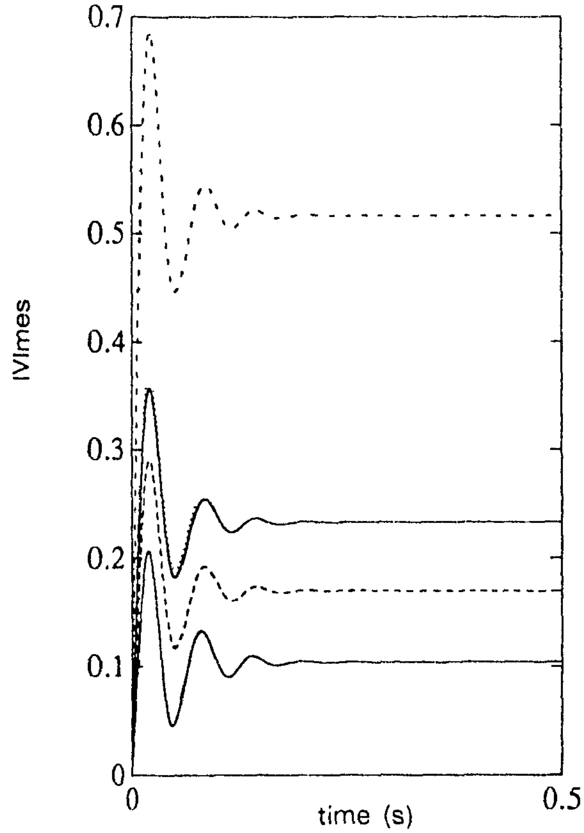

(a)

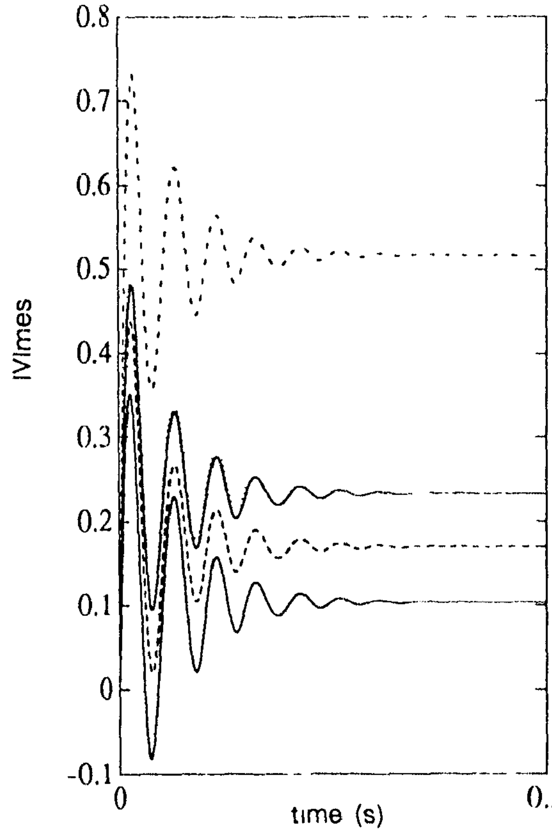

(b)

Fig 6.7. Measured voltage magnitude to voltage reference variation of the system with five SVC units
(a) SVC units with coordinated controllers
(b) SVC units with uncoordinated controllers

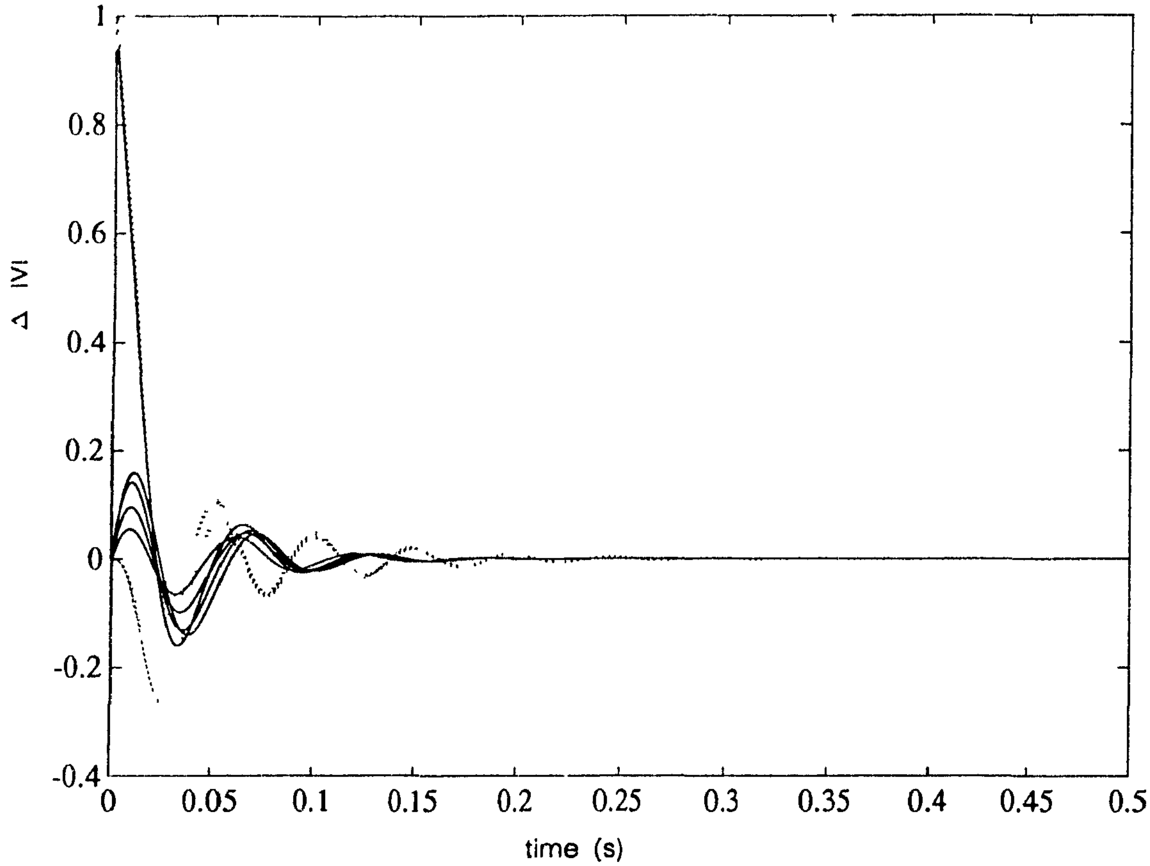

Fig 6.8. Voltage error step-responses $\Delta|V|_{svci\ trans}$ of the system with five SVC units
______ Coordinated SVC units
.... Uncoordinated SVC units

Figure 6.9 shows the step responses of the currents of coordinated and uncoordinated SVC units with the integral gains optimized for the uncoordinated SVC units system only. As before, a superior performance of the coordinated SVC controllers can be observed.

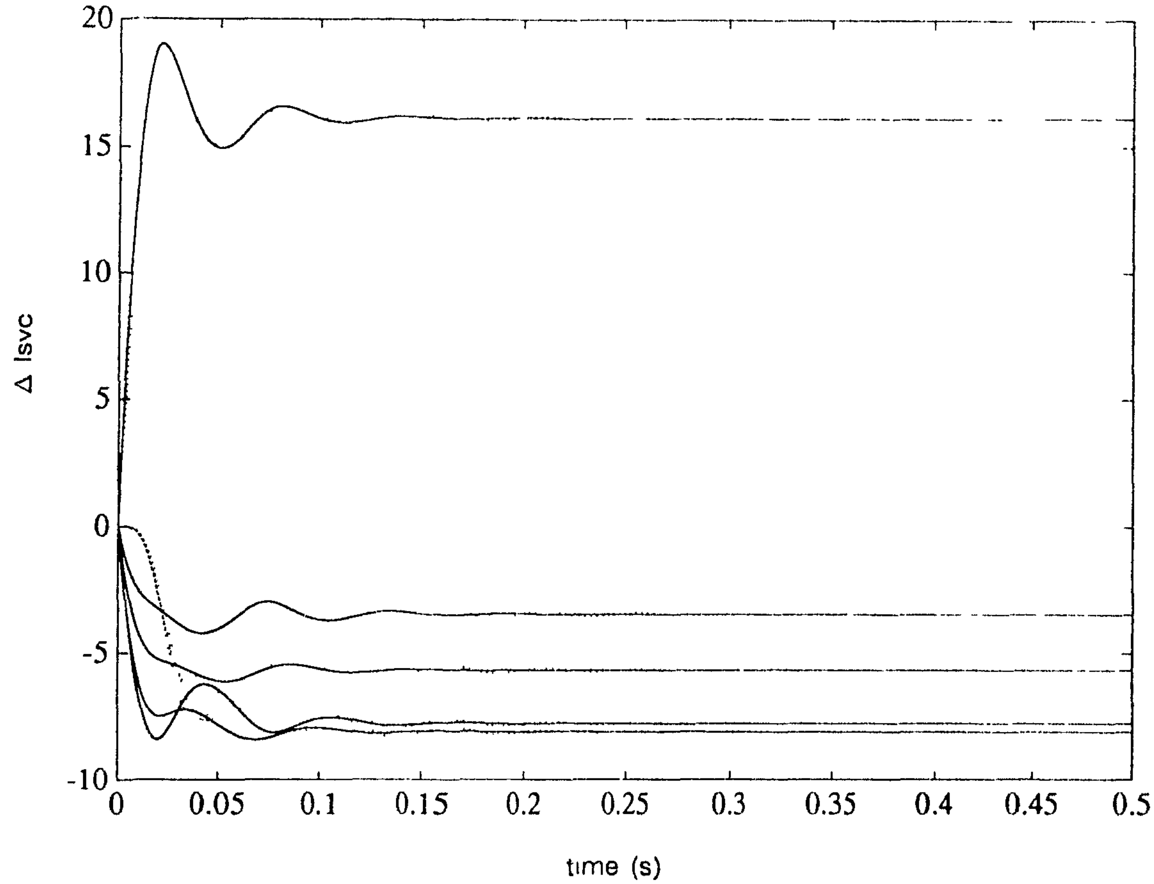

Fig 6.9. SVC current response I_{svci} of the system with five SVC units
______ Coordinated SVC units
.... Uncoordinated SVC units

Another interesting point in evaluation of the proposed coordination concept is to analyze the stability of the system with many coordinated SVCs as compared to the same system with a single SVC when the integral gain of a single SVC unit is optimized.

So to minimize the performance index defined by expression (6.1), the following integral gain was obtained :

$$I_v = 70$$

yielding the following performance index of the single SVC unit system :

$$J_{single\ min} = 0.0172$$

In the case of a five coordinated SVC units, the controller actions are fully decoupled. For that reason, each of the controller appears to be equivalent to a controller of the single SVC unit. The step-input applied to the voltage reference of any SVC unit results in the voltage error variation of that unit only. Therefore, the optimal integral gains of the coordinated controllers, (the proportional gains set to zero), are equal and assume the value identical to the one obtained for the optimal controller of the single SVC unit,

$$I_{v_i} = 70 \qquad\qquad [\ i = 1,\ 2,\ \ldots,\ 5\ ]$$

The relevant optimal performance index of the system with optimized controllers, for the unit step-input applied to the voltage reference of anyone out of five SVC controllers (SVC unit connected to bus no.19, for example), assumes the value identical to the one obtained for the optimal controller of the single SVC unit :

$$J_{co\ min} = 0.0172$$

The optimal cumulative performance index (expression 6.1), with regard to the unit step-input applied to the voltage reference of each SVC controller in sequence, assumes a five times greater value :

$$J_{co\ min} = 0.0859$$

Let us now see the comparison of the five coordinated SVCs system with the single SVC system in s-plane and time domain.

One observes clearly from Figure 6.10, that the system with five coordinated SVCs has its eigenvalues, five times repeated, and at identical locations as those of the single

SVC system. This indicates that each of the coordinated SVC system performs as an equivalent single SVC unit.

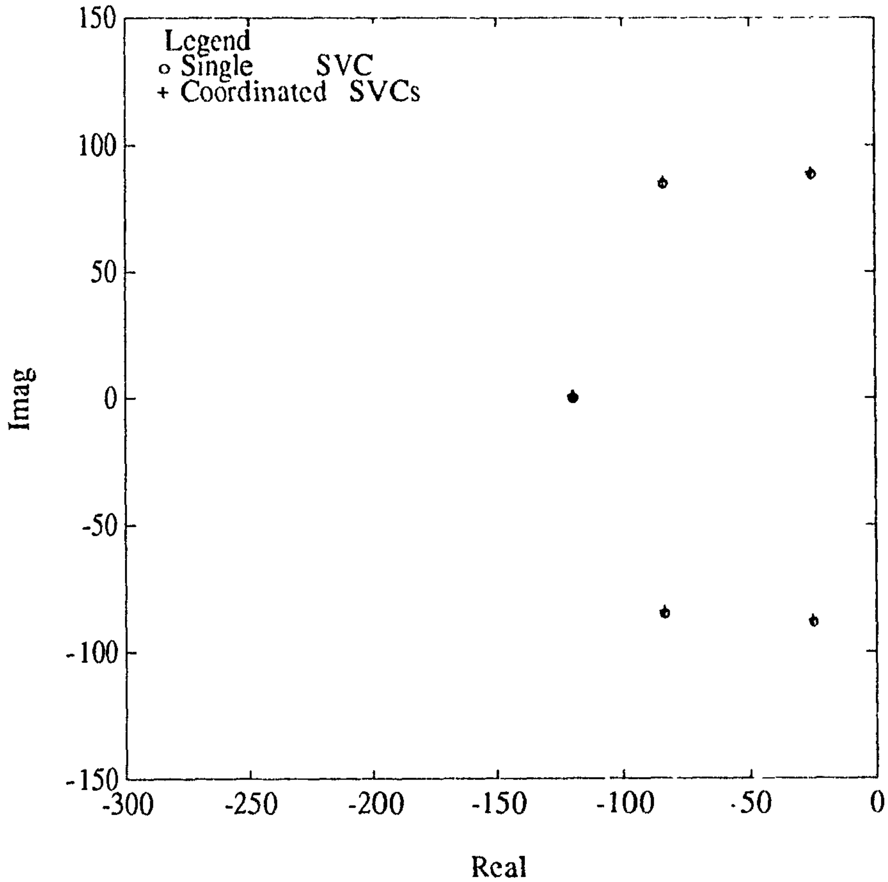

Fig 6.10. Eigenvalues of the system with five coordinated SVC units compared to a system with a single SVC unit

Similarly, the dynamic performance of the coordinated SVCs illustrated in time domain shows the voltage decoupling achieved, and its dynamic performance identical to that of the system with a single SVC unit.

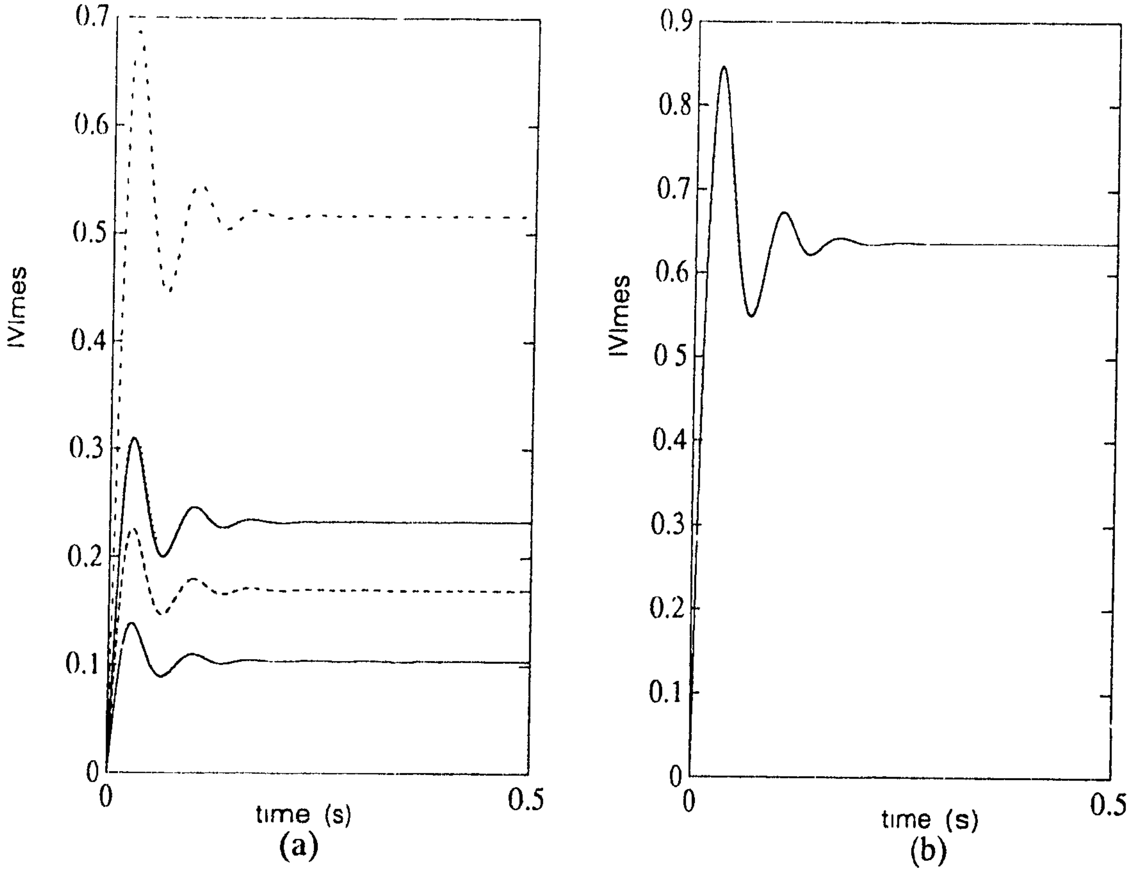

Fig 6.11. Magnitude voltage to voltage reference variation of the system
(a) with single SVC unit
(b) with five coordinated SVC units

Figure 6.11 illustrates the measured magnitude voltage response of the system with five coordinated SVC units with the magnitude voltage of a system with a single SVC system. Although the number of SVC units is five, one can see that the responses obtained in Figure 6.11a are not more oscillatory than the one of Figure 6.11b which corresponds to a single SVC case. One can also notice that the magnitude voltage appears within all the SVC controllers, which is not the case of the voltage error, as result of the compensation introduced by the added filters in the slope blocks.

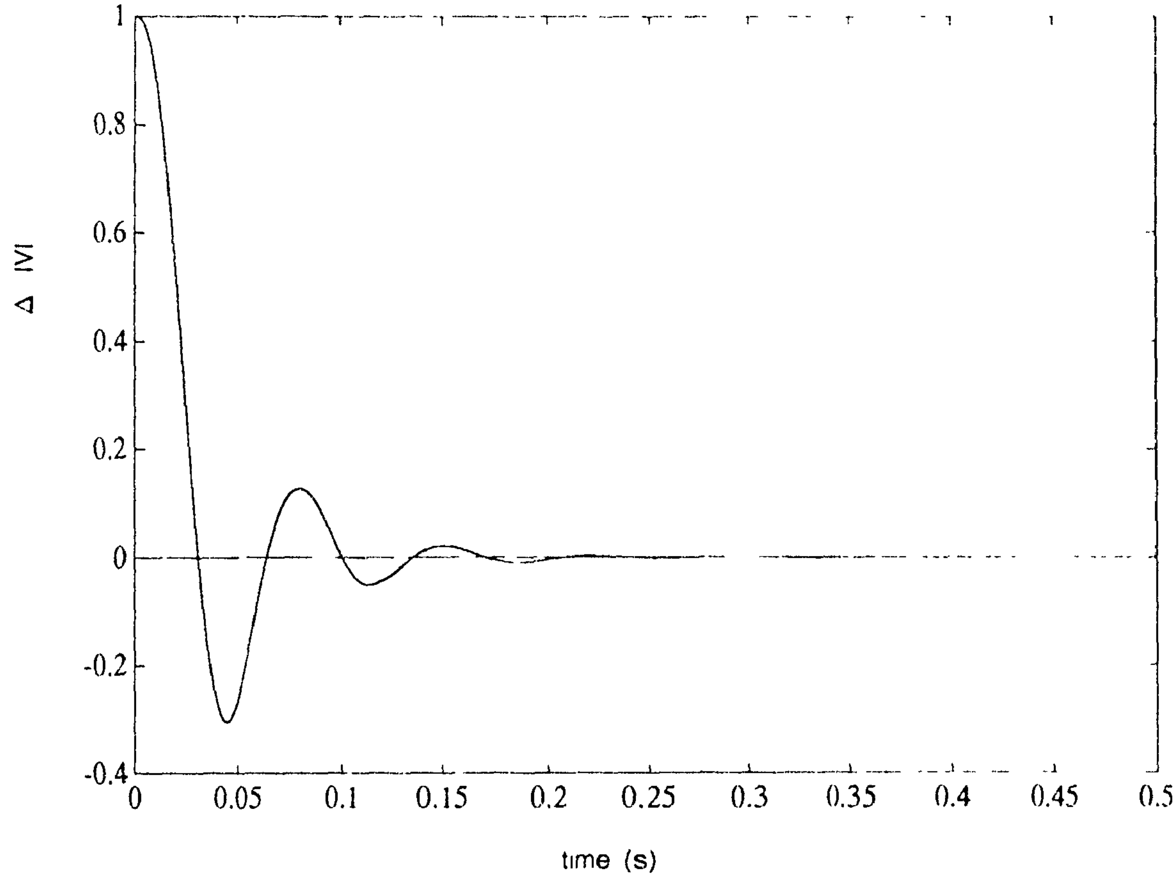

Fig 6.12. Voltage error step-response $\Delta|V|_{svc1\ trans}$ of the system
_____ with five coordinated SVC units
.. . ... with single SVC unit

Figure 6.12 shows on the same plot the five voltage error step responses of the system with five coordinated SVC units and the voltage error response of the system with a single SVC unit. It is interesting to notice that the voltage error appears only within the SVC controller to which the step-input is applied, while other four remain undisturbed. Hence, the controller reactions are fully decoupled.

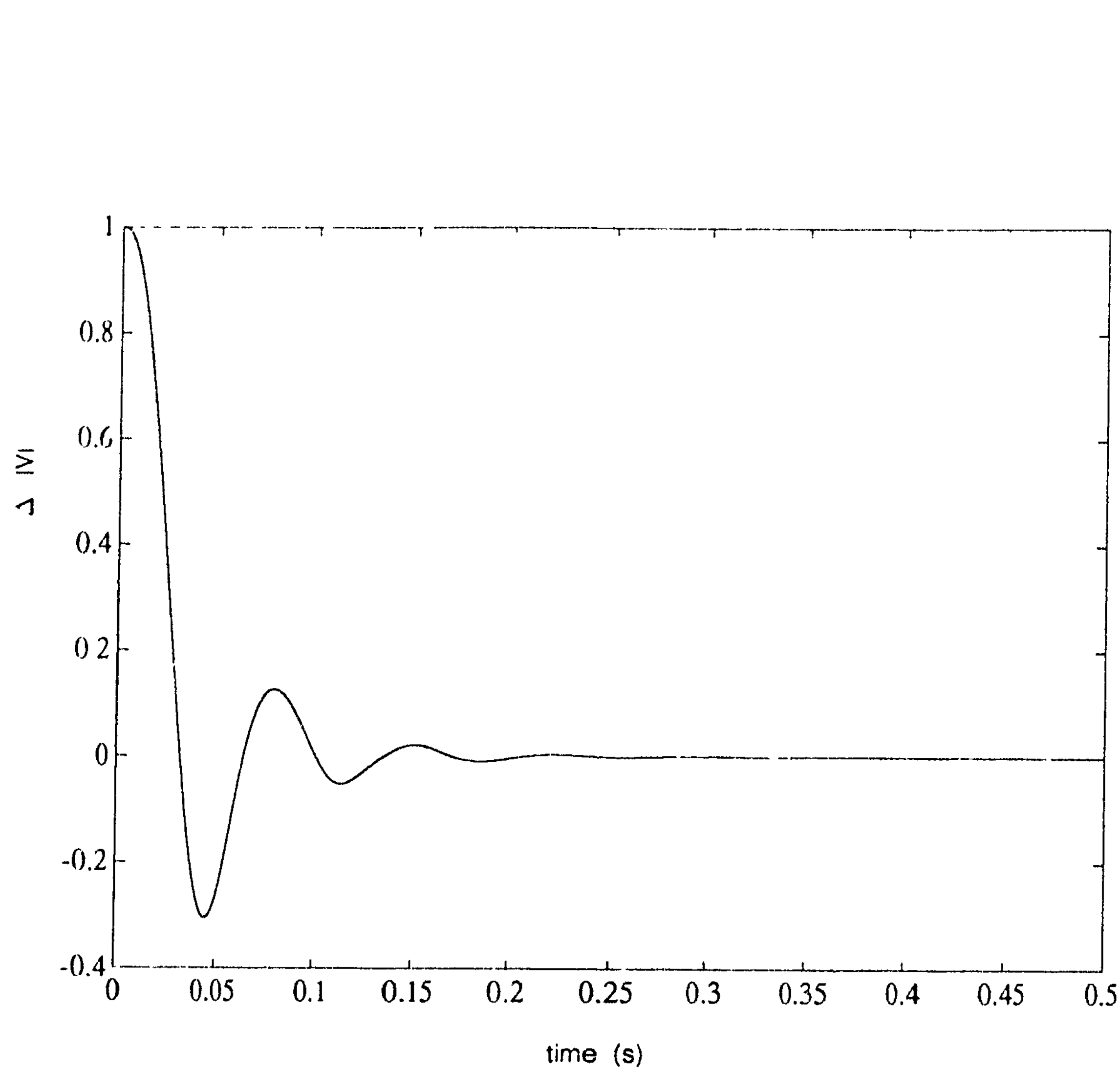

Fig 6.13. Voltage error step response $\Delta|V|_{svc1\ trans}$ of the system
______ with five coordinated SVC unit
.... with single SVC unit

Figure 6.13 is extracted from Figure 6.12. in this case, only the oscillating voltage error response of the system with five coordinated SVC units was selected for comparison with the response of the system with the single SVC unit. The two responses match identically.

Once it was proven that the proposed coordination made the SVC units performing as a system of the decoupled equivalent SVC units, it would be interesting to compare the coordinated SVC units system with the uncoordinated SVC units system, each assuming its relevant optimal controller parameters. The eigenvalues of both coordinated and uncoordinated system are shown in Table 6.2.

Table 6.2

Coordinated SVCs	Uncoordinated SVCs
-119.64	-40.74
-119.68	-56.24
-119.72	-92.90
-119.72	-120.48
-119.73	-120.48
-120.48	-120.48
-120.48	-120.48
-120.48	-120.48
-120.48	-139.02
-120.48	-189.59
-24.96 ±j 88.31	-16.43 ± j 129.47
-24.97 ±j 88.30	-44.99 ± j 99.88
-24.98 ± 88.29	-63.55 ± j 84.19
-24.98 ± 88.29	-78.55 ± j 82.49
-24.98 ± 88.29	-83.56 ± j 84.19
-84.84 ±j 88.29	-263.44 ± j 263.23
-84.84 ±j 88.29	-263.85 ± j 263.18
-84.84 ±j 88.29	-265.63 ± j 263.15
-84.84 ±j 88.29	-266.25 ± j 263.14
-84.84 ±j 88.29	-266.34 ± j 263.14
-263.29 ±j 263.19	
-263.82 ±j 263.17	
-265.63 ±j 263.15	
-266.25 ±j 263.14	
-266.34 ±j 263.14	

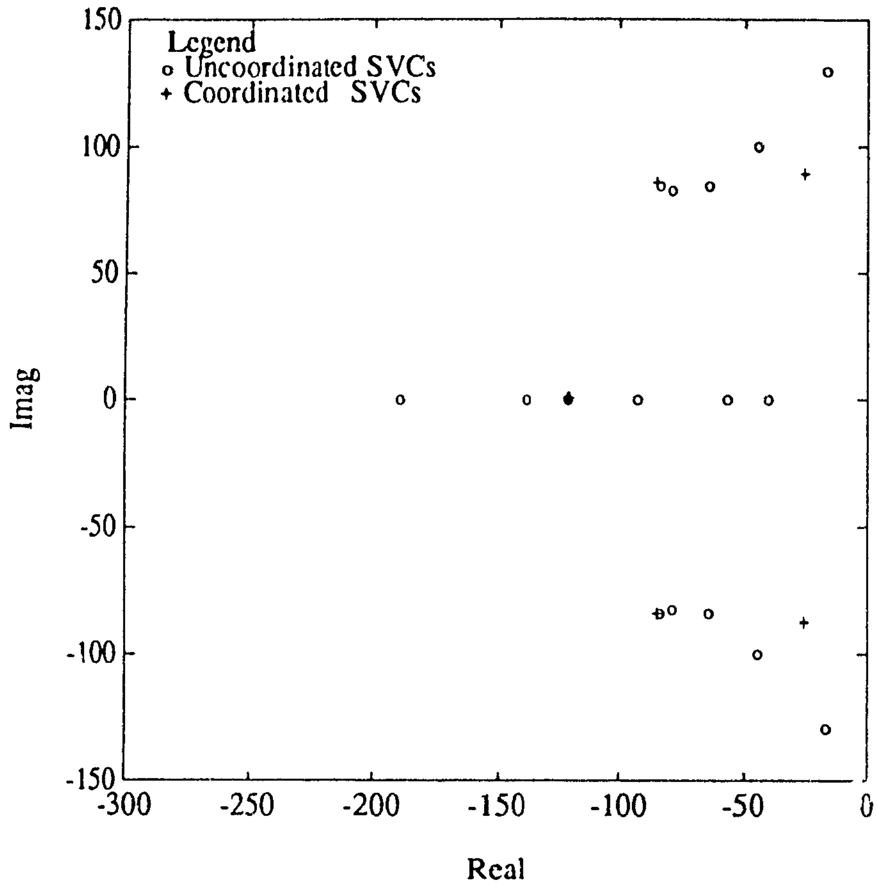

Fig 6.14. Eigenvalues of the system with five coordinated or uncoordinated SVC units

Figure 6.14 illustrates the eigenvalue locations of the system with coordinated SVC units and the system with uncoordinated SVC units. Comparing only the eigenvalues relevant to the same dynamic blocks in both coordinated and uncoordinated systems, one can see that the repeated eigenvalues of the coordinated system (at the far right of the left half of the s-plane) show an improvement in margin stability and even damping. While the uncoordinated system has its eigenvalues distributed, the coordinated system has its eigenvalues at identical locations

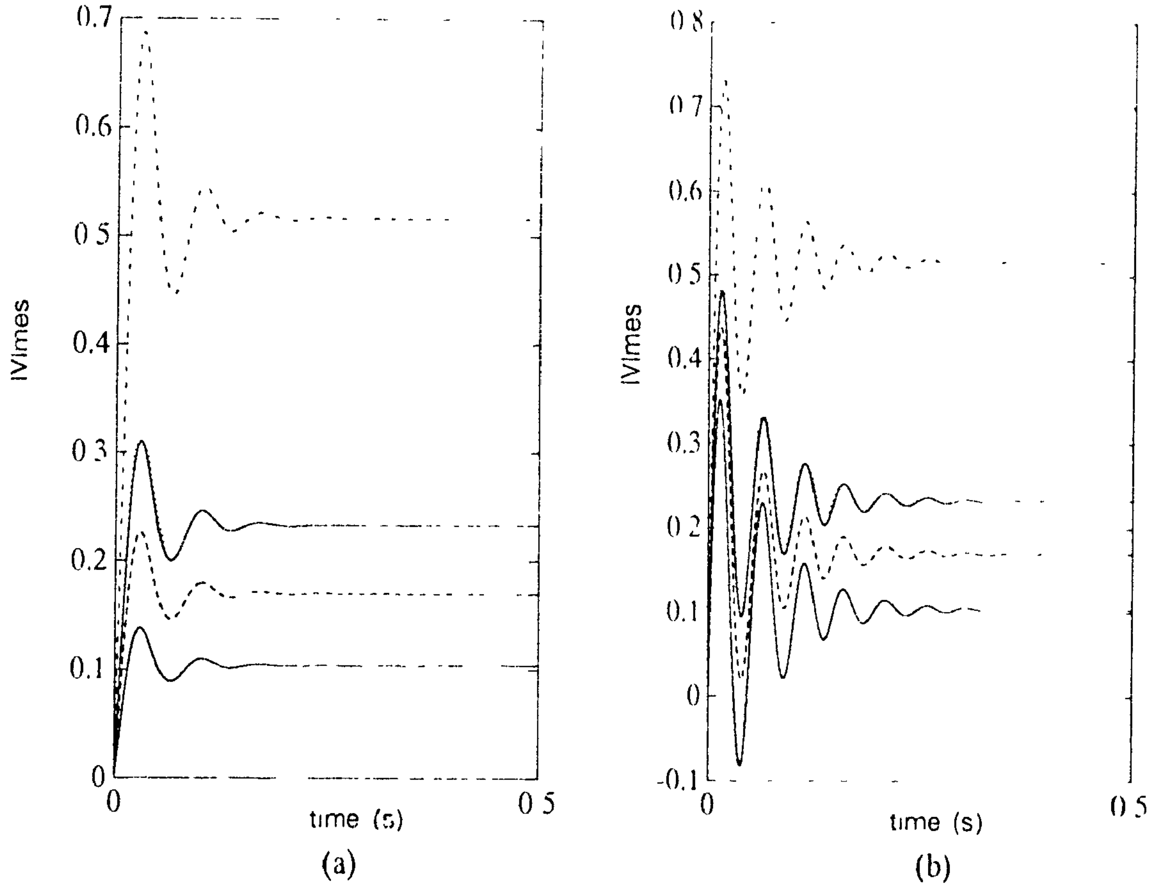

Fig 6.15. Measured voltage magnitude to voltage reference variation of the system with five SVC units
(a) SVC units with coordinated controllers
(b) SVC units with uncoordinated controllers

Figure 6.15 shows the step responses of the measured voltage magnitude of each SVC controller with and without coordination, the input being the reference voltage of the fourth SVC unit. One can see again that the coordination improves the damping of the responses and shows smaller overshoots than the responses of local SVC controllers.

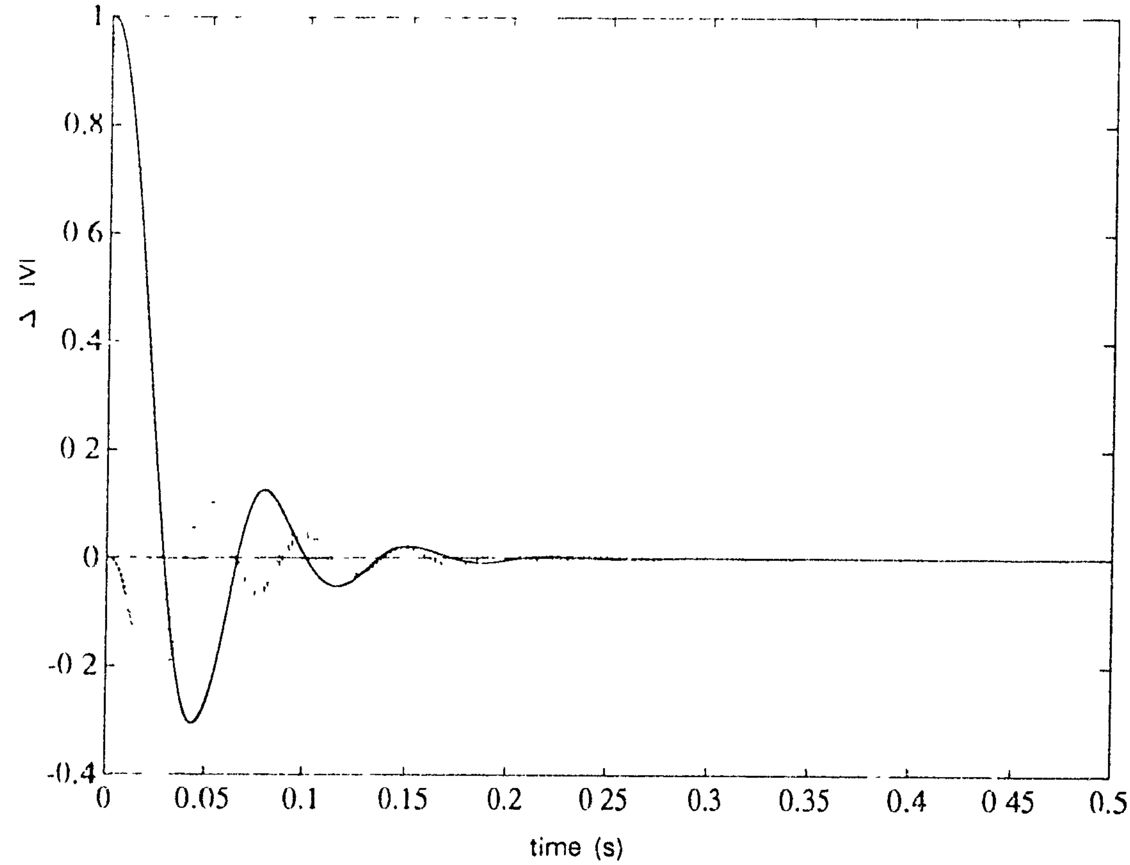

Fig 6.16. Voltage error step-responses $\Delta|V|_{svci\ trans}$ of the system with five SVC units
_____ Coordinated SVC units
. . . . Uncoordinated SVC units

Figure 6.16 illustrates the step responses of the transient voltage error of each SVC controller with and without coordination. It shows clearly that the coordinated system presents only the fourth transient voltage error step response oscillating while all others are null. This is due to the achieved voltage decoupling. As a step input was set to the fourth voltage reference, only the relevant transient voltage error oscillates. The situation is different for the uncoordinated SVC units system, as all transient voltage errors oscillate.

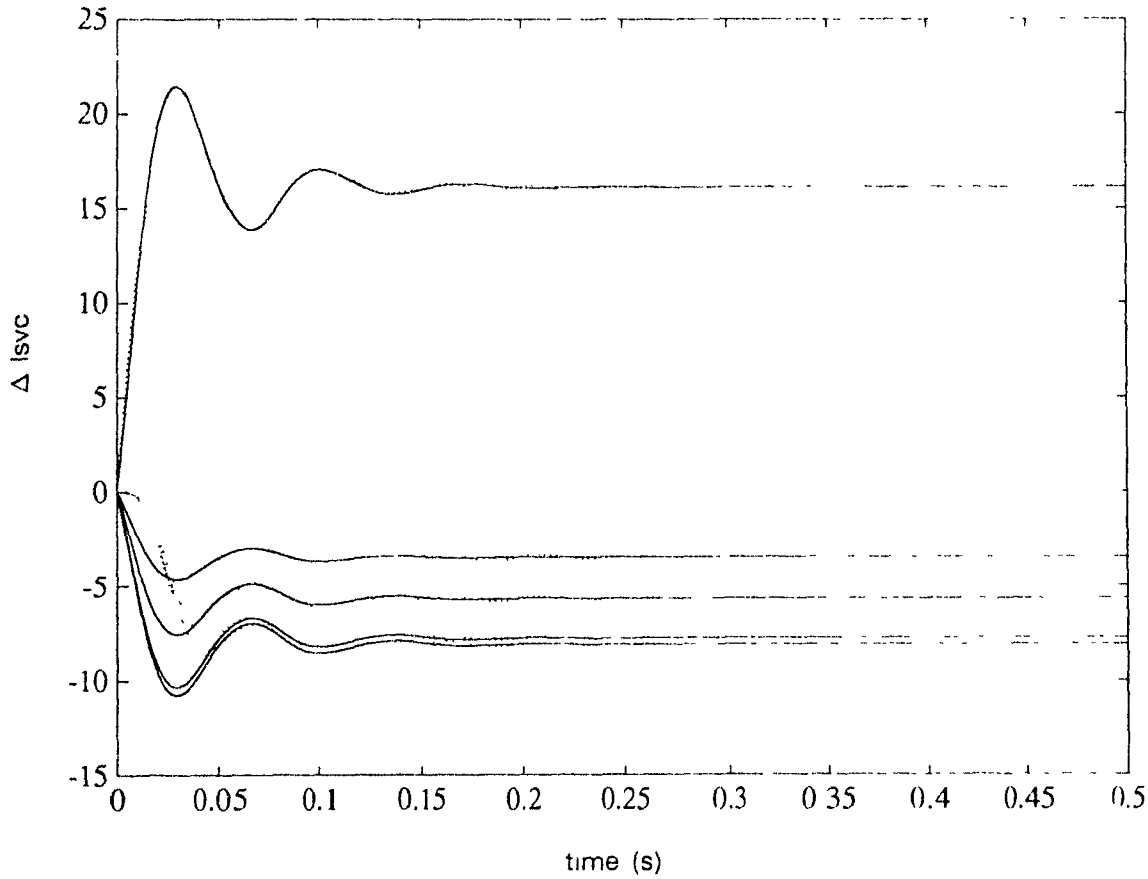

Fig 6.17. SVC current response I_{svci} of the system with five SVC units

_____ Coordinated SVC units

.... Uncoordinated SVC units

Figure 6.17 shows the step responses of the SVC currents of coordinated and uncoordinated controllers.

The relative superiority of the coordinated controllers over the local controllers increases with the number of SVC units, especially when the system stability becomes the prime concern.

6.3. IMPLEMENTATION ASPECTS

The control coordination concept relies on the coordination susceptance matrix $\mathbf{B}_{co}$ (jacobian matrix) which is a function of the system impedance matrix and the voltage vector at the operating point as shown by previous expression (5.15).

$$\mathbf{B}_{co} = [\mathrm{Im}(\mathbf{v}_o^{*}\ (\mathbf{Z} + jX_{sl})\ \mathbf{v}_o)]^{-1} \tag{6.2}$$

$\mathbf{B}_{co}$ is a full matrix which includes all the possible links when communication has to be exchanged among SVC controllers with regard to the required SVC current so that it satisfies the demanded voltage magnitude of all of them. A full matrix $\mathbf{B}_{co}$ corresponds to a full control coordination. A topological change in the network or a failure in the communication links are directly reflected on this susceptance matrix $\mathbf{B}_{co}$. For example, if the communication link between buses i and j fails, the off-diagonal elements $B_{co\,ij}$ and $B_{co\,ji}$ become zeros, and the coordination is then reduced, as $\mathbf{B}_{co}$ is no more a full matrix.

Reduced coordination can also be applied to a subset of SVC controllers within the power system, while others remain locally controlled. In this case, the only off-diagonal elements of the coordination susceptance matrix which concern the coordinated SVC controllers are non zero, while all other off-diagonal elements are null. The total reduction in coordination leads to the uncoordinated SVC units operation when all off-diagonal elements of $\mathbf{B}_{co}$ are zero. The diagonal elements represent the relevant susceptance factors for locally controlled SVC units.

In order to achieve an efficient control coordination at any system operating point (i.e load flow), the voltage phase provided by PLL circuits has to be communicated to all SVC controllers in addition to the voltage demand. In this way, the control coordination becomes load flow adaptive. Adaptation to system impedance variation due to topological changes (system contingencies) requires either a direct measurement of the driving point and transfer impedances or a computation of these impedances based on the monitored topology. In both cases, relevant processing has to be added to the SVC controllers.

The control coordination concept proposed in this thesis is very convenient with regard to its implementation and operation. It applies to new as well as to existing SVC controllers as an add-on function. The concept also enables a gradual implementation to suit growing needs for SVC control improvements. It is very important that the control security is not degraded : when a communication link fails, the relevant controller looses its performance improvement provided by the control coordination.

The following example illustrates the possibility of reduced coordination of the SVCs installed in a power system. Instead of coordinating all the SVC controllers as done before, let consider the case of coordinating only some of them, while the others operate individually. The choice of the subset of SVC units to be coordinated can be made on the judgement based on the relative proximity of the SVCs within the system. This proximity can also be evaluated by considering the off-diagonal elements $B_{co\,ij}$ of the coordination susceptance matrix $\mathbf{B}_{co}$, defining the strength of the links between the SVC units. Greater their values, the stronger the links between the corresponding SVC units in the system.

In the five SVC's system case, the analysis of the off-diagonal elements of the susceptance matrix led to the SVCs at the buses 15, 19, and 23 out-of-five existing SVC units to be chosen for coordination. Based on the performance index (6.1), the controller parameters (integral gains) were optimized as it was done when 5 SVC units were considered. However, only the coordinated SVC controllers have identical parameters, while those controlled locally have different controller parameters. We note that the general block diagram used is a combination of Figure 6.9 (for coordinated SVC controllers) and Figure 5.2 (for uncoordinated SVC controllers).

The calculated eigenvalues of the system with reduced coordination of the SVC units are given in Table 6.3 with the eigenvalues of the system with uncoordinated SVC units.

Table 6.3

Coordinated SVCs	Uncoordinated SVCs
-119.60	-40.74
-119.72	-56.24
-119.72	-92.90
-120.48	-120.48
-120.48	-120.48
-120.48	-120.48
-120.48	-120.48
-120.48	-120.48
-124.94	-139.02
-164.38	-189.59
-24.96 ±j 88.31	-16.43 ± j 129.47
-24.98 ±j 88.29	-44.99 ± j 99.88
-24.98 ±j 88.29	-63.55 ± j 84.19
-38.62 ±j 111.13	-78.55 ± j 82.49
-56.13 ±j 93.36	-83.56 ± j 84.19
-83.84 ±j 84.87	-263.44 ± j 263.23
-83.84 ±j 84.87	-263.85 ± j 263.18
-83.84 ±j 84.87	-265.63 ± j 263.15
-263.32 ±j 263.19	-266.25 ± j 263.14
-263.86 ±j 263.18	-266.34 ± j 263.14
-265.63 ±j 263.15	
-266.25 ±j 263.14	
-266.34 ±j 263.14	

Figure 6.18 illustrates the eigenvalues of the system with a reduced coordination of its SVC units together with the eigenvalues of the system with the uncoordinated SVC units. One can see that the control coordination, although limited to three out of five SVCs (other two SVCs are with local controllers), provides an improved performance and a larger margin of stability as compared to local control. One cans also see that the three coordinated SVC units have identical eigenvalues while the two uncoordinated others have different eigenvalues.

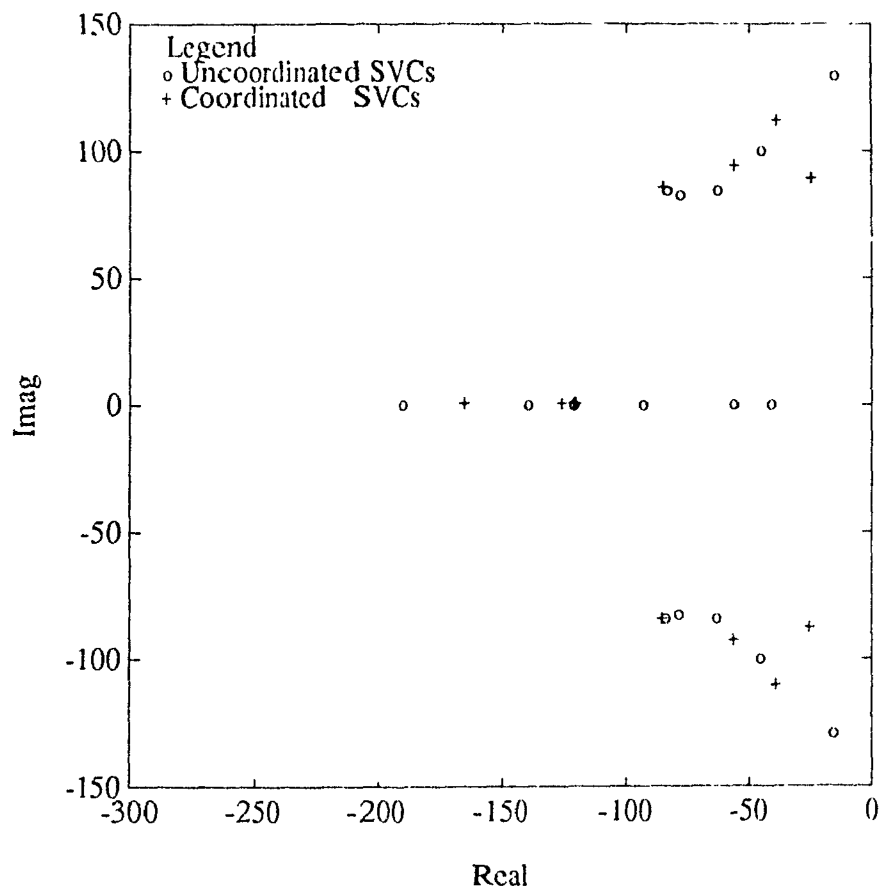

Fig 6.18. Eigenvalues of the system with five SVC units
(a) system with three coordinated and two uncoordinated units
(b) system with five uncoordinated units

Figure 6.19 illustrates the responses of the voltage error of every SVC controller of the system with reduced coordination and without coordination, the step input being applied at the reference voltage of the fourth SVC unit. One can also observe the decoupling achieved with reduced coordination as compared to the system with uncoordinated SVC units.

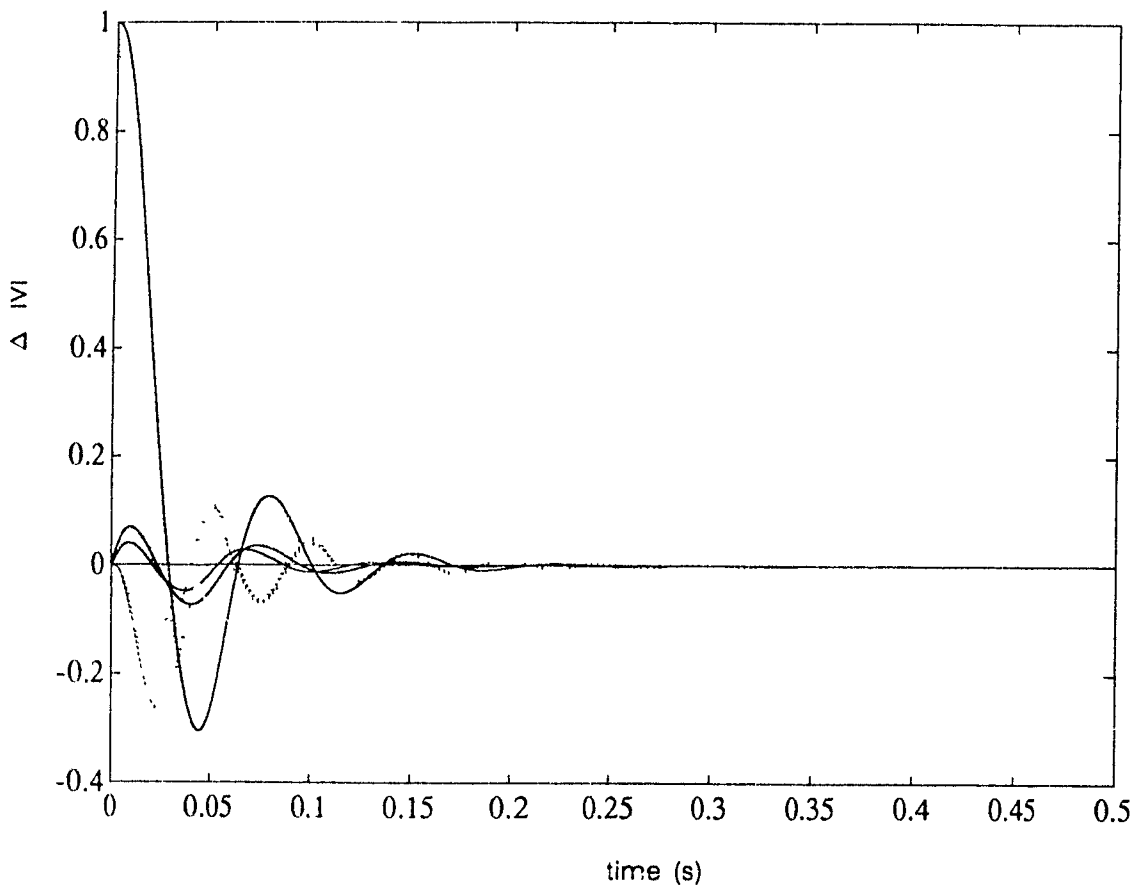

Fig 6.19. Voltage error step response $\Delta|V|_{svci\ trans}$ of the system with five SVC units

_____ Three coordinated and two uncoordinated SVCs

.... Five uncoordinated SVCs

The SVC coordination of all the SVC units gives the best SVC improvement as well as the greatest increase of the system stability margin.. However, when a full coordination is not practical, a reduced coordination can be justified, as illustrated above.

CHAPTER VII

CONCLUSIONS

Static var compensators for voltage regulation in power systems employ controllers which are local and independent. As more and more of SVC units are installed within one power system, undesirable interactions develop. Such interactions reduce, in general, their stability limits, increasing risks of instability (mutual hunting). For these reasons, the slower control settings and dynamics has to be adopted. Some studies indicate that a number of such devices has to be limited in order to ensure their operation stability.

In order to overcome the constraints imposed by such a concept of local and independent SVC controllers, two new concepts for coordination of local SVC controllers have been developed within the framework of this thesis.

The first part of the thesis presents a coordination of local controllers of SVC units operating on the same system bus. When the SVC units are uncoordinated, their dynamic participations in voltage control rely on static and dynamic characteristics of their controllers. When such controllers are different (with respect to their structures and/or parameter settings), SVC controller interactions deteriorate the dynamic performance and reduce stability margin of the entire system. The concept of control coordination developed in this thesis is based on averaging of the SVC current orders at the outputs of their controllers. The current order of each SVC controller is first summed with others, then multiplied by the ratio of its slope admittance and the equivalent slope admittance corresponding to all the SVC units together.

This proposed coordination concept improves dynamics of the SVC units operating on the same bus of the system, eliminating interactions among the SVC controllers.

The second part of this thesis presents a coordination of local controllers of many SVCs installed on different buses of a power system, based on coordination of local controllers in order to achieve a decoupled voltage regulation. In order to evaluate the conceived SVC control coordination, the IEEE 30-bus power system with five SVC units was analyzed. A comparative analysis and evaluation of the SVC systems with and without control coordination was performed in s-plane and time domain. It was determined that superiority of the coordination over local controllers increases with the number of SVC units, especially when the system stability is in question.

The control coordination concept can be conveniently implemented to new as well as existing SVC controllers as an add-on function, to suit gradually growing needs for SVC control improvements.

Another important aspect is that the control security is preserved when a communication link fails. The only consequence is that the affected controller looses the performance improvement provided by the control coordination.

The first step in further development of the concept is to extend the control coordination efficiency to become load flow adaptive. To achieve this, voltage phases have to be communicated in addition to voltage magnitude demands, to all SVC controllers. Adaptation to changes of the system topology requires a continuous updating of the driving point and transfer impedances between SVC units, either by direct measurement or by computation based on monitored topology.

BIBLIOGRAPHY

[1] L.Gyugyi, R A.Otto, T.H.Putman, "Principles and Applications of Static, Thyristor-Controlled Shunt Compensators", IEEE Trans, PAS-97, No.5, Sept/Oct., 1978, pp.1935–1945.

[2] L.Gyugyi, E.R.Taylor, Jr, "Characterisиcs of Static Thyristor-Controlled Shunt Compensators for Power Transmission system Applications", IEEE Trans, PAS-99, No.5, Sept/Oct., 1980, pp.1795-1804.

[3] A.Olwegard, K.Walve, G.Waglund, H.Frank, S.Torseng, "Improvement of Transmission Capacity by Thyristor-Controlled Reactive Power", IEEE Trans, PAS-100, No.8, August, 1981, pp.3930-3939.

[4] M.M.Gavrilovic, "Static Compensator Structures: Review and Analysis", Spring Meeting of the Canadian Electrical Association, Montreal, March 15–18, 1982.

[5] T.J.E.Miller, Editor, " Reactive Power Control in Electric Power Systems ", John Wiley & Sons, New York, 1982.

[6] R.M. Mathur. Editor, " Static Compensators for Reactive Power Control ", Canadian Electrical Association, Montreal, 1984.

[7] I.A.Erinmez, (Editor), " Static Var Compensators ", (book), Working Group 38–01, Task Force No.2 on SVC, CIGRE, 1986.

[8] L.Gyugyi, "Fundamentals of Thyristor-Controlled Static Var Compensators in Electric Power System Applications", IEEE Proceedings, Power Engineering Society Summer Meeting, 1987, pp. 8–27.

[9] H.E.Schweickardt, G.Romegialli and K.Reichert, " Closed Loop Control of Static Var Sources (SVS) on EHV Transmission Lines ", IEEE Trans., Vol. PAS-97, No.4, July/August 1978.

[10] R.L.Hauth, S.A.Miske, F.Nozari, " Role and Benefits of Static Var Systems in High Voltage Power System Applications", IEEE/PES Winter Meeting, Paper 82 WM 076-8, New York, New York, Jan. 31-Feb. 5, 1982 (Published IEEE Trans. PAS, Vol. 101, October 1982, pp. 3761-3770).

[11] D.McGillis, N.Hieu Huynh, G.Scott, " The Role of Static Compensation in Meeting AC System Control Requirements with Particular Reference to the James Bay System ", IEE Proc.C, Gener., Trans. & Distrib., 1981, 128, (6), pp.389-393.

[12] C.W.Edwards, K.E.Mattern, E.J.Stacey, P.R.Nannery, J.Gubernick, "Advanced Static Var Generator Employing GTO Thyristors", IEEE Trans. Power Del., Oct. 1988, pp. 1622-1627.

[13] R.Elsliger, Y.Hotte, J C.Roy, " Optimization of Hydro-Quebec's 735 kV Dynamic Shunt Compensated System Using Static Compensators on a Large Scale ", IEEE PES, Winter Power Meeting, New York, Paper No. A78, 107-5, January 29-February 3, 1978.

[14] L.Gerin-Lajoie, D.McGillis, G.Scott, "Static Compensator Applications and their limitations", International Symposium on Electric Energy conversion in Power Systems, Capri, Italy, May 1989.

[15] A.J.P.Ramos, "Dynamic Performance of a Radial Long Transmission System with Multiple Static Var Compensators", University Erlangen, Report Ev-Bericht F227, March 1987.

[16] R.T.Byerly, D.T.Poznaniak and E.R.Taylor, " Static Reactive Compensation for Power Transmission Systems ", IEEE 1982 Power Engineering Society Winter Meeting, Paper 82 WM 179-0, New York, January 31-February 5, 1982 (Published IEEE, PAS, Vol. PAS-101, pp 3997-4005, October 1982).

[17] M.O'Brien and G. Ledwick, " Placement of Static Compensators for Stability Improvement ", Proc IEE, Pt. C, Vol. 132, No. 1, pp 30-35, January 1985.

[18] N.Martins, L.T.G.Lima, " Determination of Suitable Locations for Power System Stabilizers and Static Var Compensators for Damping Electromechanical Oscillations in Large Scale Power Systems ", 16th Power Industry Computer Applications Conference,Seattle, WA, May 1–5, 1989 (Published in The Proceedings of The 1989 Computer Applications Conference, 1989, pp. 74–82).

[19] S.Granville, L.C.Lima, M C A.Lima and S.Prado, " Improving the Quality of Voltage Profile through Optimally Allocated Shunt Var Systems ", IERE Meeting, Rio de Janeiro, May 25-27, 1991.

[20] M.Athans, P.L.Falb, " Optimal Control ", (book), McGraw-Hill, New York, 1966.

[21] Y.Yu, K.Vongsuriya, L.N.Wedman, " Application of an Optimal Control Theory to a Power System ", IEEE Trans, 1970, PAS-89, (1), pp. 55-62.

[22] A.R.Daniels, D.H.Davis, M.K.Pal, " Linear and Nonlinear Optimization of Power System Performance ", IEEE Trans, 1975, PAS-94, (3), pp. 810-818.

[23] P.B.Reddy, P.Sannuti, " Asymptotic Approximation Method of Optimal Control Applied to a Power System Problem ", Proc. IEE., 1976, 123, (4), pp. 371-376.

[24] V.A.Venikov, V.A.Stroev, M.A.H.Tawfik, " Optimal Control of Transients in Electrical Power Systems Containing Controlled Reactors, Part. 2 : Optimal Control Solution ", IEEE Trans., 1981, PAS-100, (9), pp. 4271-4280.

[25] R.L Kosut, " Suboptimal Control of Linear Time-Invariant Systems Subject to Control Structure Constraints ", IEEE Trans, 1970, AC-15, (5), pp. 557-563.

[26] M.M ElMetwally, N.D.Rao, " Decentralized Optimal Control of Multi-Area Power Systems ", Paper A76 146-1 presented at IEEE PES 1976 Winter Power Meeting.

[27] M.Brucoli, F.Torelli, M Trovato, " A Decentralised Control Strategy for Dynamic Shunt Var Compensation in Interconnected Power Systems ", IEE Proc. C, 1985, Vol. 132, pp. 229–236.

[28] J. Belanger, G.Scott, T. Anderson and S. Torseng, "Gain Supervisor for Thristor -Controlled Shunt Compensators", CIGRE, paper No. 38–01, September 1984.

[29] J R.Smith, D A Pierre, D.A Rudberg, R M Johnson, "Robust Var Unit Control Strategies to Enhance Damping of Power System Oscillations", Proceedings, IASTED Conference on High Technology in the Power Industry, pp 238-243, March 1988.

[30] J.R.Smith, "Robust Var Unit Control Strategies for Damping of Power System Oscillations", Ph.D Thesis, Montana State University, Bozeman, MT, July 1988.

[31] J.R.Smith, D.A.Pierre, D.A.Rudberg, I.Sadighi, A P Johnson, J.F.Hauer, "An Enhanced LQ Adaptive Var Unit Controller for Power System Damping", IEEE Power Engineering Society Summer Meeting, Paper 88 SM 692-6, Portland, Oregon, July 24–29, 1988.

[32] J.R.Smith, D.A Pierre, I.Sadighi, M.H Nehrir, J.F Hauer, "A Supplementary adaptive Var Unit Controller for Power System Damping", IEEE Power Engineering Society Winter Meeting, Paper 89 WM 197–5, New York, New York, Jan. 29–Feb. 3, 1989.

[33] L.Gerin-Lajoie, G.Scott, E.V.Larsen, D.H.Baker, A.F.Imece, " Hydro-Quebec Multiple SVC Application Control Stability Study ", IEEE/PES 1990 Winter Meeting, Paper 90 WM 082–2 PWRD, Atlanta, Georgia, Feb. 4-8, 1990

[34] Electromagnetic Transients Program(EMTP), Volumes 2-4, Prepared by the University of Wisconsin at Madison.

[35] M.M.Gavrilovic, G.Roberge, P.Pelletier, J.-C.Soumagne, "Reactive and Active-Power Control by means of Variable Reactances", Proc. of the 11th Pan-American

Congress of Mechanical, Electrical and Allied Engineering Branches (COPIMERA '87), Canadian Sec., CEA, Montreal, Nov. 9-13, 1987.

[36] L.V.Martin, " Phase-Locked Loop Simulation in Transient Stability Studies ", Master thesis, McGill University, July 1989.

[37] PRO-MATLAB, User's Guide, The MathWorks, Inc., 21 Eliot Street, South Natick, MA 01760, USA, January 31, 1990.

[38] L.L.Freris, A.M.Sasson, "Investigation of the Load Flow Problem", IEE Proc., Vol. 115, No. 10, pp. 1459-1470, October 1968.

[39] A.Hellal, M.M.Gavrilovic, "Control Coordination of SVCs for Voltage Regulation in Power systems", Paper submitted for IEEE Winter Meeting, 1992.

Additional references

[40] P.K.Sinha, " Multivariable Control : An Introduction ", (book), Marcel Dekker, Inc., 1984.

[41] Charles A.Gross, " Power System Analysis ", (book), Second Edition, John Wiley & Sons, 1986.

[42] M. Brucoli, F. Torelli and M. Trovato, " Coordinated Control of Static Var Compensators in Long Distance AC Transmission Systems ", Workshop on Very Long Distance AC Transmission Systems, University of Pisa, Italy, September 1984.

[43] L.Gyugyi, W.J Lordeon, "Transmission–System Static Var Control", EPRI Technical Report, Final Report No. EPRI–EL–2754 0240P, Westinghouse Electric Corp , Dec. 1982.

[44] A.E.Hammad, "System Planning Studies for Static Var Compensation and HVDC in large EHV Networks", Brown Boveri Rev. (Switzerland), March 1982, pp. 90–94.

[45] M.E.Rahman, J.J.Keane, J.B.Svensson, "Static Var Systems Control Voltage", Electr. World, Dec. 1982, pp. 82–85.

[46] K.Reichert, Controllable Reactive Compensation", Electric Power and Energy Systems, Vol. 4, pp. 51–61, 1982.

[47] F.Aboytes, G.Arroyo, G.Villa, "Application of Static Var Compensators in Longitudinal Power Systems", IEEE PAS, Vol. PAS–102, pp. 3460–3466, October 1983.

[48] A.E.Hammad, M.El–Sadek, "Application of a Thyristor Controlled Var Compensator for Damping Subsynchronous Oscillations in Power Systems", IEEE/PES Summer Meeting, Paper 83 SM 443–9, Los Angeles, California, July 17–22,1983.

[49] G.Ledwich, "Control Algorithms for Shunt Var Systems", Electr Power Syst Res., Vol. 6, No. 2, June 1983, pp. 141–146.

[50] H.K.Patel, G.K.Dubey, "Reactive Power Compensation by Thyristor–Switched Capacitors", Conference Record of the Industry Applications Society IEEE–IAS–1983 Annual Meeting 1983, 1983, pp. 818–24.

[51] Purdue University, " Development of a Functional Representation of the Static Var Unit", Purdue Univ., Lafayette, IN, Report No. DOE/ET/29365–7, Feb. 1983

[52] Electr. Power Res. Inst., "Evaluation of Advanced Static Var Generators", Electr. Power Res. Inst., Palo Alto, CA, USA, Publ. 31 May 1984

[53] R. Gutman, J.J. Keane, M. Ea, Rahman and O. Veraas, "Application and Operation of a Static Var System on a Power System – American Electric Power Experience, Part I and II : System Studies", IEEE, PAS, Vol. PAS–104, No 7, pp. 1868–1882, June 1985.

[54] A.E.Hammad, M.El–Sadek, P.K.Dash, "Application of Static Var Compensators and HVDC Converters for Damping Subsynchronous Oscillations in Power Sys-

tems", Control in Power Electronics and Electronics and Electrical Drives. Proceedings of the Third IFAC Symposium, 1984, pp. 705–12.

[55] A.E. Hammad and M. El-Sadek, "Application of a Thyristor-controlled Var Compensator for Damping Subsynchronous Oscillations in Power Systems", IEEE, PAS, Vol. PAS-103, No. 4, pp. 811-818, April 1984.

[56] G.L. Kusic and I.A. Whyte, "Three Phase Steady-sate Static Var Generator Filter Design for Power Systems", IEEE, PAS, Vol. PAS-103, No. 4, pp. 811–818, April 1984.

[57] M.Nanba, Y.Sagisaka, Y.Mizukami, H.Yoshida, K.Murotani, M.Asano, Y.Ogihara, "Improvement of Power System Stability by Means of Static Var Compensator", Electr. Eng. Jpn. (USA), Vol. 104, No. 3, May–June 1984, pp. 40-8.

[58] T. Ohyamma, K. Yamshita, T. Maeda, H. Suzuki and S. Mine, "Effective Application of Static Var Compensators to Damp Oscillations", IEEE, PAS, Vol. PAS–104, No. 6, pp. 1405–1410, June 1985.

[59] B.T. Ooi and M. H. Banakar, "Co-ordination of Static Var Compensators with Long Distance Radial Transmission System for Damping Improvement", IEEE, PAS, Vol. PAS–103, No. 2, pp. 265-274, February 1984.

[60] E.R. Taylor Jr., J.E. O'Neil, D.T. Poznaniak, "Static Compensators Aid Long Distance Transmission", Electrical Review International (GB) Vol. 1, No. 4, pp. 44-46, May 1984.

[61] H.L.Thanawala, "Static Compensators=Fast Var Control", Electr. World (USA), Vol. 198, No. 10, Oct. 1984, pp. 74-6.

[62] K. Engberg, H. Frank and B. Klefors, "Thyristor Switched Capacitors, TSC, in theory and Practice", Fourth International Conference on AC and DC Power Transmission, IEE Conference Publication No. 255, London, September 1985.

[63] S.E.Haque, N.H.Malik, W.Shepherd, "Operation of a Fixed Capacitor-Thyristor Controlled reactor (FC-TCR) Power Factor Compensator", IEEE Trans. Power Appar. & Syst. (USA), Vol. PAS-104, No. 6, June 1985, pp. 1385-90.

[64] P. Muttik, "SVC Design and Rating Considerations", Symposium on Static Var Systems, Capricornica Institute, Rockhampton, Australia, November 1985.

[65] A.J.P.Ramos, P.C.C.Tavares and L.R.Lins, "Application of Static Compensators in Radial Power Systems", Proc. IFAC Sympos. on Planning and Operation of Electric Energy Systems, Rio de Janeiro, 1985, pp. 223-228.

[66] H.L. Thanawala, "Static Var Compensators for Transmission Systems", GEC Review, Vol. 1, No. 2, 1985.

[67] S. Torseng, "Some Utility applications of Static Compensators", Symposium on Static Var Systems. Capricornica Institute, Rockhampton, Australia, November 1985.

[68] K. Walshe, "Development of SVC Design", Symposium on Static Var Systems, Capricornica Institute, Rockhampton, Australia, November.

[69] L.J.Bohmann, R.L.Lasseter, "Equivalent Circuit for Frequency Response of a Static Var Compensator", IEEE Trans., Vol. PWRS-1, No. 4, Nov. 1986, pp. 68-74.

[70] A.E.Hammad, B.Roesle, "New Roles for Static Var Compensators in Transmission Systems", Brown Boveri Tech. (Switzerland), Jun 1986, pp 314-320.

[71] A.E.Hammad, "Analysis of Power System Stability Enhancement by Static Var Compensators", IEEE Trans. on Power Systems, Vol PWRS-1, No 4, November 1986, pp.222-227.

[72] L.Petcantchine, "Interconnected Networks: Control Algorithms for Static Var Systems (SVS)",RGE, Rev. Gen. Electr. (France), No. 8, Sept. 1986, pp 21-25.

[73] C.R.Vidyashankar, A.K.Khargekar, "A Practical fast Acting Control Scheme for Static Var Compensator", Electr. Mach. & Power Syst. (USA), Vol. 11, No. 5, 1986, pp.357–66.

[74] P.Czech, G.Scott, "Application of Static Var Compensators on Hydro-Quebec's EHV System", IEEE/PES 1987 Winter Meeting, Special Publication, Paper 87TH0187-5-PWR, Symposium on "Application of Static Var Systems for System Dynamic Performance", 1987.

[75] I.M.El-Amin, S.K.Majdhoub, "Digital Simulation of a Thyristor Controlled Reactor for Power Systems", Modelling Simulation & Control A (France), Vol. 10, No. 1, !987, pp.12–25.

[76] A.E.Hammad, "Applications of Static Var Compensators in Utility Power Systems", Proceedings of The 1987 IEEE Power Engineering Society Summer Meeting, 1987, pp.28–35.

[77] R.M.Hamouda, M.R.Iravani, R.Hackam, "Coordinated Static Var Compensators and Power System Stabilizers for Damping Power System Oscillations", IEEE Trans. Power Syst., Nov. 1987, pp.1059–1067.

[78] S.E.Haque, N.H.Malik, "Analysis and performance of a fixed filter-thyristor controlled reactor (FF-TCR) compensator", IEEE Trans. Power Syst. (USA) , Vol. PWRS-2, no. 2, May 1987, pp. 3023-9.

[79] M.Hausler, P.Huber, C.Tschudi, F.Wittwer, P.Meringdal, "Firing System and Overvoltage Protection for Thyristor Valves in Static Var Compensators", Brown Boveri Rev. (Switzerland), Vol. 74, No. 4, April 1987, pp. 206–12.

[80] Y.Hsu, C.Cheng, "Design of a Static Var Compensator using Model Reference Adaptive Control", Electr. Power Syst. Res. (Switzerland), Vol. 13, No. 2, Oct. 1987, pp. 129–138.

[81] E.V.Larsen, J.H.Chow, "SVC Control Design Concepts for System Dynamic Performance", IEEE/PES 1987 Winter Meeting, Special Publication, Paper 87TH0187-5-PWR, Symposium on "Application of Static Var Systems for System Dynamic Performance", 1987.

[82] D.E.Martin, "SVC Considerations for System Damping", Application of Static Var Systems for System Dynamic Performance, IEEE Special Publication No. 87 TH0187-5-PWR, 1987, pp. 68-71.

[83] M.O'Brien and G.Ledwich, "Static Reactive-Power Compensator Controls for Improved System Stability", IEE Proc. C., Vol. 134, 1987, pp. 38-42.

[84] A.J.P.Ramos, "Dynamic Performance of a Radial Long Transmission System with Multiple Static Var Compensators", University Erlangen, Report Ev-Bericht F227, March 1987.

[85] J.D.Ainsworth, "Phase-Locked Oscillator Control System for Thyristor-Controlled Reactors", IEE Proc., Part C, Mar 1988, pp. 146-156.

[86] C.E.Liu, T.C.Chen, C.L.Huang, "Optimal Control of a Static Var Compensator for Minimization of Line loss", Electric Power Systems Research, Vol. 15, No. 1, August 1988.

[87] D.L.Osborn , "Factors for Planning a Static Var System", Electric Power Systems Research, Vol. 17, No. 1, July 1989.

[88] A.J.P.Ramos, H.Tyll, "Dynamic Performance of a Radial Weak Power System with Multiple Static Var Compensators", IEEE Trans. Power Syst. , Nov. 1989, pp.1316-1325.

[89] E.V.Larsen, D.H.Baker, A.F.Imece,L.Gerin-Lajoie, G Scott, "Basic Aspects of Applying SVC's to Series-Compensated AC Transmission Lines", IEEE/PES 1990 Winter Meeting, Paper 90 WM 082-2 PWRD, Atlanta, Georgia, Feb. 4-8, 1990.

APPENDIX A

MODAL ANALYSIS OF LINEAR TIME-INVARIANT DYNAMIC SYSTEMS

Linear time-invariant (LTI) systems are very important in system modeling and analysis. Indeed, for small signal variations around the equilibrium point, continuous dynamic systems can be adequately modeled by linear time-invariant systems. Non linearities are usually ignored in the first phase of the control system design when a LTI system representation is used to elaborate control principles. In the second phase, the control system design is extended to the system with all nonlinearities included.

Since this approach is taken in this thesis, it is important to review the significance of eigenvalues, eigenvectors, poles, zeros and residues to control system analysis and to reveal what conclusions can be deduced from these system characteristics with regard to system dynamics in general.

A linear, time invariant system can be described in a state-space form expressed by the equations,

$$x = A\,x + B\,u \qquad \text{(A.1)}$$

$$y = C\,x + D\,u \qquad \text{(A.2)}$$

where x is the state variable vector,

y is the output vector, and

A, B, C and D are the system matrices.

The solution of LTI systems consist of two components :

the *zero-input* response which satisfies

$$\begin{aligned} x_{zi} &= A\, x_{zi} \\ y_{zi} &= C\, x_{zi} \end{aligned} \qquad \text{(A.3)}$$

with the initial state $x_{zi}(0) = x_{zi\,0}$ and

the *zero-state* response which satisfies

$$\begin{aligned} x_{zs} &= A\, x_{zs} + B\, u \\ y_{zs} &= C\, x_{zs} + D\, u \end{aligned} \qquad \text{(A.4)}$$

with $x_{zs}(0) = 0$.

The zero-input response is best studied by means of Laplace transforms. Then, equation (A.3) yields to,

$$s\, X(s) - x(0) = A\, X(s) \qquad \text{(A.5)}$$

or $$(sI - A)\, X(s) = x(0) \qquad \text{(A.6)}$$

and $$X(s) = (sI - A)^{-1}\, x(0) \qquad \text{(A.7)}$$

The solution derived from the zero-input equation is of the form,

$$x(t) = e^{At}\, x(0) \qquad \text{(A.8)}$$

Comparing equation (A.7) with (A.8), we obtain

$$\mathcal{L}[e^{At}] = (sI - A)^{-1} \qquad \text{(A.9)}$$

To determine the dynamic modes of the systems, we may write

$$(sI - A)^{-1} = \frac{Adj\ (sI - A)}{\det\ (sI - A)} \qquad \text{(A.10)}$$

The determinant is an nth-order polynomial. The co-factors of $(sI-A)^{-1}$ are also polynomials, of degree $n-1$ at most. Therefore, any particular element of $(sI-A)^{-1}$ can be expanded by partial fractions into an expression of the form

$$\frac{A_{11}}{(s-s_1)} + \frac{A_{12}}{(s-s_1)^2} + \ldots + \frac{A_{21}}{(s-s_2)} + \frac{A_{22}}{(s-s_2)^2} + \ldots \qquad (A.11)$$

where $s_1, s_2, \ldots$ are the roots of the determinant, some of which may be multiple. Using the inverse of Laplace transforms, we obtain an expression of the form

$$A_{11}\, e^{s_1 t} + A_{12}\, t\, e^{s_1 t} + \ldots + A_{21}\, e^{s_2 t} + A_{22}\, t\, e^{s_2 t} + \ldots \qquad (A.12)$$

The elements of e^{At} are sums of exponentials or time-weighted exponentials, whose exponents are the roots of the determinant.

Eigenvalues and Eigenvectors

Roots $s_1, s_2, \ldots$ satisfy the equation,

$$\det\,(sI-A) = 0 \qquad (A.13)$$

These roots are also called the eigenvalues of the matrix A. These eigenvalues characterize system modes in time domain.

An eigenvector $\mathbf{v}_i$ (modal vector) which is associated with the eigenvalue s_i is defined by the equation,

$$A\,\mathbf{v}_i = s_i\,\mathbf{v}_i \qquad (A.14)$$

$\mathbf{v}_i$ is also an eigenvector of matrix $e^{\mathbf{A}t}$, which is the solution of equation (A.13), with eigenvalue $e^{s_i t}$ as it is shown that

$$e^{\mathbf{A}t}\,\mathbf{v}_i = e^{s_i t}\,\mathbf{v}_i \qquad (A.15)$$

The significance of this relation is that the zero–input response to an initial state $x_0 = \mathbf{v}_i$ is $x(t) = e^{s_i t}\,\mathbf{v}_i$. This means that the only excited mode is s_i.

Residues, Poles and Zeros

The zero-state response is often studied by means of tran fer functions in Laplace domain. In order to derive input-output transfer function from the state equation, the following transformation were carried out,

$$s\,X(s) = A\,X(s) + B\,U(s) \tag{A.16}$$

or $$X(s) = (sI - A)^{-1}\,B\,U(s) \tag{A.17}$$

where initial conditions $x(0) = 0$ are being assumed.

The output equation yields to,

$$Y(s) = [C\,(sI - A)^{-1}\,B + D]\,U(s) \tag{A.18}$$

The transfer function is derived as follows,

$$G(s) = \frac{Y(s)}{U(s)} = C\,(sI - A)^{-1}\,B + D \tag{A.19}$$

For a multi-input-multi-output (MIMO) system, $G(s)$ has m rows(the number of ouputs) and r columns (the number of inputs). For a single-input-single-output (SISO) system, $m = r = 1$.

The time domain equivalent to equation (A.18), is given by the convolution integral,

$$y(t) = \int_0^{\infty} C\,e^{A(t-\tau)}\,B\,u(\tau)\,d\tau + D\,u(t) \tag{A.20}$$

For a MIMO system, i,j element of the matrix $G(s)$ is given by,

$$G_{ij}(s) = \frac{\mathbf{c}_i^T \, Adj\,(sI-A)\,\mathbf{b}_j + d_{ij}\,\det\,(sI-A)}{\det\,(sI-A)} \tag{A.21}$$

where $\mathbf{c}_i$ is the i-th row of matrix C,

$\mathbf{b}_j$ is the j-th column of matrix B and,

d_{ij} is the ij-th element of matrix D.

The denominator $\det\,(sI-A)$ of the transfer function $G_{ij}(s)$ is a polynomial of degree n, so is the numerator due to the term $d_{ij}\det\,(sI-A)$, while the term $\mathbf{c}_i^T \, Adj\,(sI-A)\,\mathbf{b}_j$ is of degree $n-1$.

Since the roots of the denominator are the eigenvalues of A, it follows that all poles of $G(s)$ are eigenvalues of A. The converse does not necessarily hold. If $\det\,(sI-A)$ has a factor $(s-s_i)^k$, where k is the multiplicity of s_i, it is possible that $G_{ij}(s)$ also contains this factor in its numerator, so that a cancellation takes place, hence s_i vanishes as a pole. We note that B, C and D do not influence the pole locations at all. They do, however, influence upon the system responses since they enter into the numerators.

Let the transfer function $G(s)$ be expressed as

$$G(s) = \frac{K\,(s-z_1)\ldots(s-z_n)}{(s-p_1)(s-p_2)\ldots(s-p_n)} \tag{A.22}$$

where $z_1, \ldots, z_m$ are the zeros, $p_1, \ldots, p_n$ are the poles of $G(s)$ with $m \leq n$ and K is a coefficient factor.

Equation (A.22) can be transformed to,

$$G(s) = \sum_{j=1}^{n} \frac{k_j}{(s - p_j)} \tag{A.23}$$

where k_j are residues at poles p_j.

The residues are calculated as follows :

if poles are simple, then

$$k_j = \underset{s \to p_j}{res}\, G(s) = \lim_{s \to p_j} (s - p_j)\, G(s) \tag{A.24}$$

For higher order poles, one has

$$k_j = \underset{s \to p_j}{res}\, G(s) = \frac{1}{(m-1)!} \lim_{s \to p_j} \frac{d^{m-1}}{d\, s^{m-1}} [(s - p_j)^m\, G(s)] \tag{A.25}$$

The residue k_j at pole p_j corresponds to a transient component $k_j\, e^{(p_j t)}$ as the system response to the pulse output. Therefore, the significance of the residue is that its magnitude is equal to the initial value of the corresponding transient component.

Given an input $U(s)$, the output of the system is as follows,

$$Y(s) = G(s)\, U(s) \tag{A.26}$$

Expanded by partial fraction expression (A.26) becomes,

$$G(s)\, U(s) = \sum_{j=1}^{n} \frac{k_j}{(s - p_j)} + \sum_{k=1}^{r} \frac{k_k}{(s - p_k)} \tag{A.27}$$

where n is the number of poles of $G(s)$ and r is the number of poles of $U(s)$. The inverse Laplace transformation of this equation is,

$$y(t) = \sum_{j=1}^{n} k_j\, e^{(p_j t)} + \sum_{k=1}^{r} k_k\, e^{p_k t} \tag{A.28}$$

In frequency domain, the interpretation of poles and zeros is the following. The transfer function (equation A.22) has parallel resonances at frequencies corresponding to its complex poles (high gains) and series resonances corresponding to its complex zeros (high attenuation). Therefore, the system amplifies the output signal around the poles frequency and attenuates the output signal at the zeros frequency. The real poles and zeros produce non-discriminate effects upon the input signal at all frequencies, as it could be easily seen from equation (A.22).

APPENDIX B

STATE-SPACE REPRESENTATION OF POWER SYSTEMS WITH SVCs

The details of the mathematical derivations of the state-space matrices of the complete system A_x, B_u, C_x and D_u are presented in this appendix.

The state-space representation of the SVC system (Figure 5.2) is expressed by the following :

$$x = A\,x + B_1\,|V|_{ref} + B_2\,|V| + B_3\,\theta + B_4\,I_c \tag{B.1}$$

$$\begin{bmatrix} \Delta|V| \\ |V|_{dem} \\ \Delta\theta \end{bmatrix} = \begin{bmatrix} C_1 \\ C_2 \\ C_3 \end{bmatrix} x + \begin{bmatrix} D_{11} \\ D_{21} \\ D_{31} \end{bmatrix} |V|_{ref} + \begin{bmatrix} D_{12} \\ D_{22} \\ D_{32} \end{bmatrix} |V| + \begin{bmatrix} D_{13} \\ D_{23} \\ D_{33} \end{bmatrix} \theta + \begin{bmatrix} D_{14} \\ D_{24} \\ D_{34} \end{bmatrix} I_c \tag{B.2}$$

From Figure 5.2 we also derive :

$$I_c = K\,\mathbf{B}_{co}|V|_{dem} = [E_v \quad 0] \begin{bmatrix} |V|_{dem} \\ \Delta\theta \end{bmatrix} \tag{B.3}$$

As a part of equation (A.2), we have :

$$\begin{bmatrix} |V|_{dem} \\ \Delta\theta \end{bmatrix} = \begin{bmatrix} C_2 \\ C_3 \end{bmatrix} x + \begin{bmatrix} D_{21} \\ D_{31} \end{bmatrix} |V|_{ref} + \begin{bmatrix} D_{22} \\ D_{32} \end{bmatrix} |V| + \begin{bmatrix} D_{23} \\ D_{33} \end{bmatrix} \theta + \begin{bmatrix} D_{24} \\ D_{34} \end{bmatrix} I_c \tag{B.4}$$

which can be rewritten as following :

$$\begin{bmatrix} |V|_{dem} \\ \Delta\theta \end{bmatrix} = C_{23}\ x + D_{231}\ |V|_{ref} + DD_{23} \begin{bmatrix} |V| \\ \theta \end{bmatrix} + \begin{bmatrix} D_{24} \\ D_{34} \end{bmatrix} [E_v \quad 0] \begin{bmatrix} |V|_{dem} \\ \Delta\theta \end{bmatrix}$$

(B.5)

or $$\begin{bmatrix} I_v - D_{24}E_v & 0 \\ -D_{34}E_v & I_\theta \end{bmatrix} \begin{bmatrix} |V|_{dem} \\ \Delta\theta \end{bmatrix} = C_{23}\ x + D_{231}\ |V|_{ref} + DD_{23} \begin{bmatrix} |V| \\ \theta \end{bmatrix} \quad \text{(B.6)}$$

where $$[IDE] = \begin{bmatrix} I_v - D_{24}E_v & 0 \\ -D_{34}E_v & I_\theta \end{bmatrix} \quad \text{(B.7)}$$

with I_v being the identity matrix of dimensions $(N_{svc}\ x\ N_{svc})$. N_{svc} is the number of SVCs instaleed in the power system.

From expression (B.6), we deduce :

$$\begin{bmatrix} |V|_{dem} \\ \Delta\theta \end{bmatrix} = IDE^{-1}\ C_{23}\ x + IDE^{-1}\ D_{231}\ |V|_{ref} + IDE^{-1}\ DD_{23} \begin{bmatrix} |V| \\ \theta \end{bmatrix}$$

(B.8)

or $$\begin{bmatrix} |V|_{dem} \\ \Delta\theta \end{bmatrix} = IDC\ x + IDD_1\ |V|_{ref} + IDD \begin{bmatrix} |V| \\ \theta \end{bmatrix} \quad \text{(B.9)}$$

The total SVC current as shown in Figure 4.5 is the following :

$$I_{svc_t} = I_c + I_{\Delta\theta} = K\ \mathbf{B}_{co}|V|_{dem} + K_{\theta I}\ \Delta\theta \quad \text{(B.10)}$$

or $$I_{svc_t} = [E_v \quad E_\theta\ ] \begin{bmatrix} |V|_{dem} \\ \Delta\theta \end{bmatrix} = E_{v\theta} \begin{bmatrix} |V|_{dem} \\ \Delta\theta \end{bmatrix} \quad \text{(B.11)}$$

On an other hand, deriving the magnitude and phase voltage from mesurements gives the following expression :

$$\begin{bmatrix} |V| \\ \theta \end{bmatrix} = \begin{bmatrix} J_{Rv} \\ J_{R\theta} \end{bmatrix} I_{Rl} + \begin{bmatrix} J_{Xv} \\ J_{X\theta} \end{bmatrix} I_{Xl} + \begin{bmatrix} J_{Xv} \\ J_{X\theta} \end{bmatrix} K^{-1} I_{svc_t} \tag{B.12}$$

where J_{Rv}, $J_{R\theta}$, J_{Xv} and $J_{X\theta}$ are the jacobian matrices linking the magnitude and phase voltage with load and SVC currents. In fact as shown in the power system bloc of Figure 4.5 we can derive the expressions of the jacobian matrices as follows:

$$J_{Rv} = -|\mathbf{V}|\ Re[\mathbf{V}^{-1}\ \mathbf{Y}^{-1}\ \mathbf{V}]|\mathbf{V}|^{-1} \tag{B.13}$$

$$J_{Xv} = |\mathbf{V}|\ Im[\mathbf{V}^{-1}\ \mathbf{Y}^{-1}\ \mathbf{V}]|\mathbf{V}|^{-1} \tag{B.14}$$

$$J_{R\theta} = -\ Im[\mathbf{V}^{-1}\ \mathbf{Y}^{-1}\ \mathbf{V}]|\mathbf{V}|^{-1} \tag{B.15}$$

$$J_{X\theta} = -\ Re[\mathbf{V}^{-1}\ \mathbf{Y}^{-1}\ \mathbf{V}]|\mathbf{V}|^{-1} \tag{B.16}$$

Equation (B.12) can be rewritten as :

$$\begin{bmatrix} |V| \\ \theta \end{bmatrix} = J_R\ I_{Rl} + J_X\ I_{Xl} + J_X\ K\ E_{v\theta} \begin{bmatrix} |V|_{dem} \\ \Delta\theta \end{bmatrix} \tag{B.17}$$

or $$\begin{bmatrix} |V| \\ \theta \end{bmatrix} = J_R\ I_{Rl} + J_X\ I_{Xl} + JKE \begin{bmatrix} |V|_{dem} \\ \Delta\theta \end{bmatrix} \tag{B.18}$$

Substituting equation (B.18) into (B.8) leads to :

$$\begin{bmatrix} |V|_{dem} \\ \Delta\theta \end{bmatrix} = IDC\ x + IDD_1\ |V|_{ref} + IDD\ J_R\ I_{Rl} + IDD\ J_X\ I_{Xl} + IDD\ JKE \begin{bmatrix} |V|_{dem} \\ \Delta\theta \end{bmatrix} \tag{B.19}$$

which can be rewritten as following :

$$\underbrace{[I_{v0} - IDD\ .\ JKE\ ]}_{IDK}\begin{bmatrix} |V|_{dem} \\ \Delta\theta \end{bmatrix} = IDC\ x + IDD_1\ |V|_{ref} + IDD\ J_R\ I_{Rl} + IDD\ J_X\ I_{Xl}$$

(B.20)

Deriving the magnitude and phase voltage variations from expression (B.20), gives :

$$\begin{bmatrix} |V|_{dem} \\ \Delta\theta \end{bmatrix} = IDKC\ x + IDKJ \begin{bmatrix} |V|_{ref} \\ I_{Rl} \\ I_{Xl} \end{bmatrix} \tag{B.21}$$

where $\quad IDKC = IDK^{-1}\ IDC$ (B.22)

and $\quad IDKJ = IDK^{-1}\ [IDD_1 \quad IDDJ_g \quad IDDJ_b]$ (B.23)

Resubstituting equation (B.21) into (B.18) gives :

$$\begin{bmatrix} |V| \\ \theta \end{bmatrix} = J_R\ I_{Rl} + J_X\ I_{Xl} + JKE\ \ IDKC\ x + JKE\ \ IDKJ \begin{bmatrix} |V|_{ref} \\ I_{Rl} \\ I_{Xl} \end{bmatrix} \tag{B.24}$$

or $$\begin{bmatrix} |V| \\ \theta \end{bmatrix} = J_R\ I_{Rl} + J_X\ I_{Xl} + KJC\ x + KJJ \begin{bmatrix} |V|_{ref} \\ I_{Rl} \\ I_{Xl} \end{bmatrix} \tag{B.25}$$

where $\quad KJJ = [KJJ_1 \quad KJJ_2 \quad KJJ_3]$ (B.26)

Then we can rewrite equation (B.24) as :

$$\begin{bmatrix} |V| \\ \theta \end{bmatrix} = KJC\ x + [KJJ1 \quad J_R + KJJ_2 \quad J_X + KJJ_3] \begin{bmatrix} |V|_{ref} \\ I_{Rl} \\ I_{Xl} \end{bmatrix} \tag{B.27}$$

or $$\begin{bmatrix} |V| \\ \theta \end{bmatrix} = KJC\ x + KJ_{bv} \begin{bmatrix} |V|_{ref} \\ I_{Rl} \\ I_{Xl} \end{bmatrix} \tag{B.28}$$

where $KJC = \begin{bmatrix} KJC_1 \\ KJC_2 \end{bmatrix}$ and $KJ_{bv} = \begin{bmatrix} KJ_{bv1} \\ KJ_{bv2} \end{bmatrix}$

The total SVC current can also be rewritten by substituting equation (B.21) into (B.11) as following :

$$I_{svc_t} = E_{v\theta}\ IDKC\ x + E_{v\theta}\ IDKJ \begin{bmatrix} |V|_{ref} \\ I_{Rl} \\ I_{Xl} \end{bmatrix} \tag{B.29}$$

or $$I_{svc_t} = EDK\ x + EDJ \begin{bmatrix} |V|_{ref} \\ I_{Rl} \\ I_{Xl} \end{bmatrix} \tag{B.30}$$

Rewritting expression (B.2) gives :

$$\begin{bmatrix} \Delta|V| \\ |V|_{dem} \\ \Delta\theta \end{bmatrix} = C\ x + D_2 D_3 \begin{bmatrix} |V| \\ \theta \end{bmatrix} + D_1\ |V|_{ref} + D_4\ I_{svc_t} \tag{B.31}$$

and substituting the expression (B.27) leads to :

$$\begin{bmatrix} \Delta|V| \\ |V|_{dem} \\ \Delta\theta \end{bmatrix} = C\ x + D_2 D_3\ KJC\ x + D_2 D_3\ KJ_{bv} \begin{bmatrix} |V|_{ref} \\ I_{Rl} \\ I_{Xl} \end{bmatrix} + D_{100} \begin{bmatrix} |V|_{ref} \\ I_{Rl} \\ I_{Xl} \end{bmatrix} + D_4\ I_{svc_t} \tag{B.32}$$

where $$D_{100} = [D_1 \quad 0 \quad 0] \tag{B.33}$$

Then replacing the expression of the total SVC current and regrouping the coefficients of similar elements gives :

$$\begin{bmatrix} \Delta|V| \\ |V|_{dem} \\ \Delta\theta \end{bmatrix} = C_{x1}\ x + D_{u1} \begin{bmatrix} |V|_{ref} \\ I_{Rl} \\ I_{Xl} \end{bmatrix} \tag{B.34}$$

(B.34) represents the expression of the state-space output equations, but can be rewritten in more global form including other selected ouputs of the system, such as the total SVC current I_{svc_t} and the measured voltage magnitude $|V|$. The more global expression is given as following :

$$\begin{bmatrix} \Delta|V| \\ |V|_{dem} \\ \Delta\theta \\ I_{svc_t} \\ |V| \end{bmatrix} = \begin{bmatrix} C_{x1} \\ EDK \\ KJC_1 \end{bmatrix} x + \begin{bmatrix} D_{u1} \\ EDJ \\ KJ_{bv1} \end{bmatrix} \begin{bmatrix} |V|_{ref} \\ I_{RI} \\ I_{XI} \end{bmatrix} \qquad \text{(B.35)}$$

which is :

$$\begin{bmatrix} \Delta|V| \\ |V|_{dem} \\ \Delta\theta \\ I_{svc_t} \\ |V| \end{bmatrix} = C_x\, x + D_u \begin{bmatrix} |V|_{ref} \\ I_{RI} \\ I_{XI} \end{bmatrix} \qquad \text{(B.36)}$$

The state-space form requires also to define the dynamic equations which are following. Back to expression (B.1), we have :

$$\dot{x} = A\, x + [B_2 \quad B_3] \begin{bmatrix} |V| \\ \theta \end{bmatrix} + [B_1 \quad 0 \quad 0] \begin{bmatrix} |V|_{ref} \\ I_{RI} \\ I_{XI} \end{bmatrix} + B_4\, I_{Xsvc} \qquad \text{(B.37)}$$

Substituting equations (B.27) and (B.3) into (B.37), leads to write :

$$\dot{x} = [A + B_{23}.KJC + B_4.E_{v0}.IDKC]\, x + [B_{23}.KJ_{bv} + B_z + B_4.E_{v0}.IDKJ] \begin{bmatrix} |V|_{ref} \\ I_{RI} \\ I_{XI} \end{bmatrix}$$

(B.38)

If we denote B_z and E_{v0} as,

$$B_z = [B_1 \quad 0 \quad 0] \qquad \text{(B.39)}$$

and $$E_{v0} = [E_v \quad 0] \qquad \text{(B.40)}$$

we obtain the following dynamic equation,

$$x = A_x x + B_u \begin{bmatrix} |V|_{ref} \\ I_{Rl} \\ I_{Xl} \end{bmatrix} \qquad (B.41)$$

which complete the state-space analysis by defining both expressions of the dynamic and state-space output equations.

APPENDIX C

CONTROLLER PARAMETERS OF TWO SVC UNITS OPERATING ON THE SAME BUS

	SVC1	SVC2
P_{svc} (MVars)	220	440
$K_{\theta I}$	0.955	0.955
Xsl (%)	3	3
ω_n	200	80
ζ	0.707	0.5
K_v	2	5
I_v	3000	10000
T_d	0.005	0.001
K_θ	533	450
P_θ	1	0.9
T_θ	0.0038	0.0025

APPENDIX D

DATA OF THE IEEE 30-BUS SYSTEM INCLUDING FIVE SVCs

IMPEDANCE AND LINE-CHARGING DATA (100-MVA base)

Line designation	Resistance (p.u)	Reactance (p.u)	Line charging (p.u) *
1-2	0.2399	0.4533	0
1-27	0.3202	0.6027	0
2-27	0.2198	0.4153	0
3-4	0.0132	0.0379	0.0042
3-30	0.0452	0.1852	0.0204
4-6	0.0119	0.0414	0.0045
4-12	0	0.2560	0
4-29	0.0570	0.1737	0.0184
5-7	0.0460	0.1160	0.0102
5-29	0.0472	0.1983	0.0209
6-7	0.0267	0.0820	0.0085
6-8	0..0120	0.0420	0.0045
6-9	0	0.2080	0
6-10	0	0.5560	0
6-28	0.0169	0.0599	0..0065
6-29	0.0581	0.1763	0.0187
8-28	0.0636	0.2000	0.0214
9-10	0	0.1100	0
9-11	0	0.2080	0
10-17	0.0324	0.0845	0

10-20	0.0936	0.2090	0
10-21	0.0348	0.0749	0
10-22	0.0727	0.1499	0
12-13	0	0.1400	0
12-14	0.1231	0.2559	0
12-15	0.0662	0.1304	0
12-16	0.0945	0.1987	0
14-15	0.2210	0.1997	0
15-18	0.1070	0.2185	0
15-23	0.1000	0.2020	0
16-17	0.0824	0.1923	0
18-19	0.0639	0.1292	0
19-20	0.0340	0.0680	0
21-22	0.0116	0.0236	0
22-24	0.1150	0.1790	0
23-24	0.1320	0.2700	0
24-25	0.1885	0.3292	0
25-26	0.2544	0.3800	0
25-27	0.1093	0.2087	0
27-28	0	0.3960	0
29-30	0.0192	0.0575	0

(*) Line charging is one-half of the total charging of line.

OPERATING CONDITIONS

Starting bus voltage			Generation		Load	
BUS NUMBER	Magnitude (p.u)	Phase angle degrees	MW	MVar	MW	MVar
1	1.00	0	0	0	2.4	1.2

2	1.00	0	0	0	7.6	1.6
3	1.00	0	0	0	94.2	19.0
4	1.00	0	0	0	0	0
5	1.00	0	0	0	22.8	10.9
6	1.00	0	0	0	30.0	30.0
7	1.00	0	0	0	0	0
8	1.00	0	0	0	5.8	2.0
9	1.00	0	0	0	0	0
10	1.00	0	0	0	11.2	7.5
11	1.00	0	0	0	0	0
12	1.00	0	0	0	6.2	1.6
13	1.00	0	0	0	8.2	2.5
14	1.00	0	0	0	3.5	1.8
15	1.00	0	0	0	9.0	5.8
16	1.00	0	0	0	3.2	0.9
17	1.00	0	0	0	9.5	3.4
18	1.00	0	0	0	2.2	0.7
19	1.00	0	0	0	17.5	11.2
20	1.00	0	0	0	0	0
21	1.00	0	0	0	3.2	1.6
22	1.00	0	0	0	8.7	6.7
23	1.00	0	0	0	0	0
24	1.00	0	0	0	3.5	2.3
25	1.00	0	0	0	0	0
26	1.00	0	0	0	0	0
27	1.00	0	0	0	2.4	0.9
28	1.00	0	0	0	10.6	1.9
29	1.00	0	40	0	21.7	12.7
30	1.06	0	0	0	0	0

TRANSFORMER DATA

Transformer designation	Tap setting
4–12	0.932

6-9	0.978
6-10	0.969
28-27	0.968

STATIC CAPACITOR DATA

Bus number	Susceptance (p.u) *
10	0.019
24	0.043

(*) Susceptance in p.u. on a 100-MVA base.

SVC PARAMETERS

	SVC1	SVC2	SVC3	SVC4	SVC5
P_{svc} (MVar)	5	5	5	10	1
$K_{\theta l}$	0.955	0.955	0.955	0.955	0.955
K	20	20	20	10	100
Xsl (%)	3	3	3	3	3
Ysvc p.u	1.6667	1.6667	1.6667	3.3333	0.3333
ω_n	120	120	120	120	120
ζ	0.707	0.707	0.707	0.707	0.707
K_v	0	0	0	0	0
I_v	159.22	102.18	73.64	124.24	44.23
K_θ	533	533	533	533	533
T_θ	0.0038	0.0038	0.0038	0.0038	0.0038
T_c	0.0083	0.0083	0.0083	0.0083	0.0083